CONODONT BIOSTRATIGRAPHY IN MIDDLE OSAGEAN TO UPPER CHESTERIAN STRATA, NORTH-CENTRAL OKLAHOMA, U.S.A.

By

JOHN EDWARD HUNT

Bachelor of Science in Geology

Brigham Young University

Provo, Utah

2015

Submitted to the Faculty of the
Graduate College of
Oklahoma State University
in partial fulfillment of
the requirements for
the Degree of
MASTER OF SCIENCE
December, 2017

CONODONT BIOSTRATIGRAPHY IN MIDDLE OSAGEAN TO UPPER CHESTERIAN STRATA, NORTH-CENTRAL OKLAHOMA, U.S.A.

Thesis Approved:

Dr. James O. Puckette

Thesis Advisor

Dr. Jack C. Pashin

Dr. G. Michael Grammer

ACKNOWLEDGMENTS

I have several people to thank for contributing to this thesis. First, I thank my advisor and mentor Dr. Jim Puckette. I am most grateful for his open-door policy which allowed me to ask for his help whenever I needed it. I also thank him for instilling an awareness within me that everyone has something to teach.

I thank my committee members Dr. Jack Pashin and Dr. Michael Grammer for their thoughtful critiques of this thesis. Their input and feedback helped me to ask better questions of my data and think more critically of my results. Of note, I thank Dr. Pashin for letting me borrow some of his reading materials that were relevant to this thesis, and I thank Dr. Grammer for the presentation he gave of my thesis work during the Spring 2017 Mississippian Consortium Field Trip with Devon Energy and having me join his students during their consortium-related group meetings.

I thank all past and current members of the Industry-Oklahoma State University Mississippian Consortium for their research that provided me with a solid foundation to build upon. I am especially grateful to my colleagues and fellow consortium members Cory Godwin, Jeff Miller, Ashley Dupont, and Ethan Hill for their thoughtful suggestions and help along the way that improved my methods and influenced the final interpretation of the results. I wish each of them the best in their geoscience careers.

Special thanks to my Oklahoma State colleague Tim Janousek for lending me some of his research materials so that I could better conduct my laboratory experiments and for teaching me some of his more effective conodont extraction techniques. I give special thanks to the staff at the Oklahoma Petroleum Information Center for laying out core to sample, Walter Lamle with Devon Energy for approving selected portions of this thesis to be presented at the technical conferences I attended, and Brent Johnson with OSU Laboratories at Venture One for helping me image my conodont element collection with the scanning election microscope. I also especially thank Dr. Walter Manger at the University of Arkansas–Fayetteville for the ideas and advice he gave me relative to my thesis during a field trip he led on Mississippian outcrops of the western Ozark Mountains in the spring of 2016, Dr. Phil Heckel at the University of Iowa for brainstorming ideas with me to explain my conodont recoveries during one of his visits to the University, and Dr. Scott Ritter at Brigham Young University–Provo for first introducing me to conodonts during my undergraduate years and for giving me some good advice and references to use in my thesis work. I also especially recognize my Graduate Advisor Dr. Mohamed Abdelsalam and the staff with the Boone Pickens School of Geology for handling all my graduate employment affairs and Dr. Eliot Atekwana for helping edit an early draft of this thesis.

I thank Devon Energy, the Oklahoma Geological Foundation, the Oklahoma Energy Resources Board, and Oklahoma State University for providing their financial support to this project. I could not have conducted my research without their help.

Most of all, I thank my family for their support while I worked on completing the requirements for the Degree of Master of Science in Geology at the University. I owe the most to my amazing wife, Emily, who has done so much to help care for our family during this time. I also thank my parents, sister, grandparents, and wife's parents for their moral support.

Name: JOHN EDWARD HUNT

Date of Degree: DECEMBER, 2017

Title of Study: CONODONT BIOSTRATIGRAPHY IN MIDDLE OSAGEAN TO UPPER CHESTERIAN STRATA, NORTH-CENTRAL OKLAHOMA, U.S.A.

Major Field: GEOLOGY

Abstract: The informally known “Mississippian Limestone” stratigraphic interval in north-central Oklahoma, U.S.A. bears no chronostratigraphic markers and has no formally established biostratigraphic framework to date. Conodonts collected from four “Mississippian Limestone” cores in Logan, Payne, and Lincoln Counties provide the means for better constraining the stratigraphic age of the interval over the area studied. Conodont extraction was conducted by acid digestion of whole-rock samples and heavy liquid density separation after which conodont genera and species types were identified from scanning electron microscopy. Biostratigraphically significant conodonts recovered in combination with chemostratigraphic work by Dupont (2016) and earlier studies by Thornton (1958), Curtis and Chaplin (1959), McDuffie (1959), Rowland (1964), Selk and Ciriacks (1968), and Harris (1975) indicate the “Mississippian Limestone” ranges from middle Osagean to late Chesterian in age. In general, conodont element recoveries were too low in quantity and too poor of quality for use as biostratigraphic markers. The relatively low recovery and poor preservation quality of the conodont elements are attributed primarily to the elements being reworked soon after deposition by frequent storms on a mid- to outer-ramp environment in a low-latitude carbonate ramp setting. The results of this investigation are most significant in that they help place Mississippian deposition over the area studied within the context of a global Carboniferous stratigraphy. The results also allow for the Mississippian interval in the study area to be more accurately related to time-correlative strata with similar or better age constraint for constructing more temporally meaningful depositional models of the Oklahoma basin.

TABLE OF CONTENTS

Chapter Page

LIST OF TABLES

Table Page

LIST OF FIGURES

Figure Page

CHAPTER I

FRONT MATTER

Definition of the Term "Mississippian Limestone"

The term "Mississippian Limestone" informally describes the gross Mississippian stratigraphy of the U.S. Mid-Continent. In most cases, the informal name is applied by necessity in areas where the Mississippian interval lacks age-constraint, thereby preventing it from being more formally subdivided. For example, the Mississippian interval over north-central Oklahoma was determined to be Mississippian in age based on interpretative regional-scale well-to-well cross sections and geologic mapping that revealed its coeval relationship to surrounding age-constrained Mississippian strata (e.g., Selk and Ciriacks, 1969). Where the Mississippian interval is age-constrained, formalized time-stratigraphic and lithostratigraphic names are applied to it, such as in the Ozarks region (e.g., Mazzullo et al., 2013). In the petroleum industry, the informal name "Mississippian Limestone" has been important for establishing common terminology that identifies Mississippian oil and gas reservoirs which are difficult to correlate consistently and name properly based on their lithologic descriptions and log characters alone and that do not fit the industry's other named Mississippian play concepts, such as the "Mississippian Chat". The industry's usage of the term "Mississippian Limestone" has

also been important for defining the extents of the unconventional “Mississippian Limestone” Play.

In general, “Mississippian Limestone” strata consist of cyclically stacked carbonate-siliciclastic units that have wedge-like depositional geometries (e.g., Mazzullo et al., 2009; LeBlanc, 2014; Jaeckel, 2016) and were deposited on a broad carbonate shelf to ramp environment across major regions of Oklahoma, Kansas, and Texas as well as parts of Arkansas and New Mexico (Gutschick and Sandberg, 1983). Unconventional petroleum reservoir facies of the Mississippian interval in south-central Kansas and north-central Oklahoma have been shown to have 2-3% average porosity and 0.080 mD average permeability (LeBlanc, 2014; Jaeckel, 2016). In addition, stratigraphic relationships have been shown to be very complex (e.g., Boardman et al., 2010; 2013), and they remain poorly constrained throughout much of Kansas and Oklahoma (Mazzullo et al., 2016). Therefore, new evidence that better constrains the geologic age of the Mississippian interval in areas where it is needed is crucial for more accurately correlating and naming its lithologic units and for identifying any major time-stratigraphic patterns in its distribution of oil and gas reservoir facies.

Recent Developments in the "Mississippian Limestone" Play

Within the last decade, significant advances in horizontal drilling and hydraulic fracturing techniques have made producing oil and gas from unconventional reservoirs financially competitive in the global energy market (Perry, 2014; U.S. Energy Information Administration, 2016). The “Mississippian Limestone” Play is just one example of many where new technology revitalized production in conventionally

depleted reservoirs and newly recognized tight reservoir complexes of the Mississippian (Charpentier et al., 1996; Shale Daily, 2015) (Figure 1).

Activity in the "Mississippian Limestone" Play began in 2007 when SandRidge Energy drilled its first Mississippian horizontal well in Woods County, Oklahoma (Shale Daily, 2015). The main area of renewed interest in Mississippian age reservoirs has been in south-central Kansas and north-central Oklahoma where conventional production was historically centered (Harris, 1975). Oil and gas companies' central motives for acquiring "Mississippian Limestone" assets have been that (1) drilling costs are relatively low, with the average well costing around $3 million (as of 2015) because of the shallow nature of the play (Shale Daily, 2015); and (2) extensive well data in and published literature on the Mississippian interval exists from over 50 years of industry drilling and academic study that has helped to quickly develop reservoir models and identify drilling targets.

To date, attempts to unconventionally produce the "Mississippian Limestone" have been significant, but the play itself has generally proven to be less prolific, more complicated, and much higher risk than the industry anticipated (Shale Daily, 2015). The central problems associated with "Mississippian Limestone" reservoir complexes are that (1) they frequently exhibit a high degree of lateral and vertical facies heterogeneity, making successfully tracking reservoirs in lateral drilling operations very difficult and (2) Mississippian wells tend to produce large volumes of formation water (e.g., a 1:10 oil-water cut in a single well is typical and a 1:50 oil-water cut is not unusual) (Shale Daily, 2015; Ray, 2016), which is expensive for companies to either treat or inject back into the subsurface. More recently, injection of formation water into the deep subsurface has become a publicly controversial topic because of its link to induced seismicity (Andrews

and Holland, 2015). In combination with low oil prices persisting well into 2017 since their sharp decline at the end of 2014 (McMahon, 2015) these factors have made it difficult to profit from the play, and so the petroleum industry has largely turned away from their "Mississippian Limestone" assets within the last few years. Devon Energy, for example, divested its Mississippian assets in Logan and Payne Counties, Oklahoma in 2016 (Monies, 2016).

Update on Mississippian Consortium Studies

Despite its challenges, several oil and gas companies have looked to make the "Mississippian Limestone" Play work for them by turning to consortium research. For example, in November 2012 thirteen companies teamed up with researchers at Oklahoma State University (OSU) to form the Industry-OSU Mississippian Consortium (Milam, 2013). The consortium's goals were to (1) develop high-resolution stratigraphic frameworks and depositional models; (2) analyze petrophysics; and (3) characterize reservoir types and geometries in the "Mississippian Limestone" Play area across Oklahoma and Kansas and adjacent areas of Missouri and Arkansas for the central purpose of sharing the research results with each other to better manage the risks associated with operating in the play (Milam, 2013).

To date, researchers at OSU have conducted 20 investigations in the "Mississippian Limestone", fifteen of which have been completed (including this study), in fulfillment of the consortium's goals. Figure 2 shows the geographic extent of the area studied by the consortium and where core/outcrop control exists for these studies. Several authors working outside the consortium have also published on the "Mississippian Limestone" since the time of renewed interest in the play (e.g., Mazzullo et al., 2009,

2011ab, 2013, 2016; Boardman, 2010, 2011, 2013; Wilhite et al., 2011; Farzaneh, 2012; Manger, 2012, 2014; Shoeia, 2012; Dowdell, 2013; Haynes, 2013; Matson, 2013; Unrast, 2013; Cahill, 2014; Jennings, 2014; Martin, 2015; Watney, 2015; Steinmann et al., 2017).

All prior studies conducted by the Mississippian consortium and others have helped the petroleum industry to increase its understanding of "Mississippian Limestone" deposition as it applies to reservoir quality and distribution. Nevertheless, the petroleum industry overall continues to pull its investments from the "Mississippian Limestone" Play. One major reason for the trend in divestiture is geoscientists have largely come to a consensus within the last year that wastewater injection is the central mechanism for the increased seismicity within the State of Oklahoma (Oklahoma Corporation Commission, 2017), leading the Oklahoma Corporation Commission to increase regulations on wastewater injection practices and thereby deterring the industry from wanting to operate in high water-producing reservoirs like those of the "Mississippian Limestone" Play. Currently, studies in "Mississippian Limestone" strata are most important to oil and gas companies that continue to operate in the "Mississippian Limestone" Play, such as Midstates Petroleum, White Star Petroleum, Chesapeake Energy, and SandRidge Energy because they have the greatest need for the research results. There also remains a wider interest in the industry for "Mississippian Limestone" studies to be conducted because research observations from these studies can be compared with and used as analogs in other plays of the U.S. Mid-Continent where time-correlative Mississippian reservoirs are represented, such as the STACK and SCOOP Play areas (Figure 1).

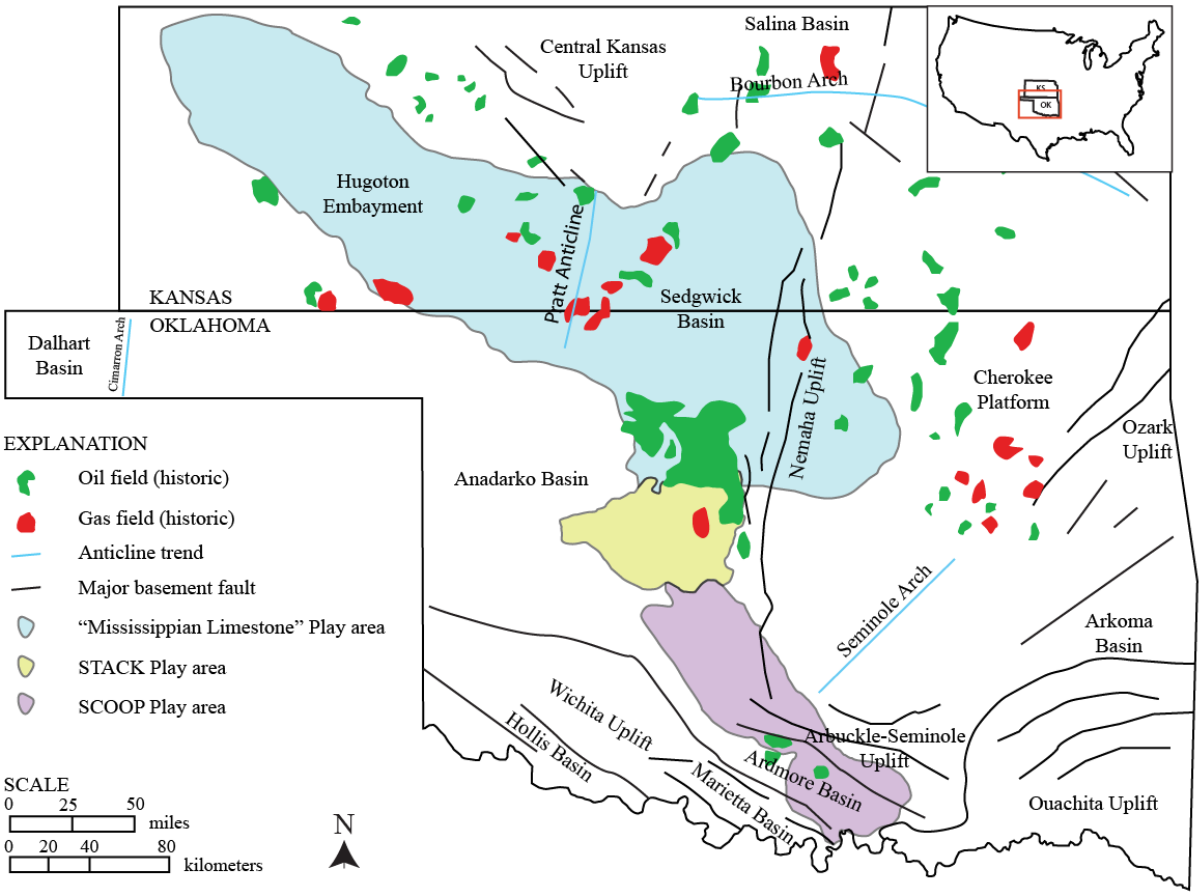

Figure 1. Map of southern Kansas and Oklahoma showing the relative locations (and names, when applicable) of major tectonic features as well as historic and current play areas involving Mississippian age reservoirs. Inset map shows the United States (lower forty-eight), with the States of Kansas and Oklahoma outlined in black and the area outlined in red represented in the enlarged figure. State lines were obtained from the Oklahoma State University Library's McCasland Map Collection (MAP ID: G4020 1975). Selected historical oil and gas field data were obtained from Harris (1975). Structural data were compiled from Northcutt and Campbell (1996) and Doll (2015, fig. 1 and references therein). "Mississippian Limestone", STACK, and SCOOP Play boundaries were estimated by compiling several maps published online (e.g., maps by Shale Experts, Wood McKenzie, and Newfield Exploration Company).

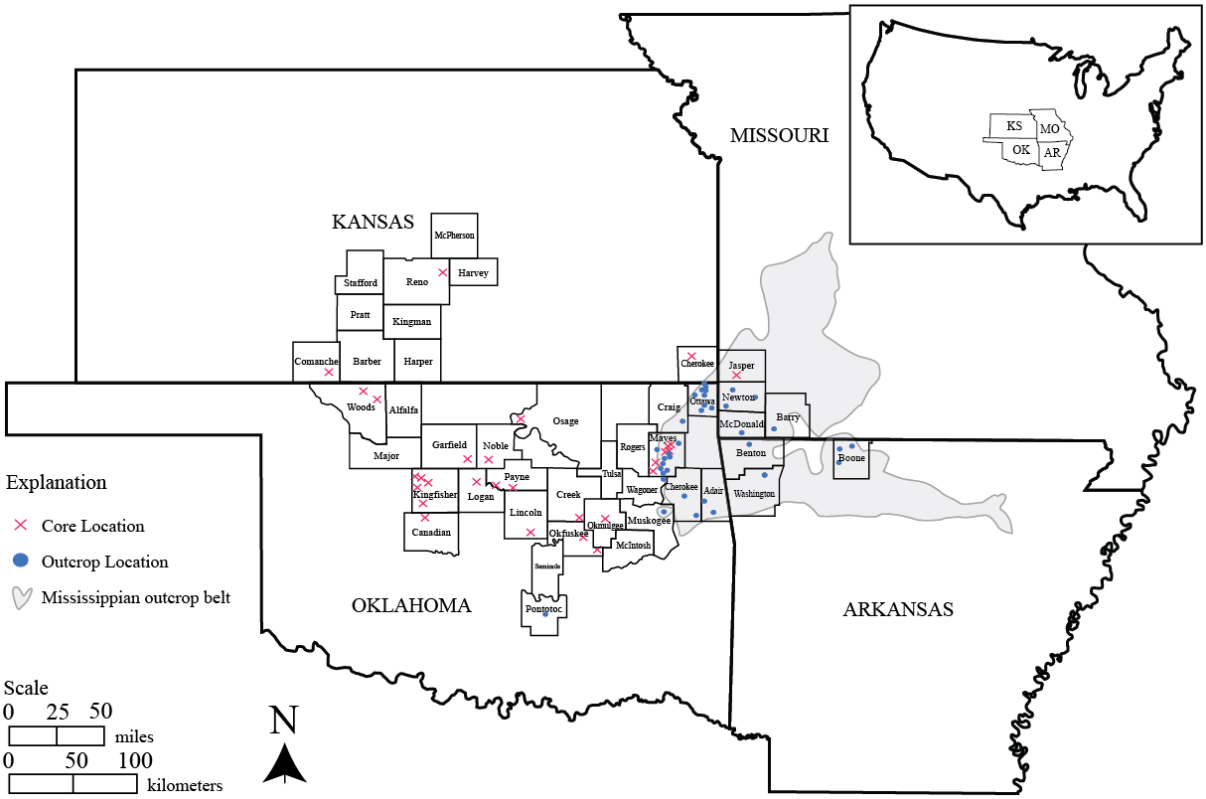

Figure 2. Map of Kansas, Oklahoma, Missouri, and Arkansas of the United States showing the main areas of investigation by the Industry-Oklahoma State University Mississippian Consortium within “Mississippian Limestone” rocks and their outcrop equivalents. Inset map shows the United States (lower forty-eight), with the state boundaries of Kansas, Oklahoma, Missouri, and Arkansas outlined in black and represented in the enlarged figure. State and county lines were obtained from the Oklahoma State University Library’s McCasland Map Collection (Map ID: G4020 1975). The simplified outline of the informally known Mississippian outcrop belt was patterned after Mazzullo et al. (2011a). Points of outcrop and core control were compiled onto this map with permission from all past and current OSU consortium researchers.

CHAPTER II

INTRODUCTION

Warrant for this Investigation

The emphasis of studies conducted by the Industry-OSU Mississippian Consortium to date has overwhelmingly been to describe the lithostratigraphy (lithofacies) of the "Mississippian Limestone" interval over southern Kansas and northern Oklahoma and in the adjacent tristate region and then place those descriptions within a sequence stratigraphic framework for better prediction of its stratigraphic distribution of oil and gas reservoir facies (Bertalott, 2014; LeBlanc, 2014; Price, 2014; Childress, 2015; Doll, 2015; Flinton, 2016; Jaeckel, 2016; Shelley, 2016). The focus of the most recent and on-going studies from the consortium is to construct regional scale maps and stratigraphic models over much of the same area for furthering understanding Oklahoma basin evolution and its depositional geometry/architecture as well as for showing large-scale trends in reservoir facies of the "Mississippian Limestone" Play (e.g., Appleseth, 2017; Elium et al., 2017; Hill, 2017; Gao and Wang, 2017).

To date, there have only been two conodont biostratigraphic analyses conducted (Miller, 2015; Godwin, 2017) and one study that attempted to apply age-dates to the Mississippian interval based on chemostratigraphic concepts (Dupont, 2016). This means

that temporal constraint for the Mississippian interval over the consortium's area of focus is almost exclusively limited to sequence stratigraphic concepts that do not directly relate rocks to the chronostratigraphic record. Placing the "Mississippian Limestone" interval within a chronostratigraphic framework is critical for establishing temporally meaningful sequence stratigraphic interpretations and depositional models that can be expanded to places where they are needed, such as in north-central Oklahoma.

No chronostratigraphic markers are known within the "Mississippian Limestone" of the U.S. Mid-Continent. As such, biostratigraphy is the method of choice for relating the Mississippian interval to the chronostratigraphic record. More specifically, conodont biostratigraphy is the method of choice for age-dating the Mississippian interval of the U.S. Mid-Continent, as this fossil group has been extensively studied and shown to have the best correlation potential for the region (e.g., Roundy, 1926; Gunnell, 1931; Branson and Mehl, 1933, 1938, 1941ab; Youngquist and Miller, 1949; Youngquist et al., 1950; Branson, 1959; Pinney, 1962; Collinson et al., 1962; 1970; Thompson and Goebel, 1963, 1968; Lane, 1967, 1974; Canis, 1968; Thompson and Fellows, 1970; Lane and Straka, 1974; Branch, 1988; Poole and Sandberg, 1991; Lane and Brenkle, 2005; Mazzullo et al., 2011b; Boardman et al., 2013; Miller, 2015; Godwin, 2017).

Other index fossil groups of the Mississippian Subsystem include brachiopods and crinoids, both of which are generally abundant in Mississippian rocks of the U.S. Mid-Continent (e.g., Lauden, 1948; Weller et al., 1948); however, both groups tend to lack the correlation potential and relatively high-resolution age-dates that conodonts provide, and both are extremely difficult to study from core. Ammonoids and foraminifera are two other index fossil groups and both are commonly used today for

age-dating Mississippian age strata because they provide relatively high-resolution age-dates relative to conodonts (Gradstein et al., 2012). However, both ammonoids and foraminifera are relatively rare in Mississippian strata over northern Oklahoma and southern Kansas (Gutschick et al., 1961) for reasons that are poorly understood. Therefore, conodonts are the most attractive of all the index fossil groups to merit biostratigraphic investigation because of the relatively high age-date resolutions they provide, their high correlation potential, and the relatively small size of individual specimens that increases their expected abundance in core.

No study to date has yielded any formalized biostratigraphic results for age-dating the "Mississippian Limestone" in north-central Oklahoma. LeBlanc (2014) developed a sequence stratigraphic framework for the "Mississippian Limestone" interval in Payne and Logan Counties from three cores, which Dupont (2016) partly reinterpreted using results from her chemostratigraphic work conducted in the same cores, and Hill (2017) has developed a sequence stratigraphic framework for the Mississippian interval from core in Lincoln County. Therefore, the opportunity arises to study the conodont biostratigraphy of the Mississippian interval in north-central Oklahoma contained in these four cores for the central purposes of (1) age-dating the interval preserved in each of the cores; (2) evaluating the work that has been done on them up to this point that relate them to the temporal domain; and (3) observing to what degree the new biostratigraphic evidence adds value to prior interpretations of the cores.

Problem Statement

The informally known “Mississippian Limestone” stratigraphic interval of Payne, Logan, and Lincoln Counties, north-central Oklahoma, U.S.A. bears no chronostratigraphic markers and has no formally established biostratigraphic framework to date. As such, it is uncertain how stratigraphic frameworks and depositional models for the Mississippian section proposed by LeBlanc (2014) and Dupont (2016) in Payne and Logan Counties and Hill (2017) in Lincoln County temporally relate to those developed in surrounding localities by the Industry-OSU Mississippian Consortium (e.g., Bertalott, 2014; Price, 2014; Jaeckel, 2016; Shelley, 2016) and to Mississippian strata in surrounding areas with age-constraint (e.g., Boardman et al., 2013; Godwin, 2017). Thus, until now the consortium and others have been limited in understanding the “Mississippian Limestone” over the area of study in the context of Oklahoma basin deposition as well as a global Carboniferous stratigraphy.

Purpose and Significance of Study

This study narrows the geologic age range of “Mississippian Limestone” strata in Logan, Payne, and Lincoln Counties using core-based conodont biostratigraphy. This study is most significant in that it (1) places the rocks within a global Carboniferous stratigraphy; and (2) establishes a locality for future comparison and correlation with other age-constrained Mississippian age strata.

Major Research Questions

Major research questions addressed in this study include:

1. What is the geological age range of the "Mississippian Limestone" interval in Logan, Payne, and Lincoln Counties, north-central Oklahoma, U.S.A.?
2. What were environmental and post-burial conditions like for conodonts in Mississippian rocks of north-central Oklahoma?
3. Is there some geological aspect(s) (e.g., gamma-ray signature, facies type, or sequence stratigraphic boundary) that predict(s) where higher conodont recoveries and preservation quality occur?
4. Is there evidence for provincialism among conodonts in the cores?
5. Do recovered conodonts identify or help constrain unconformities in the cores?
6. Can an improved lithostratigraphic nomenclature be applied to the Mississippian interval over the area of interest from the results of this investigation?
7. Do the prior chemostratigraphic and sequence stratigraphic attempts to constrain the geologic age of the "Mississippian Limestone" interval in north-central Oklahoma adequately describe its age ranges, and how do conodonts change/improve that understanding?

Hypothesis and Objectives

The hypothesis for this investigation was that conodonts–marine index microfossils capable of temporally resolving up to third-order depositional sequences (Uyeda et al., 2011; Gradstein et al., 2012), or about one million years in Mississippian age rocks of the U.S. Mid-Continent (Boardman et al., 2013; Godwin, 2017) –

demonstrate by associated geological age ranges of recovered species that the cored Mississippian intervals in Logan, Payne, and Lincoln Counties of Oklahoma are Osagean to Chesterian in age. This hypothesis is based on investigative work by Thornton (1958), Curtis and Chaplin (1959), McDuffie (1959), Rowland (1964), Selk and Ciriacks (1968), and Harris (1975) in which they propose the age of the Mississippian interval of north-central Oklahoma east of the Nemaha Uplift, south of the Kansas border, and to an area about 20 mi. (32 km) north of the study area ranges from Osagean to Chesterian in age (discussed in chapter 4). Their interpretations were based on core descriptions and log correlations of Mississippian strata over the area of interest, with very sparse biostratigraphic control available to them (Thornton, 1958; Curtis and Chaplin, 1959; McDuffie, 1959; Rowland, 1964; Selk and Ciriacks, 1968; Harris, 1975).

The research objectives that test this investigation's hypothesis are to (1) use conodonts to construct a biostratigraphic framework for the "Mississippian Limestone" in the study cores and (2) relate the biostratigraphic framework to the stratigraphic frameworks already established over the area of interest.

Core Locations and Descriptions

Drilling operations carried out by Devon Energy from 2011 to 2012 provided the cores and wireline logs for this study. Wireline logs and production information for the cored wells are available publicly through the Oklahoma Well Log Library on the Oklahoma Corporation Commission's website. Full descriptions of the cores and their depositional environment interpretations are available from LeBlanc (2014) and Hill (2017). Figures 3a and 3b provide the gamma-ray log signature and lithofacies

classifications for each of the cores and Figure 4 shows where they are positioned relative to one another.

Described from west to east, the names and locations of the cores are the Adkisson 1-33, drilled in 2012 in Logan County (36°04'24" N, 97°31'24" W, API #08323988), the Winney 1-8, drilled in 2012 in Payne County (36°03'26" N, 97°19'37" W, API #11923904), and the Elinore 1-18, drilled in 2011 in Payne County (36°01'46" N, 97°01'02" W, API #11923896). Nearly 32 mi. (51 km) due south of the Elinore 1-18, is the Doberman 1-25, drilled in 2012 in Lincoln County (35°59'39" N, 96°98'17" W, API #08124112). Distance from the Adkisson 1-33 to Winney 1-8, Winney 1-8 to Elinore 1-18, and Elinore 1-18 to Doberman 1-25 are 11.1 mi. (17.8 km), 17.4 mi. (28.0 km), and 31.4 mi. (50.5 km), respectively. Each of the cores is 4 in. in diameter and captures what has been preserved of the "Mississippian Limestone" stratigraphic interval from top to base. Thickness of the preserved Mississippian interval in each of the cores is about 324 ft. (99 m) in the Adkisson 1-33, 190 ft. (58 m) in the Winney 1-8, 143 ft. (44 m) in the Elinore 1-18, and 234 ft. (71 m) in the Doberman 1-25. LeBlanc's (2014) core descriptions indicate the Adkisson 1-33, Winney 1-8, and Elinore 1-18 were deposited largely within a mid-ramp to distal ramp crest environment, and Hill's (2017) indicate The Doberman 1-25 was deposited more within a mid-ramp to distal outer ramp environment.

In cross section, the Adkisson 1-33, Winney 1-8, and Elinore 1-18 sample the Mississippian interval in a more-or-less paleostrike direction. LeBlanc (2014) attributed the 181 ft. (55 m) difference in thickness between the Adkisson 1-33 and Elinore 1-18 over the 28.5 mi. (46 km) over which they are separated to syndepositional faulting.

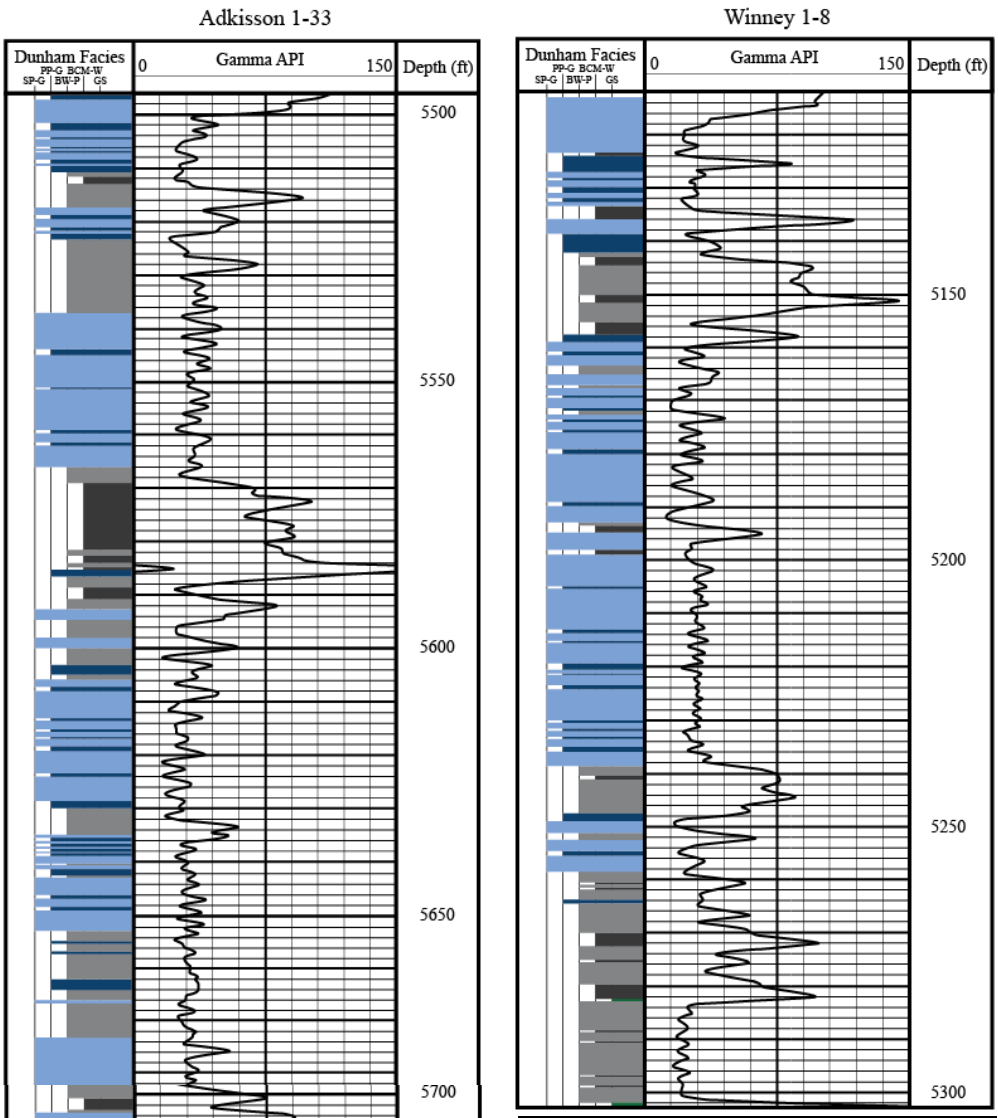

LITHOFACIES EXPLANATION	
	Dunham Facies
SP-G	Skeletal Packstone-Grainstone
PP-G	Peloidal Packstone-Grainstone
BW-P	Bioturbated Wackestone-Packstone
BCM-W	Burrowed Calcareous Mudstone-Wackestone
GS	Glauconitic Sandstone

Figure 3a. Gamma-ray curves and lithofacies types for the Adkisson 1-33 and Winney 1-8 cores. Refer to LeBlanc (2014) for full core descriptions.

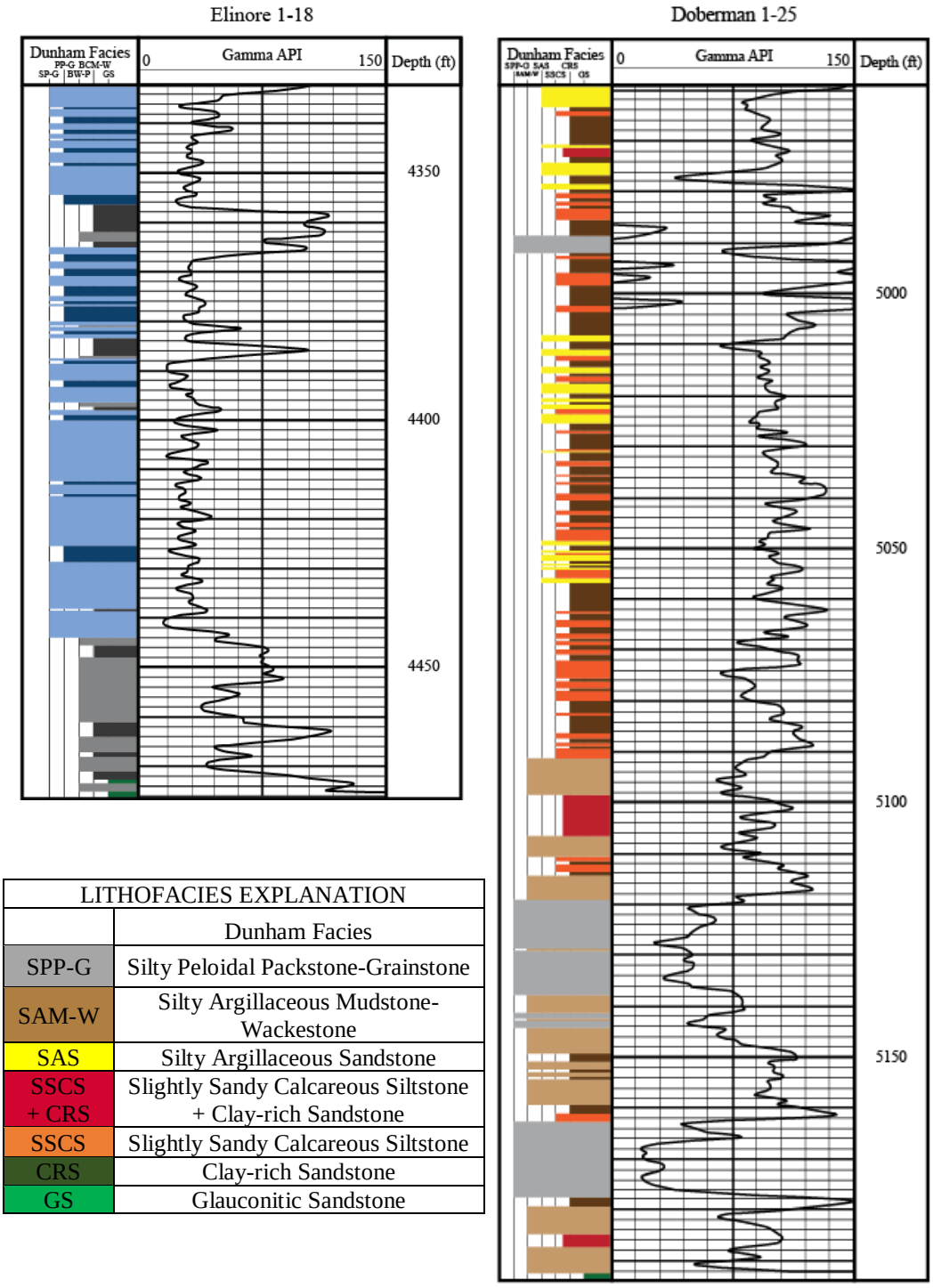

LITHOFACIES EXPLANATION	
	Dunham Facies
SPP-G	Silty Peloidal Packstone-Grainstone
SAM-W	Silty Argillaceous Mudstone-Wackestone
SAS	Silty Argillaceous Sandstone
SSCS + CRS	Slightly Sandy Calcareous Siltstone + Clay-rich Sandstone
SSCS	Slightly Sandy Calcareous Siltstone
CRS	Clay-rich Sandstone
GS	Glauconitic Sandstone

Figure 3b. Gamma-ray curves and lithofacies types of the Elinore 1-18 and Doberman 1-25 cores. See Figure 3a for lithofacies explanation of the Elinore 1-18. Refer to LeBlanc (2014) for full core description of the Elinore 1-18 and Hill (2017) for full core description of the Doberman 1-25.

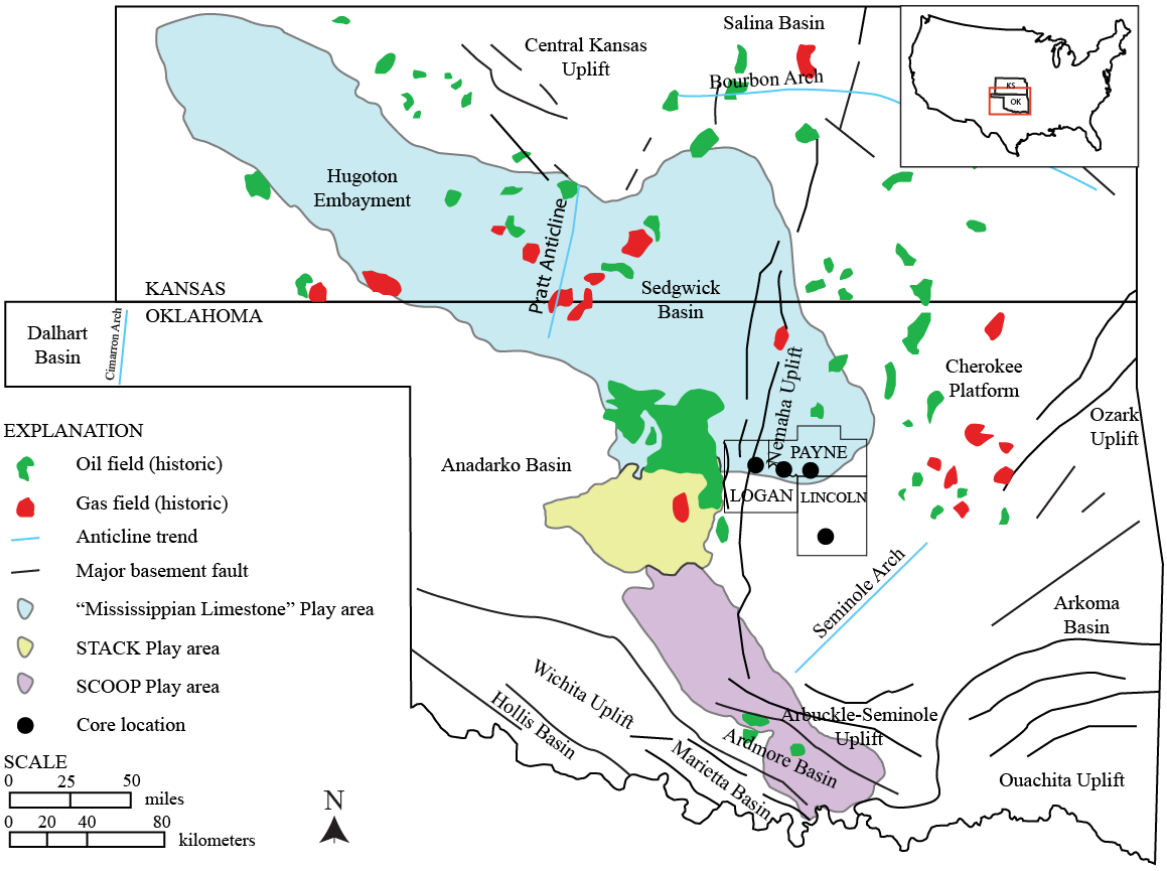

Figure 4. Map of southern Kansas and Oklahoma showing major tectonic features of the region as well as major historic and recent areas of focus in oil and gas exploration/production from Mississippian reservoirs. The geographic locations of the four cores in this study, with the counties in which they were drilled also indicated. Source data for Figure 4 same as Figure 1. Core locations were posted on the map using latitude-longitude coordinates.

CHAPTER III

GEOLOGIC SETTING

Mississippian Depositional Cyclicity in the U.S. Mid-Continent

The Mississippian Subperiod spanned from about 358.9 to 323.2 ±0.4 million years ago, totaling 35.7 million years (Gradstein et al., 2012). Mississippian strata in North America are part of the Kaskaskia (first order) megasequence (Sloss, 1963), and the Industry-OSU Mississippian Consortium has shown through detailed high-resolution sequence stratigraphic analyses that the "Mississippian Limestone" interval in the U.S. Mid-Continent is part of at least one dominantly regressive (second order) supersequence (e.g., LeBlanc, 2014; Price, 2014; Jaeckel, 2016; Shelley, 2016; Godwin, 2017). The consortium's observation that the Mississippian interval contains just one supersequence is consistent with Haq and Schutter's (2008) global interpretation of Mississippian cyclicity (Figure 5). However, given the lack of chronostratigraphic control for the Mississippian interval over the consortium's area of focus and for the basin in general, it is impossible to determine the exact number of supersequences represented without first identifying and analyzing a complete (or composite) section in the basin.

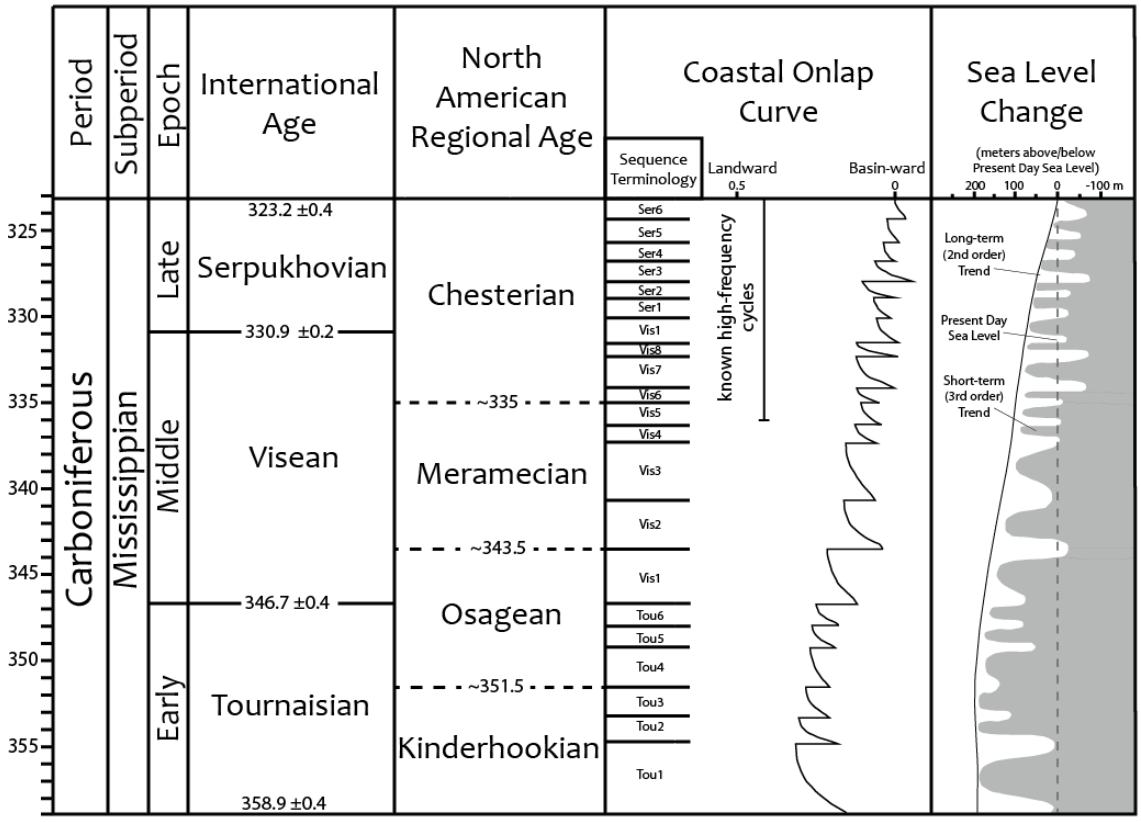

Figure 5. Coastal onlap curve for the Mississippian Subperiod. Age-dates from Gradstein et al. (2012). Coastal onlap and sea level change curves have been modified from Haq and Schutter (2008) to fit the updated geologic time scale by Gradstein et al. (2012). Sequence terminologies were compiled from Snedden and Liu (2010, 2011). Figure after Haq and Schutter (2008).

Distally-steepened Carbonate Ramp Model

Researchers with the Industry-OSU Mississippian Consortium were not the first to suggest that the character of sedimentary deposits within the Oklahoma basin is best represented with a carbonate ramp model (e.g., Handford, 1995; Franseen, 2006; Mazzullo et al., 2009). However, consortium studies were the first to suggest that the depositional setting of the Oklahoma basin across major regions of southern Kansas and northern Oklahoma can be even further classified as a distally-steepened carbonate ramp (Figure 6), per definition of the model in the literature (e.g., Read, 1982, 1985; Burchette and Wright, 1992). Key observations that supported this interpretation include the geometry of Mississippian deposits over southern Kansas and northern Oklahoma (e.g., LeBlanc, 2014; Price, 2014; Doll, 2015; Jaeckel, 2016) and presence of debris flows observed on the mid-ramp environment in the western Ozarks region (Childress, 2015).

Applying the distally-steepened carbonate ramp model in the Oklahoma basin has principally helped the consortium explain the high degree of vertical and lateral heterogeneity of lithofacies observed, especially at reservoir scales. Table 1 shows how relative sea level amplitude fluctuates based on several geologic factors acting over various time scales and illustrates why shallow-sloping carbonate ramp environments experience wide shifts in the lateral and vertical juxtapositions of their lithofacies as changes in relative sea level occur. The distally-steepened carbonate ramp model has also helped to explain the geometry of Oklahoma basin deposits, which is characterized by generally prograding carbonate-siliciclastic “wedges” or clinoforms (Figure 7) that are best observed by using interpreted third-order depositional sequence boundaries of the Mississippian interval (e.g., Doll, 2015). Conodont biostratigraphic analyses have shown

that these Mississippian clinoforms are sometimes diachronous (e.g., Boardman et al., 2010, 2013; Shoeia, 2012; Miller, 2015; Godwin, 2017), thereby illustrating the need for more biostratigraphic control in “Mississippian Limestone” strata.

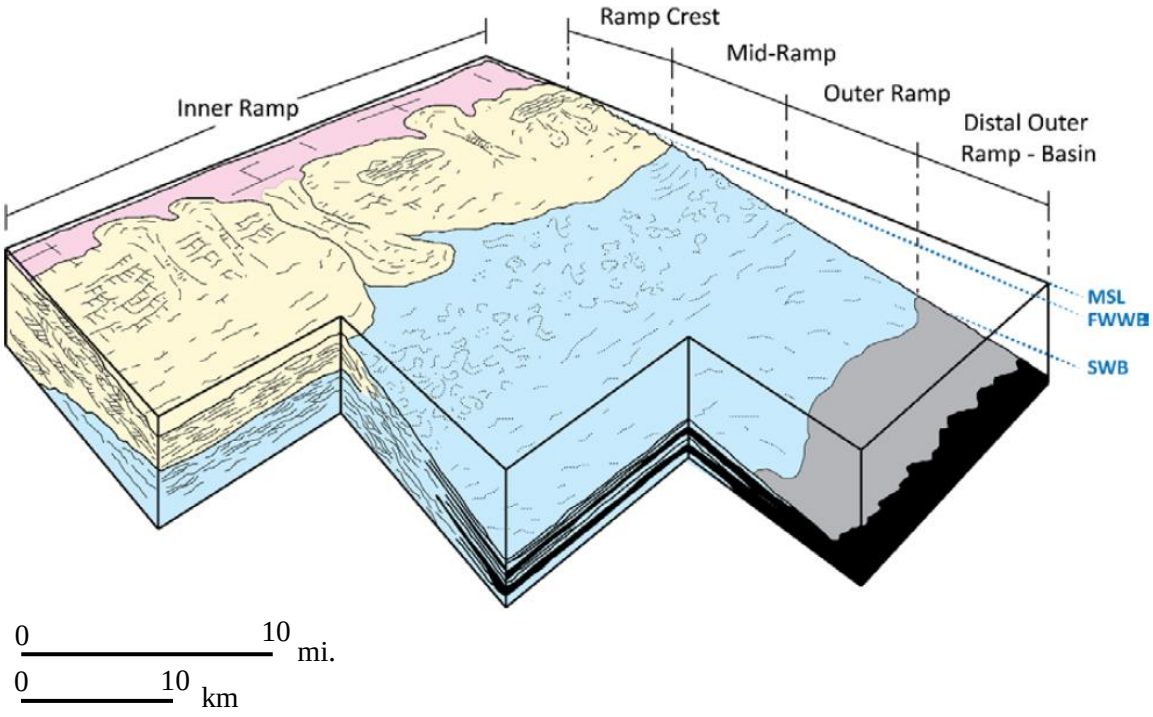

Figure 6. Conceptual block diagram of a distally-steepened carbonate ramp. Approximate locations of mean sea level (MSL), fair weather wave-base (FWWB), and storm wave-base (SWB) are given. Study cores primarily contain facies characteristic of a mid- to outer-ramp environment. Redrafted by LeBlanc (2014) after Handford (1986).

Table 1. Sequence stratigraphic hierarchy chart. Note that it is currently unclear what combination of mechanisms drive sea level rise/fall for third order depositional sequences. Data set compiled from Ross and Ross (1987ab), Kerans and Tinker (1997), and Miall (2013). Table re-drafted from Childress (2015).

Sequence Stratigraphy Hierarchy Chart					
Tectono-Eustatic Cycle Order	Sequence Stratigraphic Unit	Duration (My)	Relative Sea Level Amplitude ft (m)	Relative Sea Level Rise/Fall Rate in/ky (cm/ky)	Major Control(s) on Sea Level Rise/Fall
First	Megasequence, or Supersequence Set, or Megacycle	200 – 400	n/a	<0.4 (< 1)	Tectonics (i.e., Wilson Cyclicity)
Second	Supersequence, or Supercycle	10 – 100	164 – 328 (50 – 100)	0.4 – 1 (1 – 3)	Tectonics, Ocean Floor Spreading, and Global Ice Volume
Third	Depositional Sequence, or Composite Sequence	1 – 10	164 – 328 (50 – 100)	0.4 – 4 (1 – 10)	Tectonics and Continental Ice Volume?
Fourth	High-frequency Sequence, Parasequence, or Cycle Set	0.1 – 0.4	3 – 492 (1 – 150)	16 – 197 (40 – 500)	Milankovitch Cyclicty (i.e., Eccentricity)
Fifth	High-frequency Cycle, or Parasequence	0.02 – 0.04	3 – 492 (1 – 150)	24 – 280 (60 – 700)	Milankovitch Cyclicty (i.e., Obliquity and Precession)

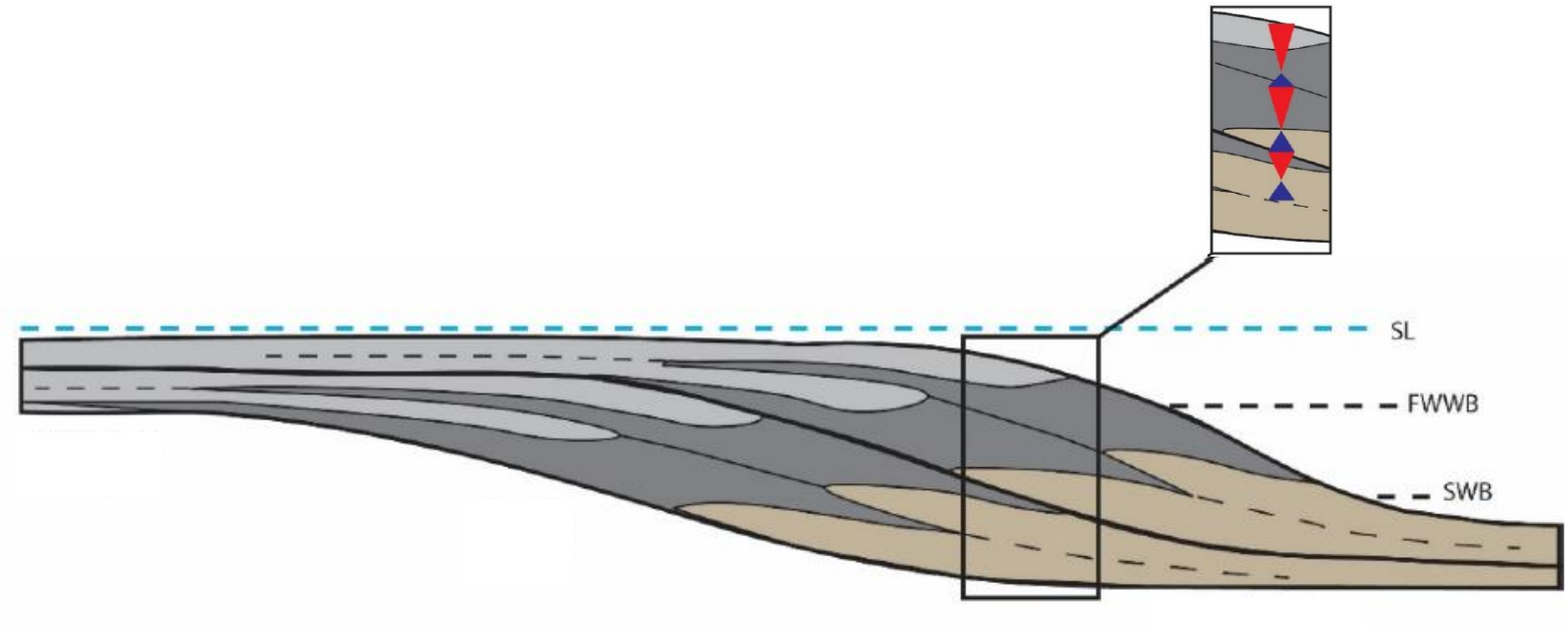

Figure 7. Conceptual diagram showing prograding clinoforms in cross section view that are characteristic of the Oklahoma basin. Grainy, high-energy lithofacies (light gray), intermediate lithofacies (dark gray), and muddy, low-energy lithofacies (tan) indicate inner-ramp, mid-ramp, and outer-ramp to basin environments, respectively. Approximate locations of mean sea level (SL), fair weather wave base (FWWB), and storm wave base (SWB) on the ramp are provided. Inset image conceptualizes a generic sequence stratigraphic stacking pattern for the clinoforms. Modified from Jaeckel (2016).

Paleoenvironmental Conditions

Figure 8 is a paleogeographic map of late Early Mississippian deposition in the U.S. Mid-Continent. The map has been modified several times by OSU consortium researchers (inclusive of this study) and is most frequently used to demonstrate that during the Mississippian Subperiod ancestral Oklahoma was positioned in a low-latitude setting and was covered by an epicontinental sea, which allowed a broad carbonate platform to ramp environment to form along the southern margin of the Transcontinental Arch in response. The name for the gross depositional setting of this marine carbonate-dominated environment is the Burlington Shelf (coined by Lane, 1978).

Figure 8 is largely based on work by Lane and DeKeyser (1980) and Gutschick and Sandberg (1983) and includes updates to the map from the consortium, but it also incorporates data from other paleoclimatic studies that reflect the current understanding of paleodepositional conditions in the late Early Mississippian over the U.S. Mid-Continent (Rowley et al., 1985; Ross and Ross, 1987a; Witzke, 1990; Golonka et al., 1994; Scotese, 1997; Mii et al., 1999). Therefore, the paleogeographic map that is presented in this thesis is one of the best visual representations of late Early Mississippian paleogeography for the U.S. Mid-Continent currently available.

A relatively limited body of literature exists for Middle to Late Mississippian strata over much of the U.S. Mid-Continent in comparison with studies for Early Mississippian stratigraphy over the same region. As such, paleogeographic maps for the Middle and Late Mississippian in the Oklahoma basin are not as robust as the one the consortium uses for Early Mississippian paleogeography. Figure 9 is one of Blakey's (2017) paleogeographic maps of the early Middle Mississippian (~345 Mya) for the

Laurussian supercontinent and northern part of Gondwana. Blakey maps are best used "in time sequence [to] show…broad patterns of Earth history" (Deep Time Maps, 2017); therefore, Figure 9 is most useful when compared with Figure 8 to highlight changes in overall depositional conditions of the U.S. Mid-Continent from the Early to Middle Mississippian. Blakey does not currently have a paleographic map of the U.S. Mid-Continent available for the Late Mississippian, nor is there one available in the literature that is representative of the major shifts in understanding Oklahoma basin deposition because of recent studies; therefore, no paleogeography map of the U.S. Mid-Continent during the Late Mississippian is presented here. Additional work is needed for creating a modern paleogeographic map of the Late Mississippian in the Oklahoma basin.

Overall, climatic conditions on the Burlington Shelf during the Early to Middle Mississippian were generally tropical to subtropical (e.g., Parrish, 1982; Witzke, 1990; Golanka et al., 1994; Scotese, 1997; Buggisch et al., 2008) and paleosea conditions were overall non-restricted (Steinmann et al., 2017). However, studies have suggested more arid, cooling, and restricted conditions were established by the early Middle Mississippian and that they became more regionally persistent during the remainder of the Mississippian Subperiod (e.g., Noble, 1993; Franseen, 2006; Buggisch et al., 2008), probably related most directly to the suture of Laurussia and Gondwana.

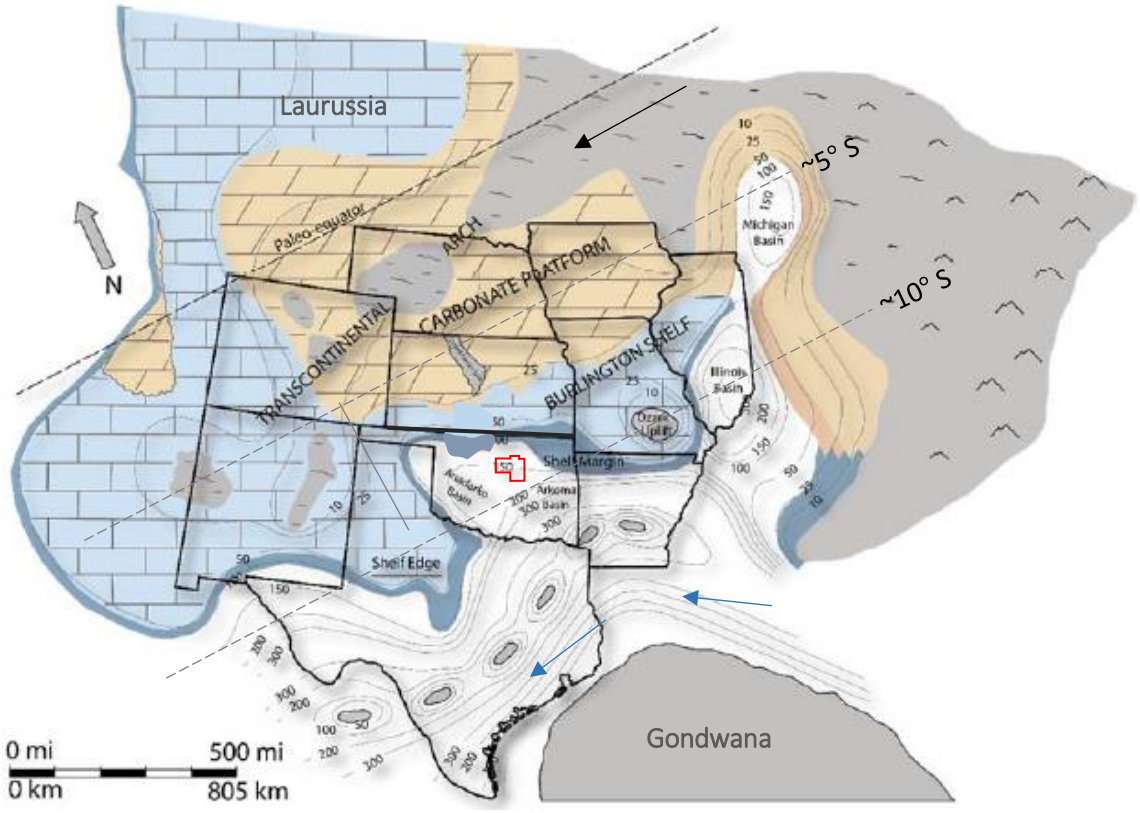

Figure 8. Paleogeographic map of the late Early Mississippian for the U.S. Mid-Continent. Map compiled from various authors' observations. Study area outlined in red. Areas of uplift (gray) and areas of dominant dolomite (tan), limestone (light blue), fine-grained (dark blue), and basin (white) facies indicated. Water depth contours in 50 m (164 ft.) intervals. Warm ocean current direction (blue arrows) from Ross and Ross (1987a) and Mii et al. (1999). Wind direction (black arrow) from Witzke (1990) and Golonka et al (1994). Lines of latitude estimated by georeferencing this figure with map data from Google Earth in ArcGIS. Figure modified from Jaeckel (2016), originally redrafted by LeBlanc (2014) after Gutschick and Sandberg (1983) and Lane and DeKeyser (1980). Compare with Figure 9.

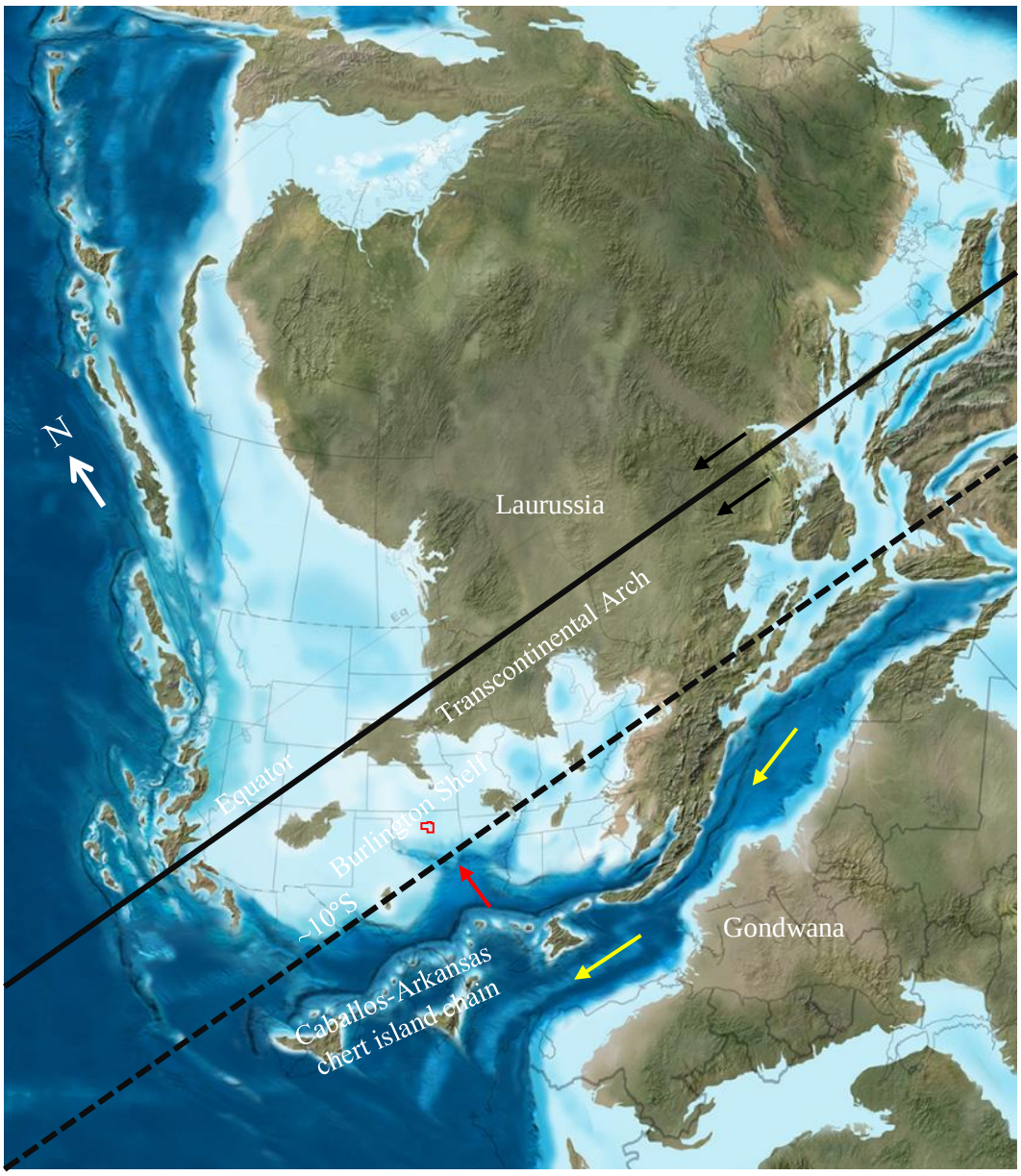

Figure 9. Paleogeographic map of ancestral North America during the early Middle Mississippian (~345 Mya). Study area outlined in red. Direction of upwelling (red arrow) from Parrish (1982). Dominant wind directions (black arrows) from Witzke (1990) and Golonka et al. (1994). Cool ocean currents (yellow arrows) inferred from Buggisch et al. (2008) and their direction from Mii et al. (1999) and Mazzullo et al. (2009). Lines of latitude estimated by scaling this figure with map data from Google Earth. Image modified from Blakey (2017). Compare with Figure 8.

Structural Background

The four cores in this study are positioned along the southwestern part of the Cherokee Platform and the eastern edge of the Nemaha Uplift Geologic Provinces in north-central Oklahoma (Charpentier et al., 1996; Johnson, 2008) (Figure 4). For a concise summary on the evolution of the geologic provinces of Oklahoma, refer to Johnson (2008). Relative to this study, just two structural elements of Oklahoma merit further discussion. They are: (1) the Nemaha Uplift and (2) the Kanoka Ridge.

Nemaha Uplift

Geoscientists have not yet arrived at a clear consensus for exactly how or when the structures of the Nemaha Uplift formed, though several models with evidence for their formation and timing have been proposed (e.g., Gay, 2003ab; McBee, 2003; Friess, 2005; Steen, 2017). Regardless of the nature and timing of faulting on the Nemaha, there is a consensus among petroleum geologists that movement along faults complicated stratigraphic relationships of the "Mississippian Limestone" by compartmentalizing oil and gas reservoirs, and in some areas of uplift, significantly or entirely eroding the Mississippian interval (Gay, 2003ab; LeBlanc, 2014; Hill, 2017). Therefore, biostratigraphic results are meaningful in that age-dates help to constrain unconformable surfaces, such as those between the Woodford-Mississippian, Mississippian-Pennsylvanian contacts, or those within the Mississippian interval (e.g., the Tournaisian-Visean contact), which may help to highlight mass extinction events or climatic changes. Future high-resolution biostratigraphic studies may also help to constrain unconformities related to the Mississippian for better narrowing the timing of faulting related to the Nemaha structure.

Kanoka Ridge

Handford (1995) was first to speculate that an east-west trending fore-bulge arch might exist somewhere in the subsurface of northern Oklahoma and Arkansas, along the northern end of the Arkoma Basin. Mazzullo et al. (2011a) followed up with Handford's (1995) speculation by demonstrating that Lower and Middle Mississippian strata in parts of southeastern Kansas and southwestern Missouri prograded northward, while the same time-correlative strata in northeastern Oklahoma and northern Arkansas prograded southward. To explain the discrepancy, the authors proposed that an Early Mississippian age structural high ran through the present-day Oklahoma-Missouri-Arkansas tristate region and along the Oklahoma-Kansas border (Mazzullo et al., 2011a). They speculated that the structural high caused sediments of the Lower and Middle Mississippian to prograde in opposite dip directions along its northern and southern flanks and proposed that the so-called east-west trending structural high would have represented the fore-bulge arch of the Arkoma Basin (Mazzullo et al., 2011a).

Suneson (2012) was first to respond to the evidence for the fore-bulge arch of the Arkoma proposed by Mazzullo et al. (2011a). He added his own observation that some Early Pennsylvanian sandstone units of the Jackfork Group in Choctaw County, Oklahoma appeared to have been sourced from the south while other units within the same group formation were sourced from the north (Suneson, 2012). This meant that if the Pennsylvanian age units were also somehow related to the same fore-bulge arch proposed by Mazzullo et al. (2011a), then the structure must have been active at least from the Early Mississippian to the Early Pennsylvanian, consistent with the overall timing of the formation of the Arkoma Basin (Suneson, 2012). Mazzullo et al. (2016)

later provided evidence for there being depositional onlap onto an east-west trending series of magnetic anomalies positioned along the Oklahoma-Kansas border and the adjacent tristate region observed in Devonian and Carboniferous age strata, demonstrating that this string of anomalies must represent an area of uplift active from sometime in the Devonian throughout most of the Carboniferous. The authors named their interpreted structural high the Kanoka Ridge (Figure 10) and claimed that it represents the missing fore-bulge arch of the Arkoma (Mazzullo et al., 2016), though not all experts in Oklahoma basin evolution fully agree with the interpretation, such as Dr. Walter Manger at the University of Arkansas–Fayetteville (personal communication, 2017).

The Kanoka Ridge is significant to any study conducted in the Oklahoma basin because it helps explain why uniform lithostratigraphic naming conventions cannot easily be applied to "Mississippian Limestone" strata when correlating the interval across the northern and southern flanks of the structure that once sustained separate depositional environments (Figure 11). The ridge further demonstrates why geoscientists must rely on biostratigraphic evidence to properly correlate rocks of the "Mississippian Limestone" from southern Kansas into northern Oklahoma, or from the Ozarks region into parts of northeastern Oklahoma. It is for this reason that Mazzullo et al. (2016) asked for conodont biostratigraphic work be conducted in the Mississippian interval across northern Oklahoma for expanding the time-stratigraphic correlations and unifying lithostratigraphic nomenclature they have previously applied to the Mississippian interval in the Ozark region (Mazzullo et al., 2013).

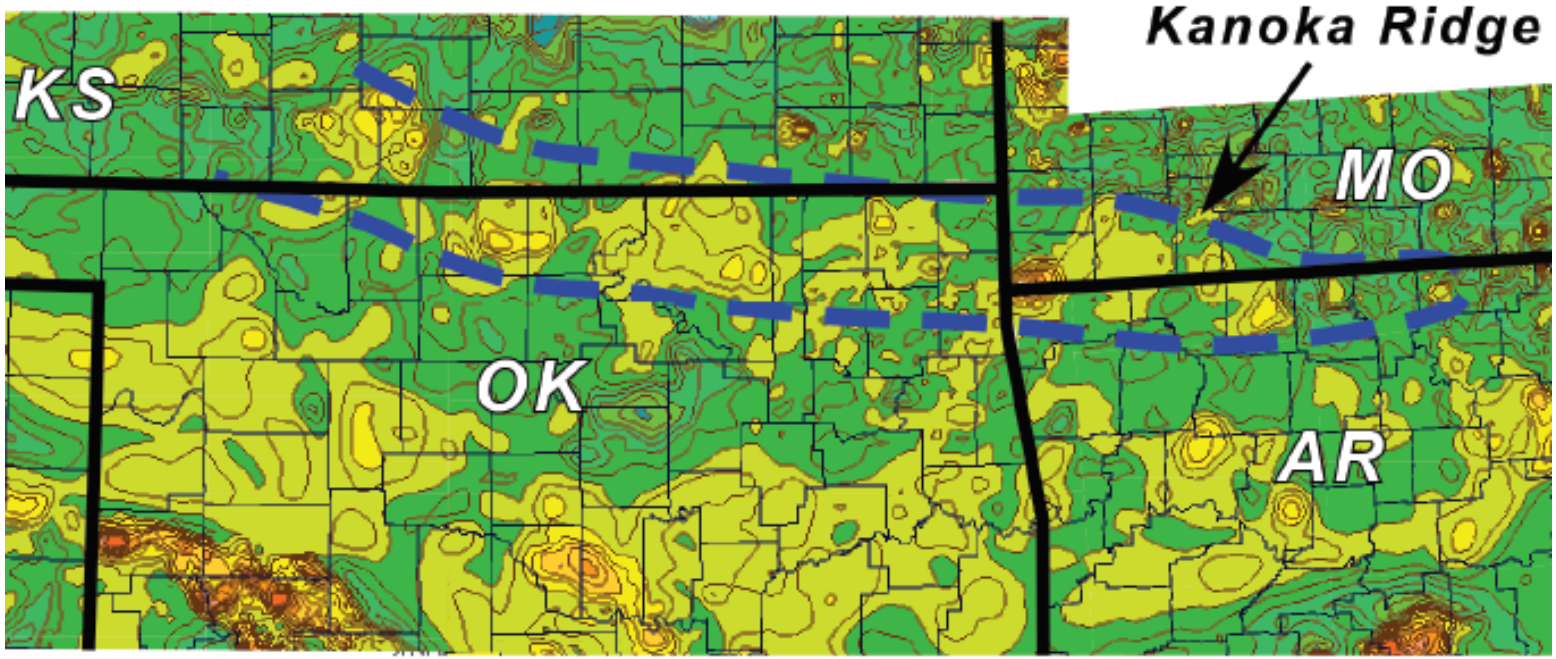

Figure 10. Magnetic anomaly map showing the approximate trend (blue dashed lines) of the Kanoka Ridge throughout parts of the Oklahoma-Missouri-Arkansas tristate region and along the Kansas-Oklahoma State line. Warmer colors in the magnetic anomaly data correspond to areas of greater magnetic susceptibility, interpreted to correlate with greater areas of uplift. Contour intervals are in 100 nT. Source data for the map can be found at https://www.uwgb.edu/dutchs/StateGephMaps/OklaGphMap.HTM. Image reproduced from Mazzullo et al. (2016).

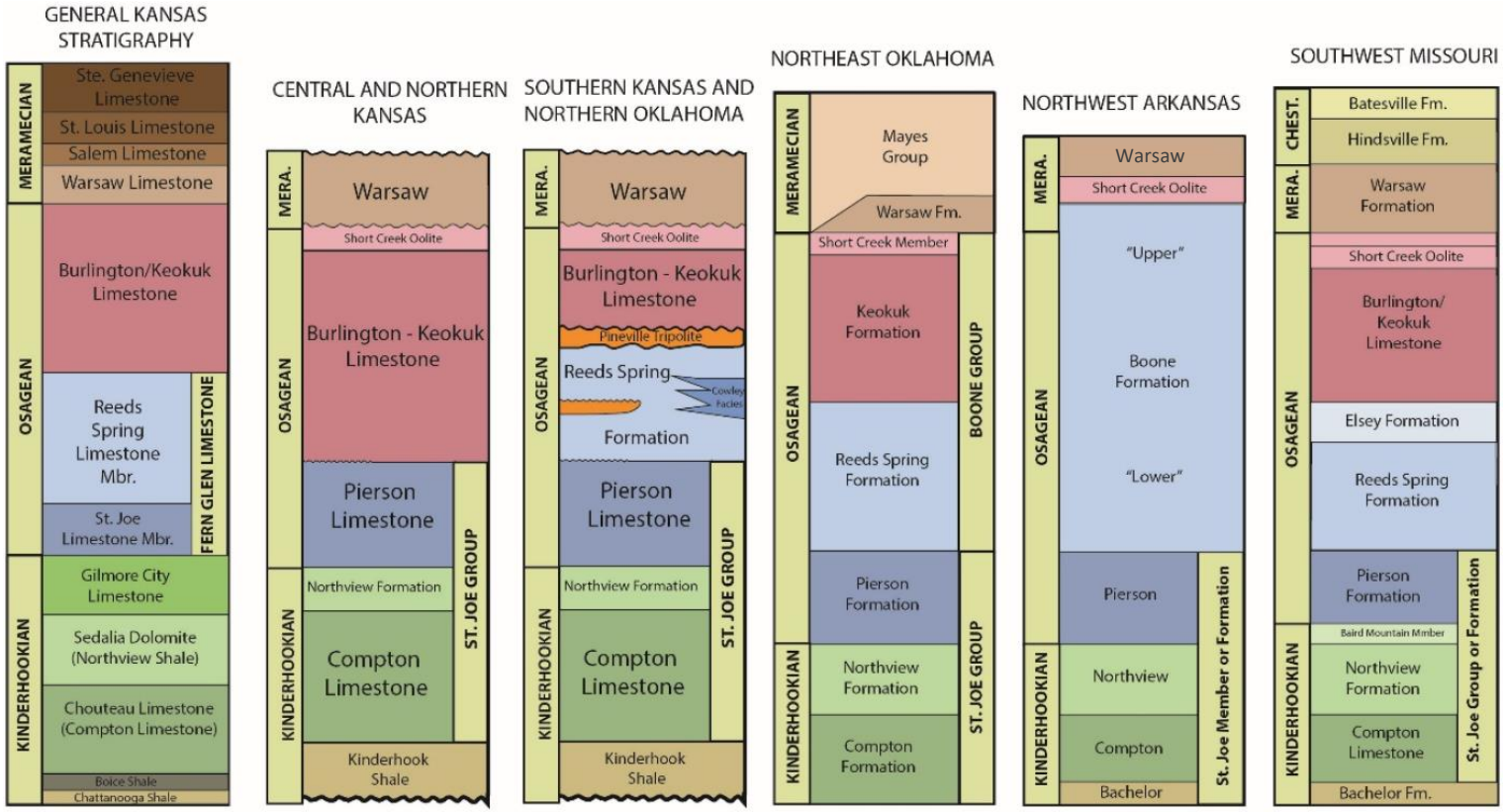

Figure 11. Comparison of several stratigraphic columns showing the conventions applied in different regions for naming "Mississippian Limestone" lithostratigraphic units of Kinderhookian, Osagean, and Meramecian of the U.S. Mid-Continent. Figure reproduced from Jaeckel (2016) after Mazzullo et al. (2011b, 2013) and Zeller (1968).

CHAPTER IV

PREVIOUS WORK

Relevant Age-dating Studies Conducted in the "Mississippian Limestone"

Studies by Thornton (1958), Curtis and Champlin (1959), McDuffie (1959), Rowland (1964), Selk and Ciriacks (1968), and Harris (1975) attempted to narrow the geologic age range of the Mississippian section in north-central Oklahoma, including the area directly in and west of the study area in Logan and Payne Counties, by relating Mississippian units of that region to areas with age-constrained Mississippian strata in southern Kansas and northwestern Oklahoma through lithologic-based log correlations. Based on their correlations it was suggested that the Mississippian interval of Logan, Payne, and Lincoln Counties, Oklahoma contains the full Meramecian interval, some of the Osagean below, and some or all the Chesterian above (Thornton, 1958; Curtis and Champlin, 1959; McDuffie, 1959; Rowland, 1964; Selk and Ciriacks, 1968; Harris, 1975). Figure 12 is a generalized model of what previous authors have expected the Mississippian interval to look like from a time-stratigraphy perspective within an area just 20 miles north of the Elinore 1-18.

The central problem with the previous authors' log correlations for the "Mississippian Limestone" in north-central Oklahoma is that they were using concepts of

lithostratigraphy to match time-stratigraphic horizons (Thornton, 1958; Curtis and Champlin, 1959; McDuffie, 1959; Rowland, 1964; Selk and Ciriacks, 1968; Harris, 1975). Lithostratigraphic boundaries do not necessarily honor time-stratigraphic ones; therefore, they cannot be relied on to provide accurate age-dates of the Mississippian interval in the Oklahoma basin.

Of all the previous authors to attempt to age-date the Mississippian interval in north-central Oklahoma, work by Selk and Ciriacks (1968) is the most relevant to this study because they attempted to incorporate conodont data from cores in Noble and Payne Counties to their lithostratigraphic-based correlations. However, Selk and Ciriacks (1968) failed to publish their methods used to process conodonts and any of the details of the work or images of the conodonts they collected, thereby informalizing their biostratigraphic results. Their collection of conodont elements presently resides at the Paleontology Repository at the University of Iowa. Interestingly, Cory Godwin (personal communication, 2017), a researcher with the Industry-OSU Mississippian Consortium and conodont biostratigrapher visited the repository at the University of Iowa to review the work of Selk and Ciriacks (1968) and has indicated to the author that he is personally overall supportive of their age-dating interpretation. Still, the biostratigraphic results of Selk and Ciriacks (1968) have been questioned/disputed in the literature (e.g., Rogers, 2001) and remain informalized; therefore, there is present need to provide more formalized biostratigraphic evidence to the Mississippian interval in north-central Oklahoma.

In a recent attempt to age-date the Mississippian interval in north-central Oklahoma, Dupont (2016) used carbon isotopes obtained from whole-rock samples in the

same cores LeBlanc (2014) described and the author sampled for his biostratigraphic analysis. Dupont's (2016) interpretation was that a complete "Mississippian Limestone" interval is represented by the subsurface sections, basing her conclusion on comparisons with her data to other North American carbon isotopic charts with some age constraint (Mii et al., 1999; Saltzman, 2002, 2003; Batt et al., 2007; Koch et al., 2014). However, using chemostratigraphic evidence alone is a rather new method for applying age-dates to rocks; therefore, there remains questions of the limitations of this chemostratigraphic approach. Since the results of Dupont (2016) and all the other previous studies discussed herein provide some basis for determining the geologic age range of the Mississippian interval in north-central Oklahoma, biostratigraphic evidence is required to more effectively assess previous authors' interpretations.

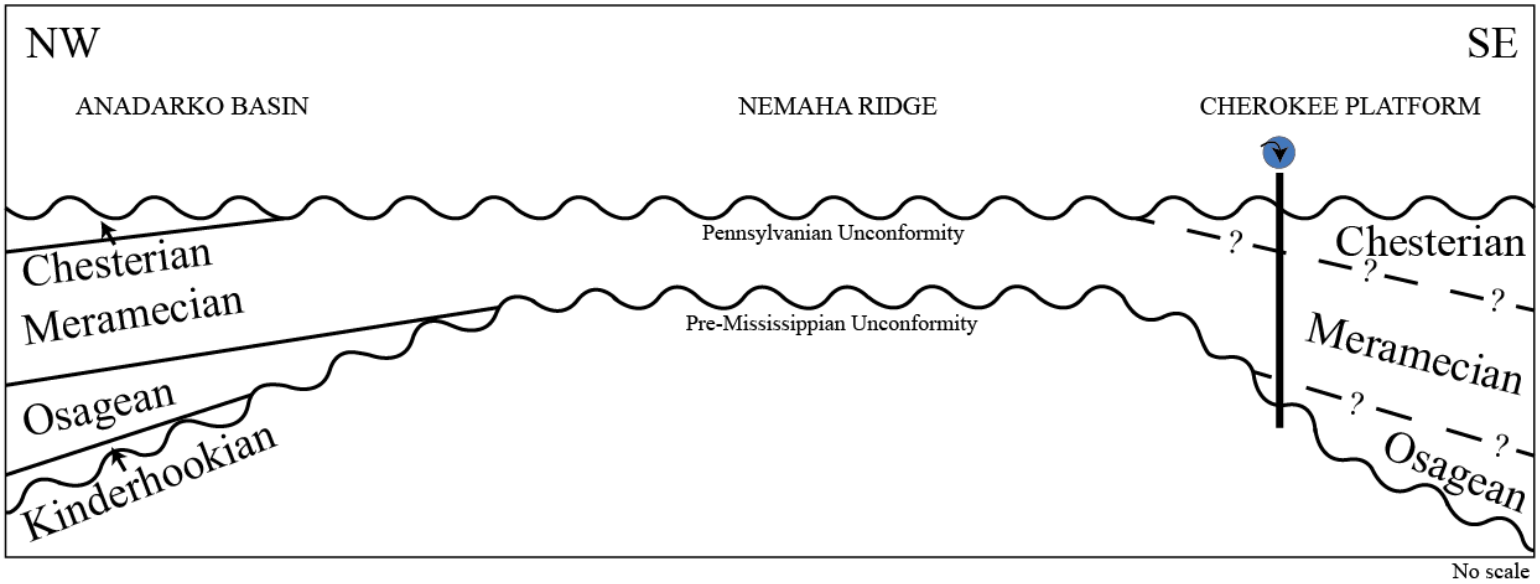

Figure 12. Generalized depositional model for the "Mississippian Limestone" interval of north-central Oklahoma. The well symbol with the blue dot and arrow through it represents the approximate location of the cored wells in this study. The estimated well location estimates the relative geologic age range that Thornton (1958), Curtis and Champlin (1959), McDuffie (1959), Rowland (1964), Selk and Ciriacks (1968), and Harris (1975) predicted would exist for the Mississippian interval in north-central Oklahoma.

CHAPTER V

CONODONT BIOSTRATIGRAPHY

Landmark Studies on Conodonts

Conodonts were first discovered and described in 1856 by German paleontologist Christian Pander. Pander (1856) described conodonts by their only hard parts, which he termed "elements," and wrote that conodont elements are tiny teeth-like fossils which probably belonged to a group of primitive soft-bodied fish related to the modern-day hagfish or lamprey eel. Over the next seventy years, geoscientists regarded conodonts as curious paleontological occurrences, but they were otherwise ignored (Sweet and Cooper, 2008).

In 1926, Ulrich and Bassler demonstrated that stark commonalities among conodont elements collected from all over the world could be seen in Paleozoic strata that were understood to be relatively the same age and that element forms of conodonts seemed to systematically change through time. This meant there was potential for conodont elements to be used as biostratigraphic markers. Roundy (1926) was first to test Ulrich and Bassler's (1926) hypothesis and used his collection of conodont elements from Mississippian age outcrops in Texas to compare with other conodont collections globally and to each other, demonstrating that conodont elements are useful

biostratigraphic markers. Since then, conodont elements have been collected and described extensively all over the world and have proven to be one of the more readily available and useful biostratigraphic markers for sedimentary rocks of middle Cambrian to Late Triassic age (at which time conodonts went extinct). Within the last ten years, conodont elements have also shown potential for yielding direct age-dates through (U-Th)/He thermochronology (e.g., Peppe and Reiner, 2007).

In the late 1970's, nearly 50 years after Roundy (1926) confirmed conodonts as being useful biostratigraphic tools, geoscientists realized that this curious group of fauna was valuable for more than just applying age-dates to rocks. It was known at the time that conodont elements change color (Sweet and Cooper, 2008), but it was Epstein et al. (1977) who first reported on how conodont element color changes relate to subsurface temperature and percent fixed carbon, demonstrating that the elements could be useful indicators for estimating the burial history of strata as well as hydrocarbon maturation. The authors created the first Conodont Alteration Index (CAI) –a chart generated from their lab observations and field work–useful for estimating the maximum burial depth of strata, maximum subsurface temperature strata attained during diagenesis, and thermal maturity of hydrocarbons in them (Epstein et al., 1977). Harris (1979) later published a more robust CAI that related conodont element color changes to another optical index of thermal maturation (i.e., vitrinite reflectance), and his is the more commonly used chart today (Figure 13). The petroleum industry has found the CAI useful for assessing burial histories and hydrocarbon potential in rock formations where conodont elements are abundant (McCarthy et al., 2011).

By the 1980's, it became commonplace for authors to make interpretations based on conodont biofacies because enough ecological evidence regarding the creatures had been collected up to that point. Within the last 20 years, conodonts were shown to be useful for another geological application. Wenzel et al. (2000) and later Buggisch et al. (2008) for example, demonstrated that elemental oxygen isotopes are generally reliable paleosea thermometers, meaning that conodont elements are useful tools for reconstructing paleosea conditions and showing trends in major climatic changes (e.g., eustatic glaciation). This relatively new methodology has been questioned recently, (e.g., Terrill, 2015), but overall the use of conodonts for reconstructing paleosea conditions is well-received among experts in the geoscience community.

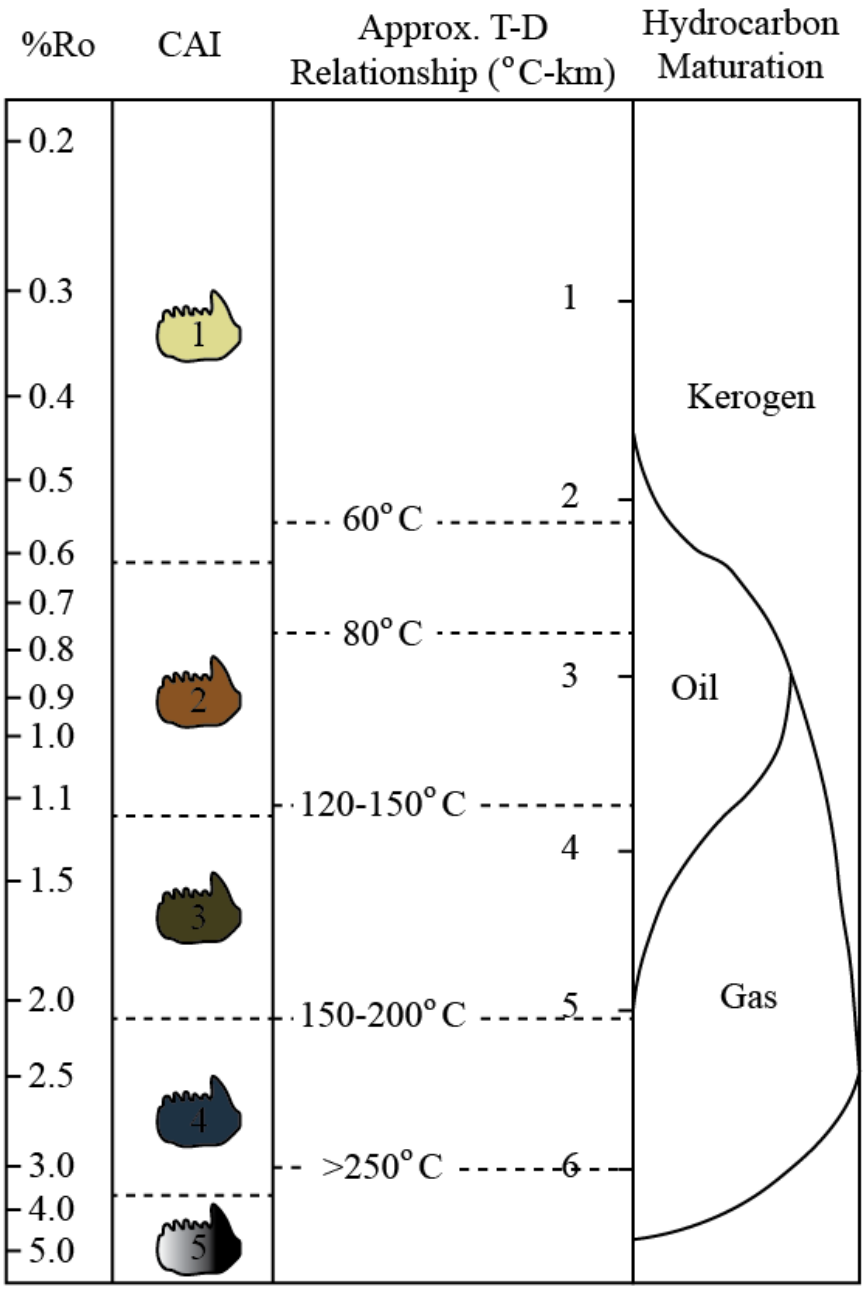

Figure 13. Conodont Alteration Index (CAI) compared with changes in vitrinite Reflectance values (%Ro), temperature (T) and depth (D), and the hydrocarbon maturation window. All data were experimentally derived from Epstein et al. (1977) and Harris (1979). Figure redrafted from Harris (1979).

The Enigmatic Conodont Animal

Although conodont elements were discovered over 160 years ago and have been studied extensively from a biostratigraphic perspective, much less is known to date about the conodont animal and its ontologic, paleozoological, and phylogenetic affinities. It was not until 1983 that the first conodont animal (body fossil) was observed and described. Briggs et al. (1983) made the discovery as they worked in the Granton "shrimp beds" of Edinburgh, Scotland and came across a peculiar soft-bodied specimen preserved along a bedding plane of a limestone. The specimen had a jawless, bulbous, and bi-lobed head with two large eyes and an arrangement of in-situ conodont elements with a narrow eel-like body that showed evidence for a notochord, chevron-shaped muscle tissue, and an asymmetrically-shaped rayed fin at its tail (Figure 14).

With the discovery of the first body fossil of the conodont animal (Briggs et al., 1983) and a few others since, geoscientists have reinterpreted their understanding of the clade's ontology and phylogenetic affinities using various statistical and digital modeling methods. Knell (2012) published a comprehensive summary of these landmark studies on conodonts. In general, the current consensus among paleontologists is that conodonts are a group of extinct agnathan soft-bodied marine chordates (Purnell and Donoghue, 1997; Donoghue et al, 2000) that have for now been placed into their own class called the Conodonta (Murdock et al., 2013). There exists a growing body of literature that suggests conodonts are vertebrates with phylogenetic ties to the modern hagfish (Terrill, 2015). Based on all analyses, conodonts are thought to be overall nektonic creatures that grew up to 6 in. (15 cm) long and lived within the photic zone of most marine nearshore to open marine environments (e.g., Dzik, 2000; Aldridge and Briggs, 2009; Knell, 2012).

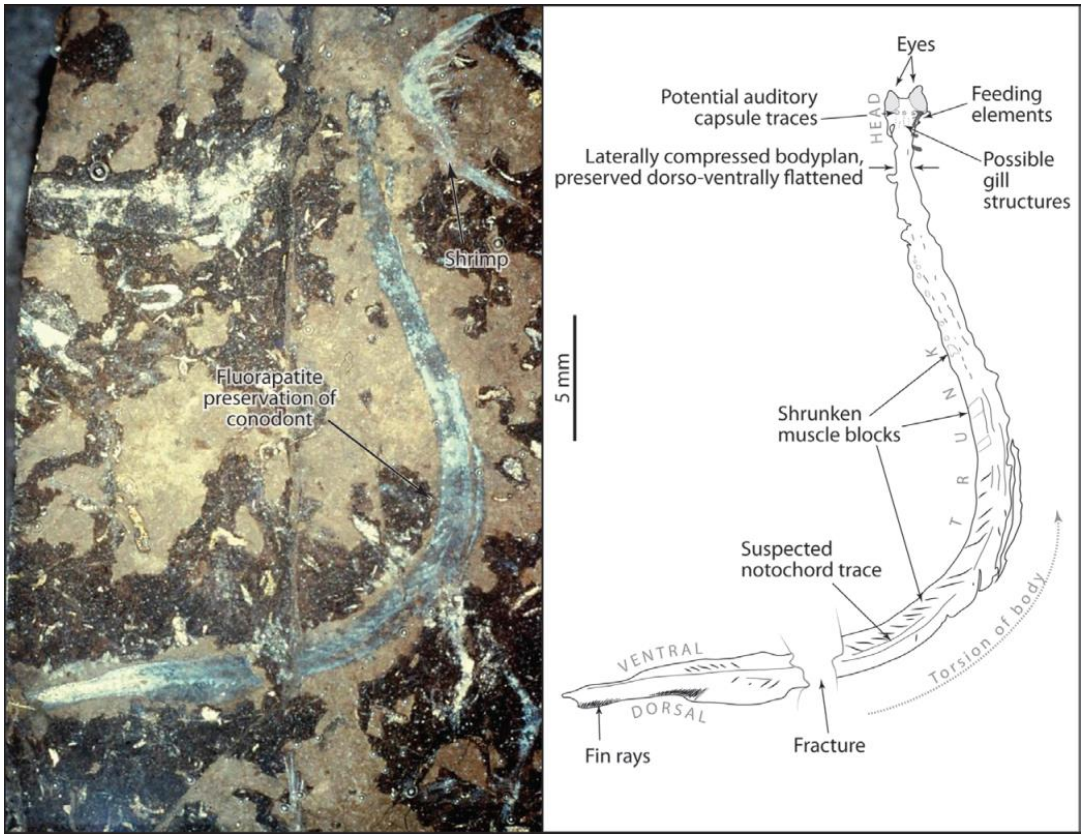

Figure 14. Soft-body plan of a conodont. The conodont specimen photographed (left) is from the Granton "shrimp beds" of Edinburgh, Scotland and has several of its soft-bodied features preserved, which are identified (right). Note the shrimp body fossils preserved in the photo as well as the diagenetically altered fluorapatite (blue-green mineralization) of the exceptionally well-preserved conodont. Photograph and schematic drawing both from Briggs et al. (1983).

Conodont Elements

Chemically, conodont elements consist of francolite, which is a form of calcium phosphate (apatite) that is enriched in carbonate and fluorine (Sweet and Cooper, 2008). The stable mineral apatite resists chemical and physical alteration, but fluorine–an important minor constituent found in conodont elements–helps to simplify the mineralogical structure of apatite and further increase its resistivity to ion substitutions and other diagenetic alterations (Marshall and Marshall, 2014). As a witness to their chemical and physical resistivity during diagenetic alternation, conodont elements have been found relatively well-preserved in Paleozoic and Early Mesozoic metasedimentary rocks from all over the world, including marbles and gneisses (McCarthy et al., 2011). It is the chemically resistive nature of conodont elements that helps to preserve their delicate morphologic structures and original isotopic signatures and enables them to be useful for various geologic applications.

Collections of conodont elements found in-situ, as they would have been placed in a living conodont, have been shown to be part of a larger, bilaterally symmetrical feeding apparatus that begins in a conodont's pharyngeal (throat region) (e.g., Purnell, 1994) (Figure 15). Several conodont genera have been shown to have occlusional function in some areas of their feeding apparatus based on multi-element analyses and statistical reconstructive modeling (e.g., Wickström and Donoghue, 2005; Jones et al., 2012; Murdock et al., 2013), meaning that most conodonts used their feeding apparatus with associated muscle groups to grasp, impale, and even slice or "chew" their prey (Purnell, 1994; Purnell and Donoghue, 1997; Martínez et al., 2014).

Conodont elements are classified into three groups based on differences in their overall morphology and where they belong on a feeding apparatus (Figure 15). M-elements (coniforms or "cones") are the simplest and generally have the appearance of a cone shape. M-elements are located at or near the anterior (front) of a typical feeding apparatus, and they usually display much larger denticles (teeth-like structures) compared with other element types on a single apparatus. S-elements (ramiforms or "bars") are the longest and generally fit directly behind the M-elements in a tubular-, cone-, or "arrowhead"-shaped fashion that narrows towards the posterior (back) end of a conodont's pharyngeal. S-elements also generally make up most the elements per conodont animal, and have the appearance of serrated rods.

P-elements (pectiniforms or "platforms") are the most complex on a conodont's feeding apparatus and come in sets of two which are located at the very most posterior end of a conodont's pharyngeal. Both sets provide occlusional function by using a pendulum-like motion to allow the conodont to slice its prey after it has grasped and impaled its prey repeatedly with its M- and S-elements. P_1-elements are located at the most posterior end of a conodont's pharyngeal and are the most useful in biostratigraphic analyses that rely on traditional form taxonomy for species identification (e.g., this study) because they display the most obvious, and in many cases, only characteristic features for defining species. Some studies have indicated that P_1-elements diversified the most, in general, among conodonts because these creatures had to rely on them most for consuming their prey, making it advantageous for their forms to develop better P_l-elements through geologic time (Donoghue et al., 2000; Wickstrom and Donoghue, 2005).

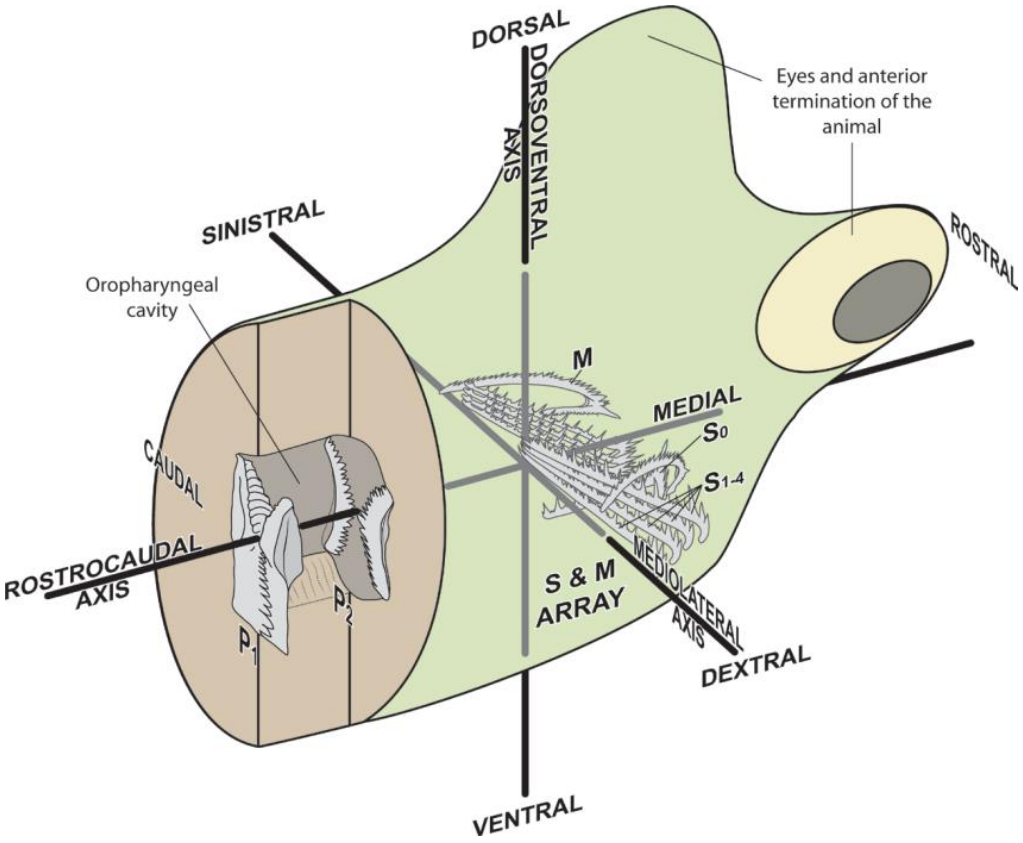

Figure 15. Schematic illustration showing the arrangement of elements in a conodont's feeding apparatus. Note the three classifications of conodont elements (M-, S-, and P-elements) are indicated. P-elements are the most critical for identifying species. Schematic from Barham (2015).

Biostratigraphic Application of Conodont Elements

Biostratigraphy is the subdiscipline of stratigraphy that uses the distribution of fossil remains to organize strata into distinct units. The latest techniques for relating biostratigraphic units are to the chronostratigraphic record is summarized in Gradstein et al. (2012). Simply put, this is done by identifying a fossil succession within a rock layer and comparing it with other rock layers that bear the same fossil succession. The rock layers with the same fossil succession are then correlated across an area or region until they are confidently traced to where rock layers with the same/similiar fossil succession are constrained by absolute age-dating. The fossil succession of all the rock layers bearing the same/similar fossil succession and shown to be coeval is then bracketed by absolute age-date(s), and the fossil succession becomes pseudo direct evidence for that geologic age range in future studies. Future work refines the geologic age range of each fossil succession and breaks them into smaller zones (called biozones), allowing them to become more precise and better able to be correlated over larger areas.

Ideally, every fossil succession is constrained by assignment of absolute age-dates at its top and base. However, rarely does this occur because of several factors, including (1) the punctuation of the rock record; (2) the time-transgressive nature of stratigraphic deposits and how faunal groups diversify and are distributed through time; and (3) the preservation quality of the fossils themselves. To this end, several graphic, statistical, and computational techniques, which are described in detail by Gradstein et al. (2012), are used by paleontologists to estimate the absolute age of a biozone.

Conodonts are widely accepted as reliable index fossils. This means that conodont elements are overall (1) globally widespread; (2) representative of relatively short periods

of geologic time; and (3) found in high abundances in most sedimentary rock types. Conodont global biozones of the Mississippian are presently constrained at a maximum of about three or four million years (Gradstein et al., 2012). In contrast, several authors have argued that conodont biozones for the U.S. Mid-Continent represent sub-one million year intervals (Boardman et al., 2013; Godwin, 2017). It is very common for higher age-dating resolutions of a fossil group to exist over a region in comparison with a global distribution of the same group because of something called provincialism (discussed later). Interestingly, work by Uyeda et al. (2011) has suggested that it may not be practical for future conodont biostratigraphic work conducted in the U.S. Mid-Continent to further constrain age-dating resolutions far below one million years because of a theory called long-term evolution.

The theory of long-term evolution states that changes in organisms' bone and other hard part structures, such as when a conodont adds a row of denticles to its platform, accumulate slowly (Uyeda et al., 2011). In the case of conodonts, that "slowness" is estimated to be about one million years (Uyeda et al., 2011). This makes distinguishing between new species of conodonts based on changes in structural changes of their hard parts almost impossible unless other lines of evidence, such as ornamentation, soft-tissue, or element function are considered because they tend to preserve more obvious differences between species types at resolutions in geologic time much smaller than one million years. The problem with conodont species of the Mississippian is that they tend to lack many ornamentation features in comparison with species of other periods in geologic history, such as several of the conodont species of the Devonian and Pennsylvanian. It is important to note that this theory does not imply

anything about the true rate of evolution in conodonts, nor does it mean that it is impossible for preserved conodont species of the Mississippian to have age-resolutions far below a one-million-year time scale, since given the right conditions (e.g., provincialism and natural selection) species types are known to diversify over periods much shorter than millions of years.

Conodont Provincialism

Provincialism is when a group of fauna or flora is restricted to an area for a prolonged period and new species emerge because of the restricted area's unique set of environmental conditions that force the group of fauna or flora to adapt. Gradstein et al. (2012) summarized the evidence for showing there is provincialism observed among Mississippian conodont populations of the U.S. Mid-Continent; however, there is no universally accepted theory that explains what caused it. Previous authors have suggested that mass extinction events (e.g., Lauden, 1949), active tectonics and high-frequency sea level change (e.g., Noble, 1993), basin restriction (e.g., Franseen, 2006), long-term effects of eustatic glaciation (e.g., Buggisch et al. 2008), and even a meteorite impact event (Evans et al, 2011) all had roles in causing or promoting Mississippian conodont provincialism within the U.S. Mid-Continent.

The author of this study is of the opinion that periodic basin restriction best summarizes why conodont species of the U.S. Mid-Continent are different from other global populations of the Mississippian and that the collision of Laurussia with Gondwana during the Mississippian in combination with relative sea level change were the principal drivers for causing the isolating basin conditions. Noble (1993) speculated along these same lines, arguing that microcontinents caught in between the colliding

Laurussian and Gondwanan continents were uplifted and therefore provided regional barriers to basins across the ancestral United States and shifted or inhibited seaway current pathways that prevented marine faunal groups, such as foraminifera and ammonoids, from colonizing the Oklahoma basin.

Figure 5 shows how sea level fluctuated during the Mississippian, and although the curve by Haq and Schutter (2008) does not show sea level change for the Oklahoma basin alone, several of the lowstands correspond with minor mass extinction events in the U.S. Mid-Continent. For example, Laudon (1948) reported an apparent mass decline among certain families of echinoderm and brachiopod populations of the western U.S. Mid-Continent in rocks of the middle Osagean and noted that some families in both groups completely disappeared at the Osagean-Meramecian boundary (Laudon, 1948) (about the same time paleoclimatic studies have shown more restricted basin conditions were established within the basin), with significant evolutionary changes present in the families of both groups that survived the localized extinction event. Ausich et al. (1994) later observed there is no other evidence for a mass extinction among the same echinoderm or brachiopod faunal groups that Lauden (1948) described in any other basin around the world at the Osagean-Meramecian contact (though there was one during the middle Osagean); therefore, the authors determined that the localized disappearances observed in these faunal groups may be best explained by prolonged restricted basin conditions. For example, because most echinoderm families are stenohaline and prefer open-water circulation conditions (Russell, 2013), if basin conditions were restricted for prolonged periods such that both salinity and circulatory conditions changed even just

moderately, the echinoderm populations of the Oklahoma basin certainly would have suffered.

Another factor to consider for the mass regional decline among echinoderm and brachiopod populations that Lauden (1948) observed is from a meteor impact. Evans et al. (2011) provided evidence for a meteor impact that occurred in southwestern Missouri during the latest Osagean to earliest Meramecian. Ausich et al. (1994) observed, however, that the decline and subsequent diversification of crinoids and brachiopods during the Osagean-Meramecian was gradual and that it started in the early Osagean, indicating that a single impact event would not fully explain the gradual decline in brachiopod and crinoid families that is observed in the basin. However, a meteor impact at the Osagean-Meramecian boundary coupled with a prolonged period of basin restriction in the Oklahoma basin may help explain why it has historically been more difficult to study the "Mississippian Limestone" from a biostratigraphic perspective for rocks of Meramecian and Chesterian age, as Godwin (2017) has noted.

CHAPTER VI

MATERIALS AND METHODS

Whole-rock Sample Collection

With permission, whole-rock samples were obtained from the butt-end of each core at the Oklahoma Petroleum Information Center in Norman, Oklahoma. Permission to sample the cores was given to the author with the understanding that all samples would be obtained using a precise methodology that preserved as much of the cores as possible. Therefore, the author chose, in general, to limit all sampling in the cores to their top and base, above and below major time-stratigraphic surfaces and lithologic changes, and in organic-rich intervals, such as maximum flooding surfaces (condensed sections), where conodont elements were assumed to be most abundant. This means that collection priority in the Adkisson 1-33, Elinore 1-18, and Winney 1-8 cores was placed (1) at or near core tops and bases for obtaining their maximum age range; (2) above and below third order sequence boundaries established by LeBlanc (2014) for observing any time-stratigraphic control on conodont element abundances; (3) in lithologic units where abundant macrofauna were present (excluding skeletal grainstone facies) for isolating intervals of high biodiversity with relatively high preservation potential (i.e., high

biodiversity intervals preserved in low-energy depositional conditions); and (4) in "hot" shales where the gamma-ray curve read ≥100 API and which corresponded to the darkest colored rock unit relative to its surroundings (proxy for condensed sections) (Figures 16a-c). In the Doberman 1-25, no sequence boundaries had been picked by Hill (2017) at the time the whole-rock samples were collected. In addition, samples were collected later and permission was given to sample much less of the Doberman 1-25 in comparison with the other cores; therefore, the collection method in the Doberman 1-25 was the same as in the other three cores but without sampling around known sequence stratigraphic boundaries and by limiting sample collection to about a 7-ft. spacing to ensure there was maximum coverage of the cored interval (Figure 16d). For a full list of all samples in each of the cores, refer to Appendix A.

Whole-rock samples measured 0.25 ft. to 1.25 ft. from top to base and about 9 in. around their circumference, with the average sample measuring 0.5 ft. long and weighing approximately 6 lbs. Samples were collected at thinly spaced intervals of about 0.5 ft. along a 5-ft. continuous stratigraphic interval for more precisely measuring the depth interval from which conodont elements were recovered, as the methodology used to process each of the samples was destructive. In total, 369 whole-rock samples were collected from the four cores, 123 of which came from the Adkisson 1-33, 145 from the Winney 1-8, 67 from the Elinore 1-18, and 34 from the Doberman 1-25. The total footage sampled in each of the cores by percent was 25%, 51%, 31%, and 4.9% in the Adkisson 1-33, Winney 1-8, Elinore 1-18, and Doberman 1-25 cores, respectively. The relatively large variation in the total footage of samples collected from each core is due in part to the limiting permissions granted to the author, especially evident in the Doberman 1-25.

The footage variation is also due to the natural variation in the amount of facies present in the cores that were ideal for sample collection. For example, the Adkisson 1-33 and Elinore 1-18 contain more organic-rich, non-skeletal grainstone macrofauna-bearing intervals to sample than the Winney 1-8, which contains much grainier and less organic-rich facies. To compensate for the lack of ideal sampling intervals in the Winney 1-8 core, whole-rock samples were collected from a relatively larger portion of skeletal grainstone facies than were collected from the other cores. Sample collection from skeletal grainstone facies were generally avoided otherwise because it was assumed that the coarse-grained, high-energy facies would have poor preservation potential for conodont elements, which are susceptible to fragmentation and winnowing.

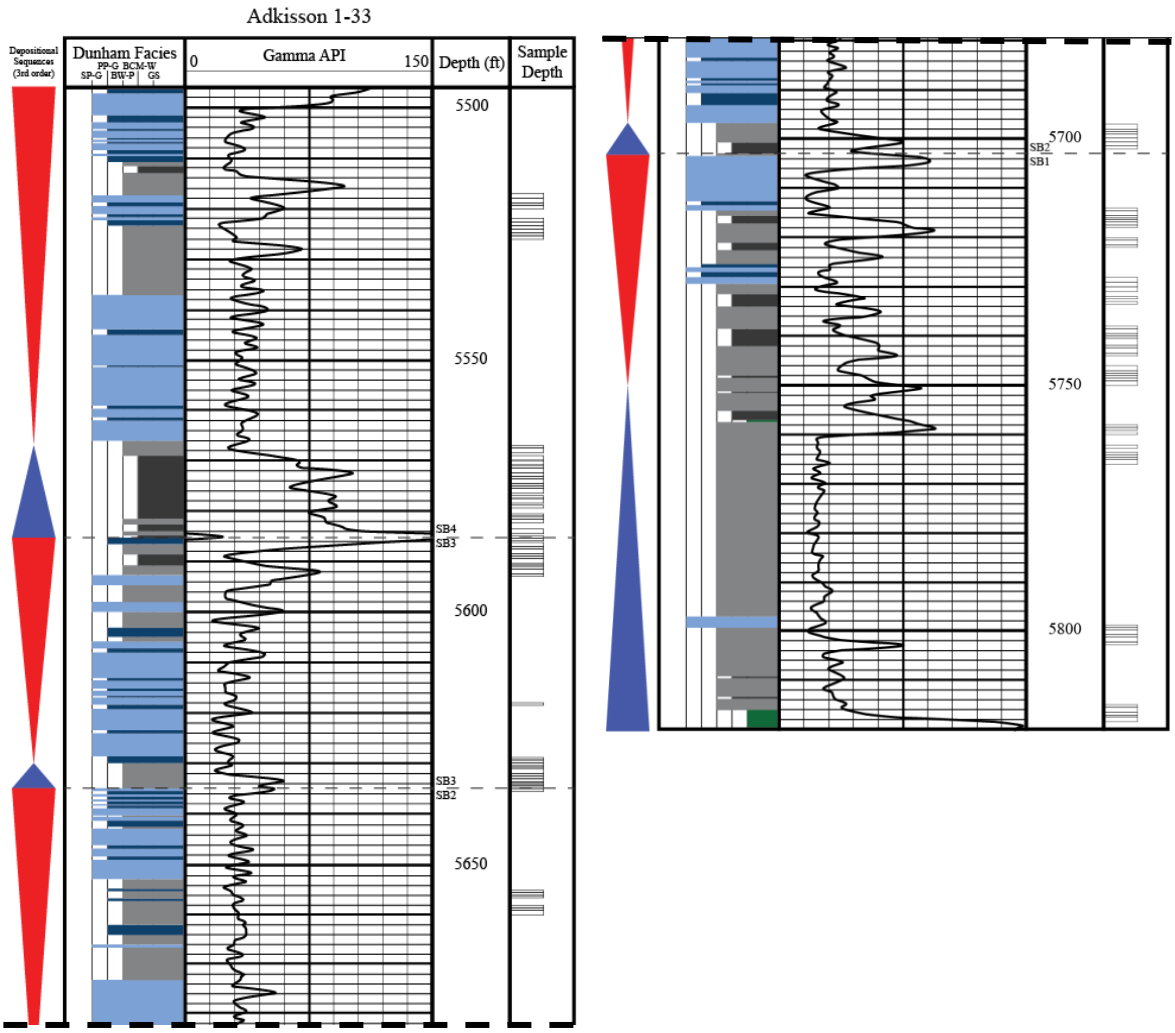

Figure 16a. Part of figure 3a presented again, but this time showing the intervals where whole-rock samples were collected for conodont element analysis in the Adkisson 1-33. The bolded dashed line indicates where the log was cut to display its full length in this figure. All depth tracks have been converted to log depth, though in this core the log and core depths are equivalent. Dashed lines labeled SB# represent third-order sequence boundaries established by LeBlanc (2014).

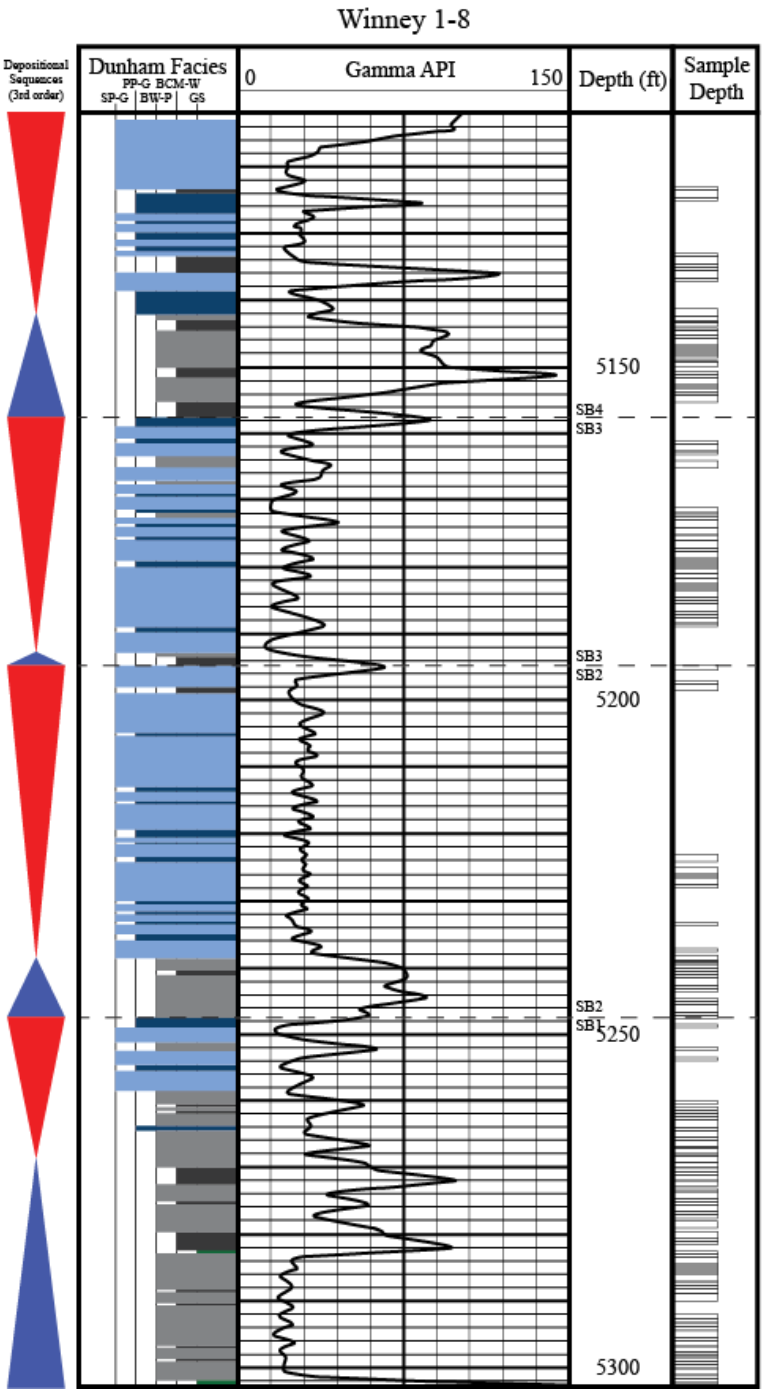

Figure 16b. Part of figure 3a presented again, but this time showing the intervals where whole-rock samples were collected for conodont element analysis in the Winney 1-8. All depth tracks have been converted to log depth, and in this core the log depth is 10 ft. above the core depth. Dashed lines labeled SB# represent third-order sequence boundaries established by LeBlanc (2014).

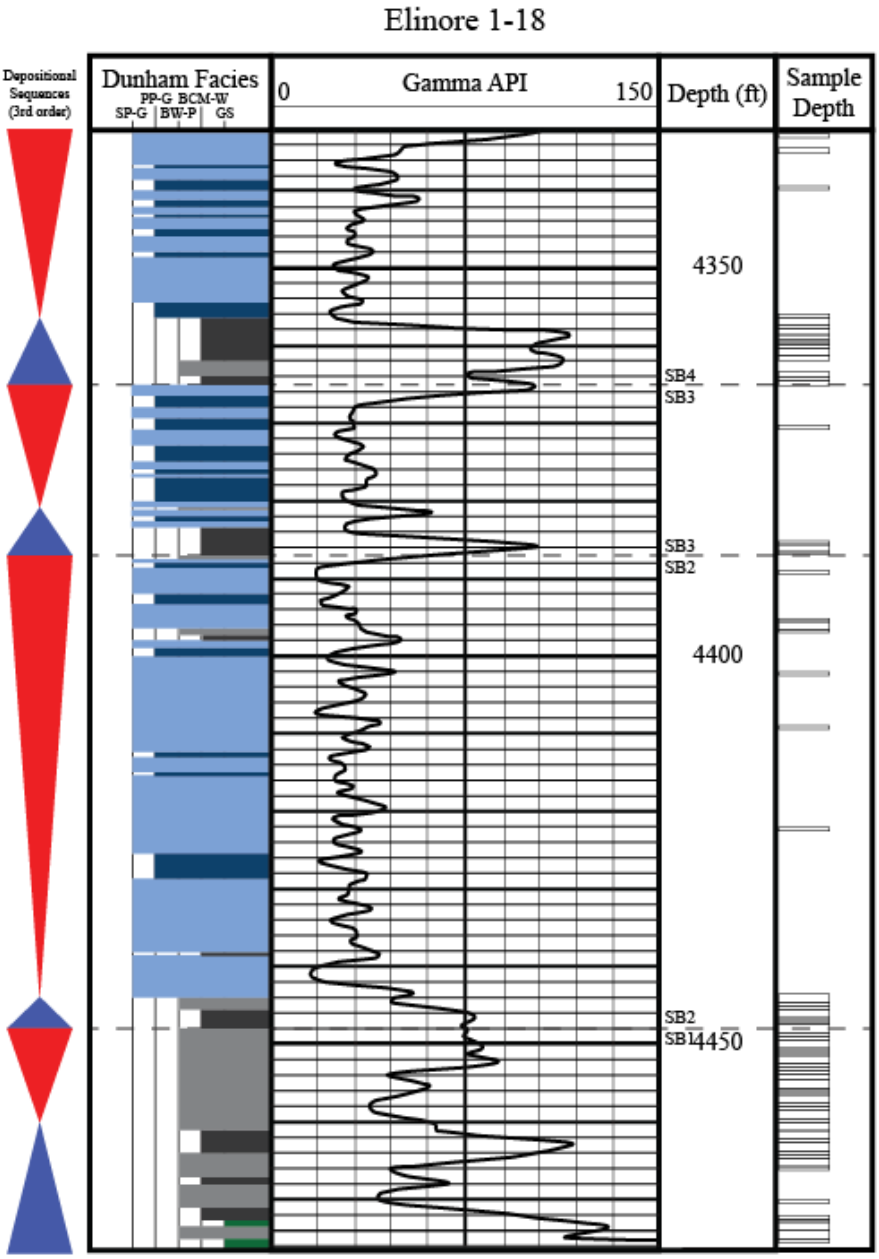

Figure 16c. Part of figure 3b presented again, but this time showing the intervals where whole-rock samples were collected for conodont element analysis in the Elinore 1-18. All depth tracks have been converted to log depth, and in this core the log depth is 6 ft. above the core depth. Dashed lines labeled SB# represent third-order sequence boundaries established by LeBlanc (2014).

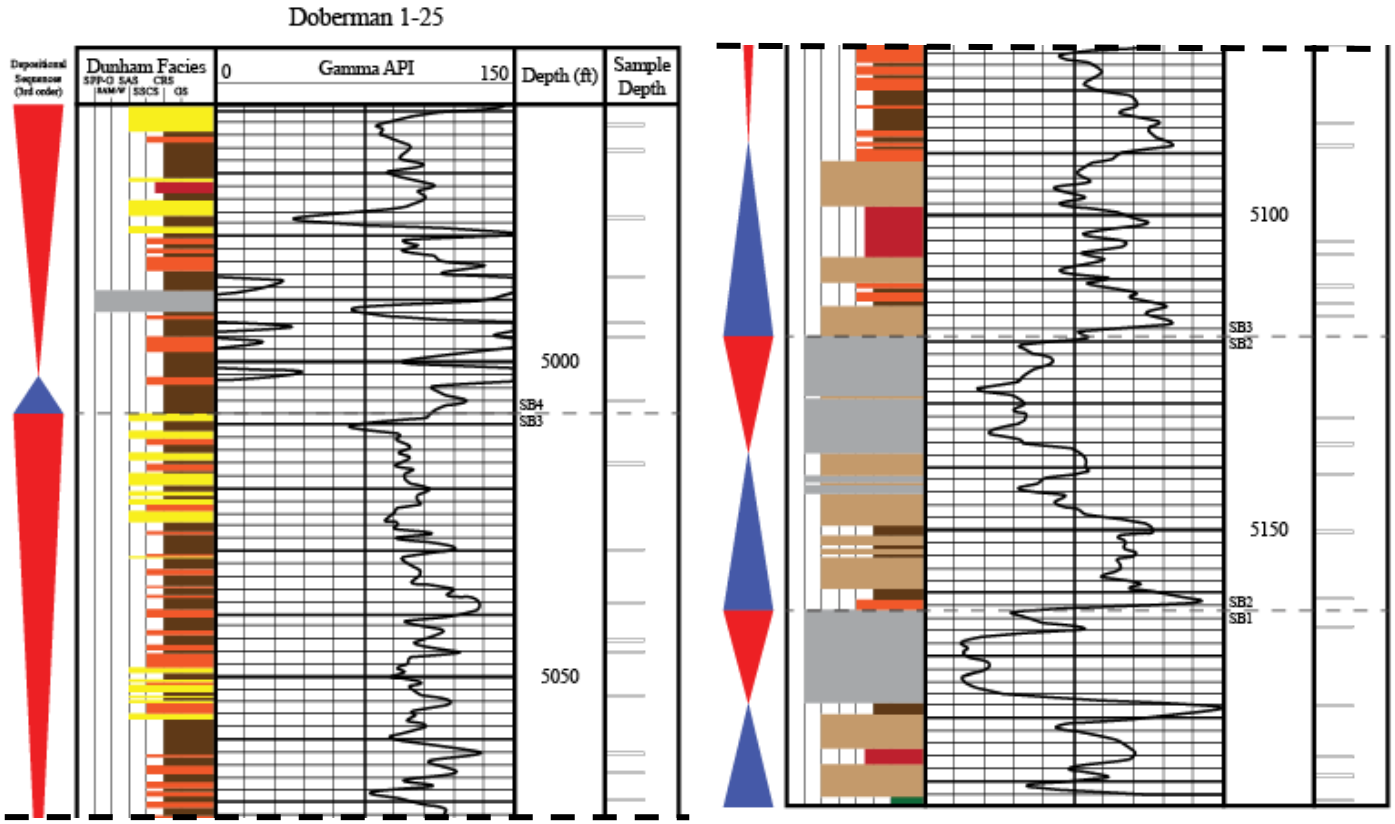

Figure 16d. Part of figure 3b presented again, but this time showing the intervals where whole-rock samples were collected for conodont element analysis in the Doberman 1-25. The bolded dashed line indicates where the log was cut to display its full length in this figure. All depth tracks have been converted to log depth, and in this core the log depth is 6 ft. above the core depth. Dashed lines labeled SB# represent third-order sequence boundaries established by LeBlanc (2014) for the Elinore 1-18 and correlated to the Doberman 1-25 by Hill (2017).

Whole-rock Sample Processing

All whole-rock sample processing was conducted at the Hazardous Reactions Laboratory at Oklahoma State University. Figure 17 is a generalized workflow that summarizes how the whole-rock samples were processed to extract conodont elements in each of the cores. The samples were processed using several standardized techniques, including sample disaggregation, acid digestion, and heavy liquid density separation. Each sample underwent at least two acid treatment baths and some that were more difficult to digest had up to seven acid treatments applied to them (each acid treatment had a duration of 24 hrs.). For samples that underwent more than three acid treatments, the spent acid from the prior acid treatment was saved and reused as a buffering agent, with its pH kept above 2.8 in the next acid treatment to protect conodont elements from corrosion, discoloration, or partial dissolution from prolonged exposure to acid treatment (Dzik, 2000). For a detailed description of the techniques used to process whole-rock samples and extract conodont elements, refer to Appendix B. For a full list of the type and number of acid baths applied to whole-rock samples, refer to Appendix A.

Observations made by the author coupled with x-ray diffraction (XRD) data available on select whole-rock samples in each of the cores showed that coarser-grained, siliciclastic-rich facies were most difficult to digest in acid. This means that samples containing siliceous sponge spicules or rich in glauconitic sandstone, such as in the Adkisson 1-33, Elinore 1-18, and Winney 1-8, and the sandstone and siltstone facies of the Doberman 1-25 were the most difficult to process.

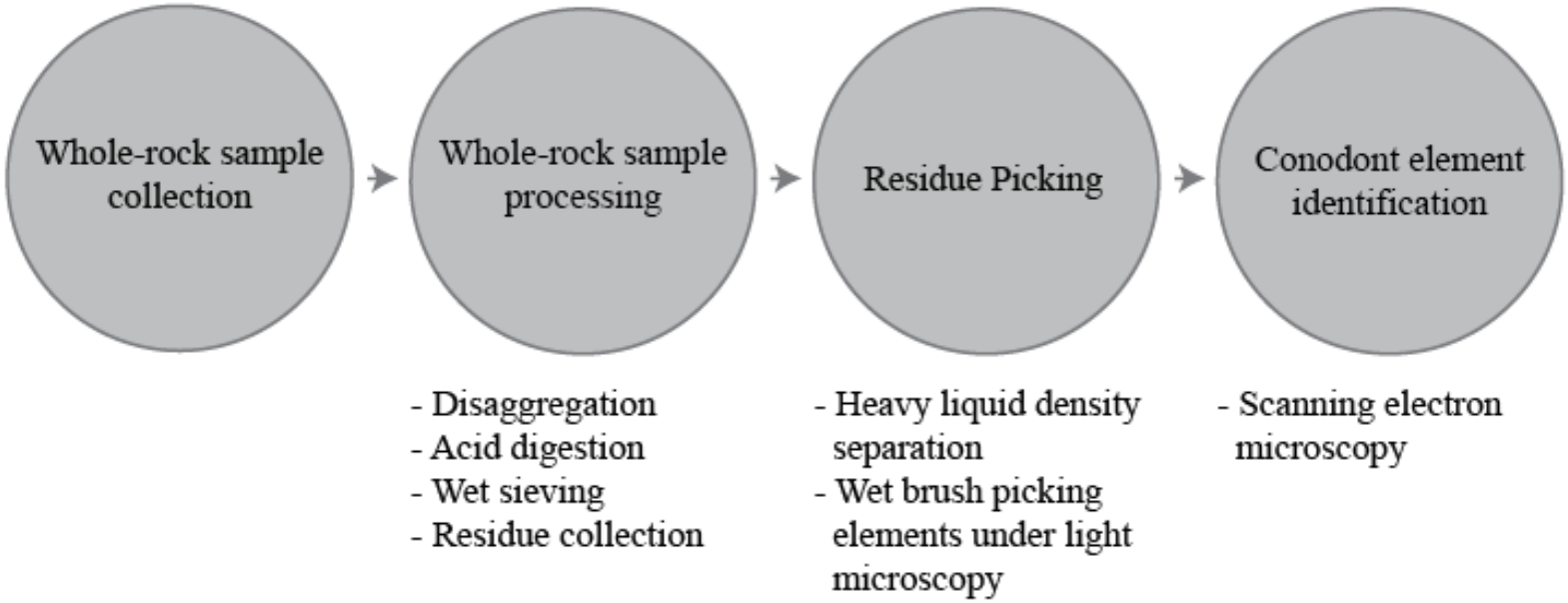

Figure 17. Generalized workflow for extracting conodont elements from whole-rock samples.

Residue Picking and Conodont Element Identification

Upon acid treatment, each whole-rock sample produced a residue. Residue from an acid treated whole-rock sample consisted of gravel-sized to fine sand grains, which were then sorted by decanting the spent acid, residue, and remaining whole-rock sample through a mesh sieve stack. Sieve sizes included #120, #35, and #4, arranged from bottom to top. Residues were then collected from both the #35 and #120 mesh sieves. The residue in the #35 mesh sieve was scanned for conodont elements to check for larger specimens that might not have made it into the #120 mesh sieve. No conodont elements were ever recovered from the #35 mesh sieve. The residue from the #120 mesh sieve contained a collection of grains that ranged from medium to fine sand, or from 1/200 to 1/48 in. (0.125 to 0.5 mm). Average conodont elements of the Mississippian have been shown to range in size from 1/128 to 1/48 in. (0.2 to 0.5 mm) (Barrick, 2001); therefore, the portion collected the #120 mesh sieve was checked most thoroughly for conodont elements using the heavy liquid density separation technique as described in Appendix B.

After residues were collected, conodont elements as well as all other identifiable fossils and heavy minerals were wet brush picked using a Leica L2 light microscope set at 20x magnification, following the methods of Miller (2015). All conodont elements–whether fragmentary or whole–were picked and included in the results (discussed in the next chapter). Picked elements not well-preserved were placed on gridded microscope slides while well-preserved specimens (i.e., specimens the author thought would be ideal for additional work) were mounted to carbon tape, set on aluminum stubs, and positioned in their proper orientations for imaging with the scanning electron microscope (SEM). All mounted specimens were then coated in gold-palladium for analysis with the SEM.

The tiny morphologic features that define each species of conodont can only be resolved using relatively high magnification (40x). Since conodont elements' morphologic features are micrometers in size, imaging them with scanning electron microscopy was necessary. The SEM resides at the Venture 1 Research Facility in Stillwater, Oklahoma. Scanning electron microscopy works by shooting electrons out an electron gun and focusing them through a series of electromagnets to form a narrow beam of energy that reflects off the surface of a sample (e.g., a conodont element), producing secondary (surface) electrons that are in turn caught by a Faraday cage and analyzed by a series of sensors connected to computer software. The sensors and software interpret the varying energy levels and orientations of the incoming secondary elections to create an image at a single sampled location. The software then shifts the beam of electrons, "scanning" the specimen and rendering a high-resolution image (up to about 0.4 nm) within a couple of seconds. All conodont elements were analyzed with the SEM set at 20 kV, which provided a maximum resolution slightly below 1 nm.

Dataset Limitations

This study is limited primarily by the fact that whole-rock sampling was done from core. Core samples are not as ideal for obtaining conodont elements as outcrop samples are because (1) one cannot easily return to a locality rich in elements to obtain additional whole-rock samples and (2) there is far less rock available to process, meaning that fewer conodont elements are expected to be recovered relative to similar studies conducted in outcrop that have access to larger quantities of rock for processing. As permission was not granted to process whole-rock samples along the entire length of

core, the biostratigraphic results of this study are further restricted in that it was impossible to analyze conodont elements that may be contained within unsampled sections of the cores. Also, because of sampling restrictions, a facies bias was introduced to this dataset for maximizing conodont element recoveries, though it may be that relatively more conodonts occur within the lithofacies that were not sampled as frequently. Additionally, residues of whole-rock samples represented on average only about one half of the total rock volume processed because of the inability of the acids used to fully digest the samples. This means conodont specimens likely remain in unprocessed portions of the samples analyzed.

Collection Repository

Conodont elements and all other materials examined in this study (i.e., wet-brush picked minerals, fish scales and teeth, as well as SEM imaged crinoid stems and siliceous sponge spicules) reside with the Paleontology Repository in the Department of Earth and Environmental Sciences at the University of Iowa, 115 Trowbridge Hall, Iowa City, IA, 52242, U.S.A.

CHAPTER VII

RESULTS AND DISCUSSION

Conodont Biostratigraphic Results and Interpretation

Biostratigraphic results indicate the "Mississippian Limestone" interval of north-central Oklahoma in the study cores ranges from middle Osagean to upper Chesterian (uppermost Tournaisian to Visean), consistent with the study's initial hypothesis and previous predictions of others (i.e., Thornton, 1958; Curtis and Chaplin, 1959; McDuffie, 1959; Rowland, 1964; Selk and Ciriacks, 1968; Harris, 1975). Conodont species that were relatively age diagnostic and key for defining age boundaries in the study cores included the following: (1) *Polygnathus bischoffi* in the lower part of the first (lowermost) third order depositional sequence of the Elinore 1-18, indicative of the middle Osagean and a key specimen within the *anchoralis-latus* Zone of North America (Perri and Spaletta, 1998); (2) *Gnathodus texanus*, *G. bulbosus*, *G. linguiformis*, *G. cuneiformis*, and *G. pseudosemiglobular* in the upper part of the first (lowermost) third order depositional sequence of the Elinore 1-18, indicative of the upper Osagean and equivalent to the *Gnathodus bulbosus* and lower and middle parts of the *G. texanus* Zones of North America (Collison et al., 1970; Boardman et al., 2013; Miller, 2015); (3) *G. species A* and *G. sp. 15 (aff. punctatus)* in the second (from the base) third order

depositional sequence of the Elinore 1-18, indicative of the basal-lower Meramecian and equivalent to the upper part of the *G. texanus* Zone of North America (Thompson and Fellows, 1970; Boardman et al., 2013; Godwin, 2017); (4) *Vogelgnathus campbelli* and *Lochriea commutata* in fourth (uppermost) third order depositional sequence of the Adkisson 1-33 and Elinore 1-18, indicative of the basal-lower Chesterian and characteristic of the *G. bilineatus-Cavusgnathus charactus* Zone of North America. (Dunn, 1970; Perri and Spaletta, 1998; Godwin, 2017); (5) *Adetognathus unicornis* in the third (from the base) third order depositional sequence in the Doberman 1-25, indicative of the upper Chesterian and equivalent to the lower part of the *A. unicornis-Rhachistognathus muricatus* Zone of North America (Repetski and Henry, 1983; Morrow and Webster, 1991; Bahrami et al., 2014); and (6) *Rhachistognathus muricatus* transitional form to *R. websteri* and *R. minutus minutus* in the fourth (uppermost) third order depositional sequence of the Doberman 1-25, indicative of the uppermost Chesterian and equivalent to the upper part of the *A. unicornis-Rhachistognathus muricatus* Zone (Baesemann and Lane, 1985; Morrow and Webster, 1991; Krumhardt et al., 1996). Figures 18 and 19 summarize key conodont biostratigraphic results and Figures 20-24 provide examples of some of the important conodont species in this study. Refer to Appendix C for a section on systematic paleontology and Appendix D for SEM images (plates) of selected conodont species.

Of note, most of the conodonts identified in this study are moderate to deeper-water species, such as the polygnathids and gnathodids of the Osagean and lower Meramecian as well as the vogelgnathids and lochrieids of the lower Chesterian. Interestingly, the upper Chesterian conodont fauna, which include the adetognathids and

rhachistognathids are more closely associated with shallow-water conodont biofacies, indicating the overall Mississippian depositional environment shallows upward.

Conodont element recoveries were too sparse for the author to assign biozones in the cores (discussed later). As such, age boundaries (not biozones) were assigned to the cores and constrained by allowing conodont age-dated intervals to be representative of a single third order depositional sequence, or to the nearest major change in lithology that could be traced in all the cores where conodont control was sufficient above and below the change in lithology for establishing multiple ages within a single third order depositional sequence (Figure 19). The author assumed he could rely on the third order sequence stratigraphic boundaries that were previously established by LeBlanc (2014) and Hill (2017) because major changes in conodont species were consistently noted around them, and conodont species of the same relative age were recovered from the same correlated third order depositional sequences, such as between the fourth (uppermost) third order depositional sequence of the Adkisson 1-33 and Elinore 1-18 (Figure 18), confirming the validity of the correlations to the author. The sequence stratigraphic correlations were also validated by fossil evidence in the transgressive system tracts of each third order depositional sequence which showed there were predictable patterns in the fossil evidence, suggesting a genetic relationship between them (Table 2).

Interestingly, no valuable conodont biostratigraphic information was recovered in the third (from the base) third order depositional sequence of the Adkisson 1-33, Winney 1-8, and Elinore 1-18 (Figure 18). The author is confident, however, that the depositional sequence without age control is Meramecian for at least two reasons: (1) average

representations of the type of sponge spicules in this depositional sequence were recovered from the Adkisson 1-33 and Winney 1-8 and imaged with the SEM (Figure 25) and found that triaxon spicules dominated the sequence, while only a few monaxon and tetraxon spicules were ever recovered. Franseen (2006) and others have shown that triaxon spicules dominate the Meramecian interval in the Oklahoma basin, monaxon forms dominated in the Osagean, and triaxon and tetraxon forms dominated in the Chesterian. Therefore, the dominance of triaxon spicules provides strong evidence that the depositional sequence without any age control is at least Meramecian. (2) The third order depositional sequence below and above the interval without age constraint from conodonts is basal-early Meramecian and basal-early Chesterian, respectively, indicating that a Meramecian (late Meramecian?) age designation for the interval best fits the data set and established sequence stratigraphic framework.

A tentative position for the Tournaisian-Visean contact was assigned in the Adkisson 1-33, Winney 1-8, and Elinore 1-18 (Figure 19). This assignment was principally based on the occurrence of conodont species *Polygnathus bischoffi* in the Elinore 1-18, which is only known to occur within the *anchoralis-latus* Zone (Perri and Spaletta, 1998). The top of the *anchoralis-latus* Zone (Perri and Spaletta, 1998), or alternatively the bottom of the *Gnathodus bulbosus* Zone (Lane and Brenkle, 2005; Boardman et al., 2013) marks the position of the Tournaisian-Visean contact. Because *G. bulbosus* specimens were the dominate conodont fauna recovered from the Elinore 1-18 just above where *P. bischoffi* was noted and there was a relatively major change in lithofacies that could be traced from the Adkisson 1-33, Winney 1-8, and Elinore 1-18, it is thought that enough evidence is present in the cores to tentatively assign the position of

the Tournaisian-Visean contact there. Importantly, because it is unclear where the lower limit of the *anchoralis-latus* Zone is in the Adkisson 1-33, Winney 1-8 and Elinore 1-18, an earlier part of the Osagean may be represented in the cores, particularly in the Adkisson 1-33 and Winney 1-8 where no age-diagnostic conodont species were found. Addressing whether the Visean-Superkovian contact is represented in any of the cores, the author compared the Chesterian conodont fauna from this study to Chesterian conodonts from other North American basins and their biozonations and found that the Chesterian conodont taxonomic forms in this study are not representative of Superkovian age conodonts. Therefore, no Visean-Superkovian contact was assigned in any of the study cores. Identification of the Tournaisian-Visean and Visean-Superkovian contacts are important for placing the Mississippian interval of north-central Oklahoma within a global Carboniferous stratigraphy.

Because there are no real indicators of relatively significant periods of missing geologic time in the Mississippian interval in the study cores (i.e., there is no evidence for major unconformities within the Mississippian stratigraphy studied), the biostratigraphic evidence is also meaningful in that it supports a more-or-less continuous production of some kind of organic material and inflow of sediments into the Oklahoma basin from the middle Osagean to the late Chesterian. Also, the thickness of the Chesterian section is more than double that of the Meramecian, and both the Meramecian and Chesterian sections are interpreted to have been deposited within a mid- to outer-ramp environment, indicating that the rate of sedimentation increased as did the rate of basin subsidence, both of which may be related to Late Mississippian orogenic activity of the Ouachita and/or Nemaha systems.

The age-dates assigned to the Mississippian interval in the study cores also provide important constraint for better determining their proper lithostratigraphic names. Future work is needed to assign a more formalized lithostratigraphic nomenclature to the Mississippian interval over the area studied.

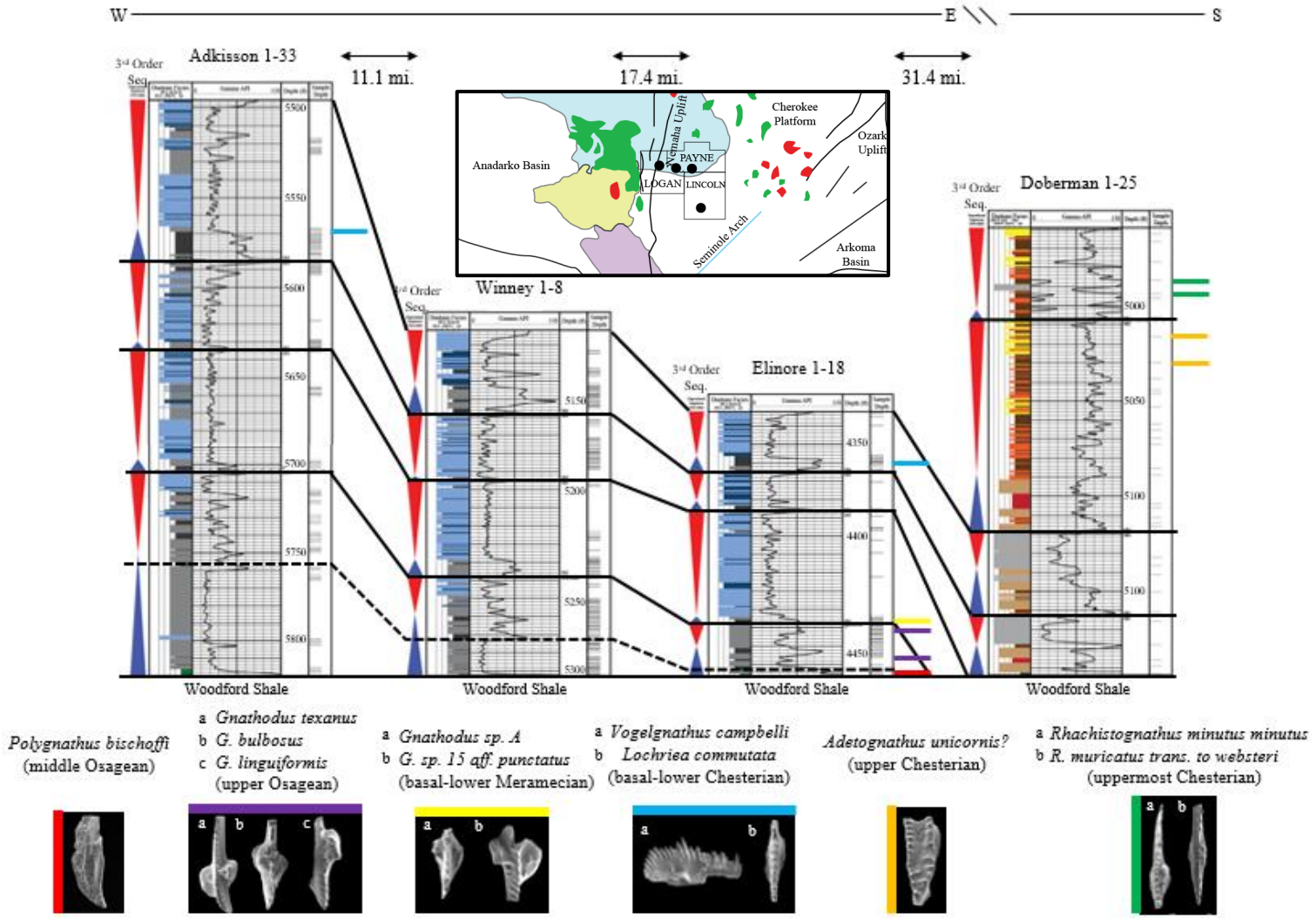

Figure 18. Summary of biostratigraphic results. Important conodont species are indicated toward the bottom of the figure, and they are color-coded and correspond to the depths where they were recovered in each of the cores. Note that the difference in thickness among the three cores oriented east-west along paleostrike is likely due to syndepositional faulting (LeBlanc, 2014). The solid black lines are third order depositional sequence boundaries established by LeBlanc (2014) in the Adkisson 1-33, Winney 1-8, and Elinore 1-18 and Hill (2017) in the Doberman 1-25 and from the Doberman to the Elinore 1-18. The dashed black line divides the middle from the upper Osagean and tentatively represents the Tournaisian-Visean contact.

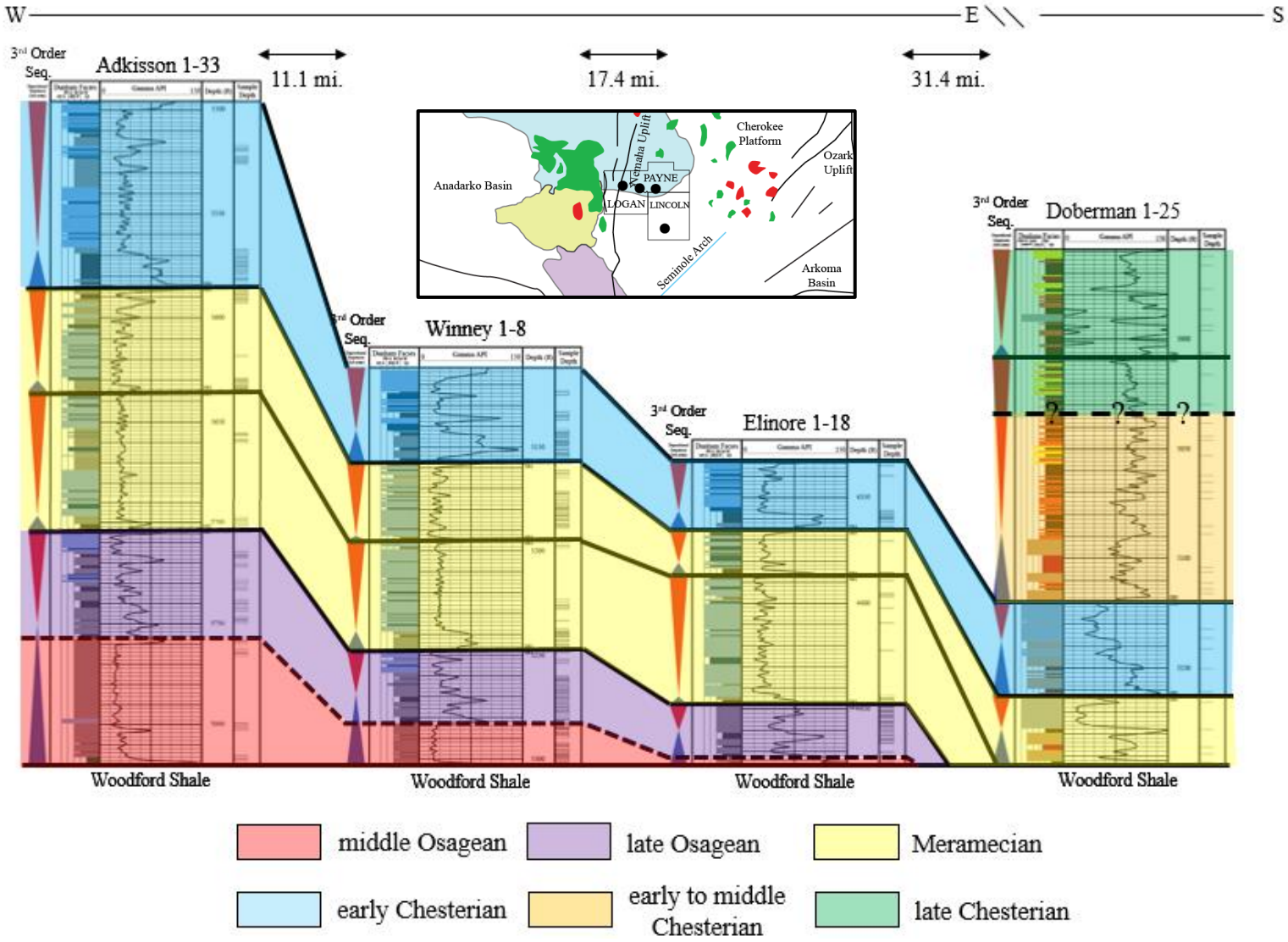

Figure 19. Summary of the interpreted geological ages and their boundaries of the "Mississippian Limestone" in north-central Oklahoma. The solid black lines are third order depositional sequence boundaries established by LeBlanc (2014) in the Adkisson 1-33, Winney 1-8, and Elinore 1-18 and Hill (2017) in the Doberman 1-25 and from the Doberman to the Elinore 1-18. The dashed black line divides the middle from the upper Osagean and tentatively represents the Tournaisian-Visean contact.

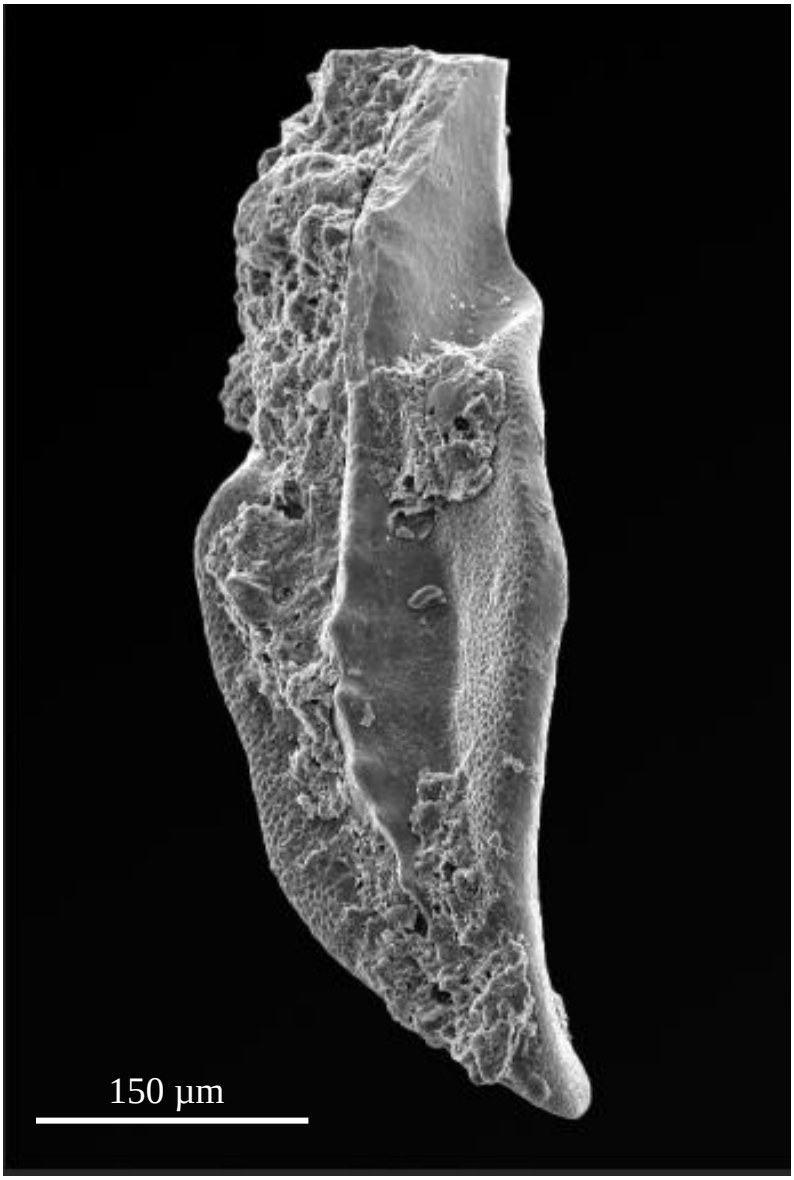

Figure 20. SEM image of *Polygnathus bischoffi*, recovered from the Elinore 1-18 a few feet above the Woodford-Mississippian contact. *Polygnathus bischoffi* is characteristic of the middle Osagean and has been noted as a key species for defining the *anchoralis-latus* Zone just below the Tournaisian-Visean contact (Perri and Spaletta, 1998).

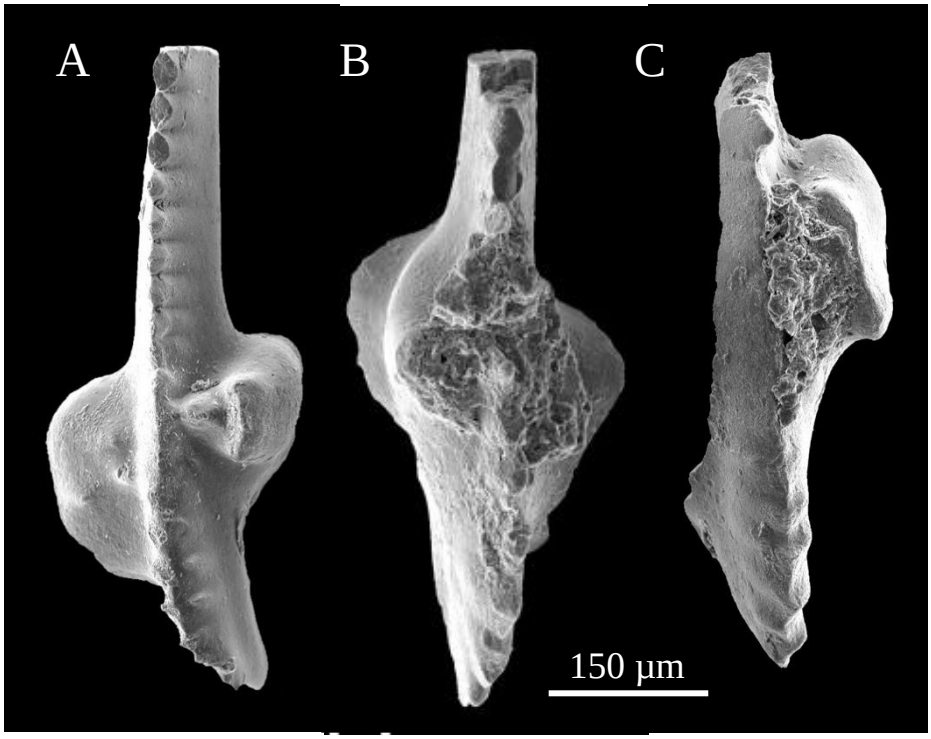

Figure 21. SEM images of (A) *Gnathodus texanus*, (B) *G. bulbosus,* and (C) *G. linguiformis*, recovered from the Elinore 1-18 a few feet below the bottom of the second (second the base) third order depositional sequence boundary. Together, these three species are most characteristic of the upper Osagean in the Oklahoma basin (e.g., Miller, 2015; Boardman et al., 2013).

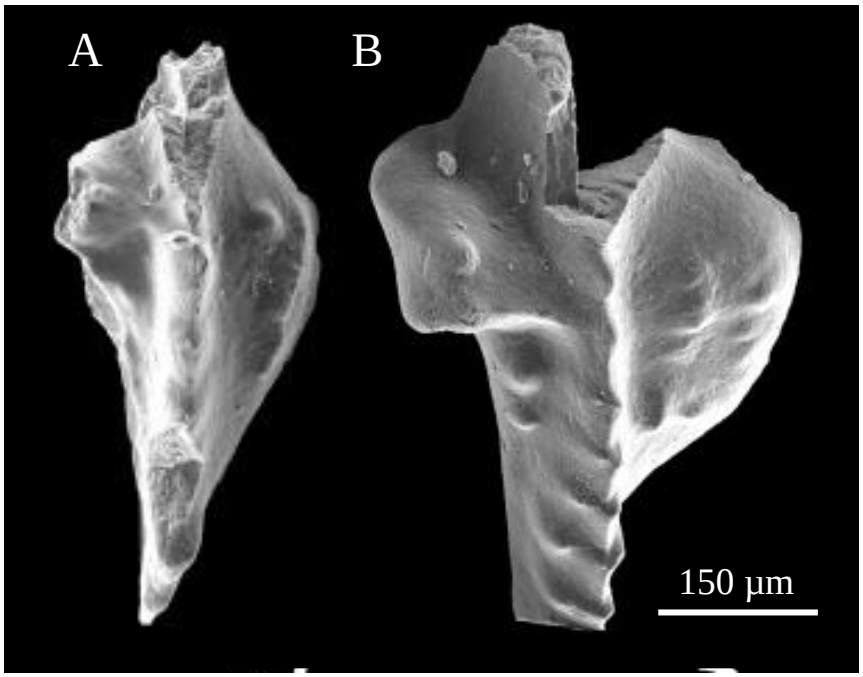

Figure 22. SEM images of (A) *Gnathodus sp. A* and (B) *G. sp. 15 (aff. punctatus)* recovered from the Elinore 1-18 just above the top of the second (from the base) third order depositional sequence boundary. Both species are characteristic of the basal-lower Meramecian in the Oklahoma basin (e.g., Boardman et al., 2013; Godwin, 2017).

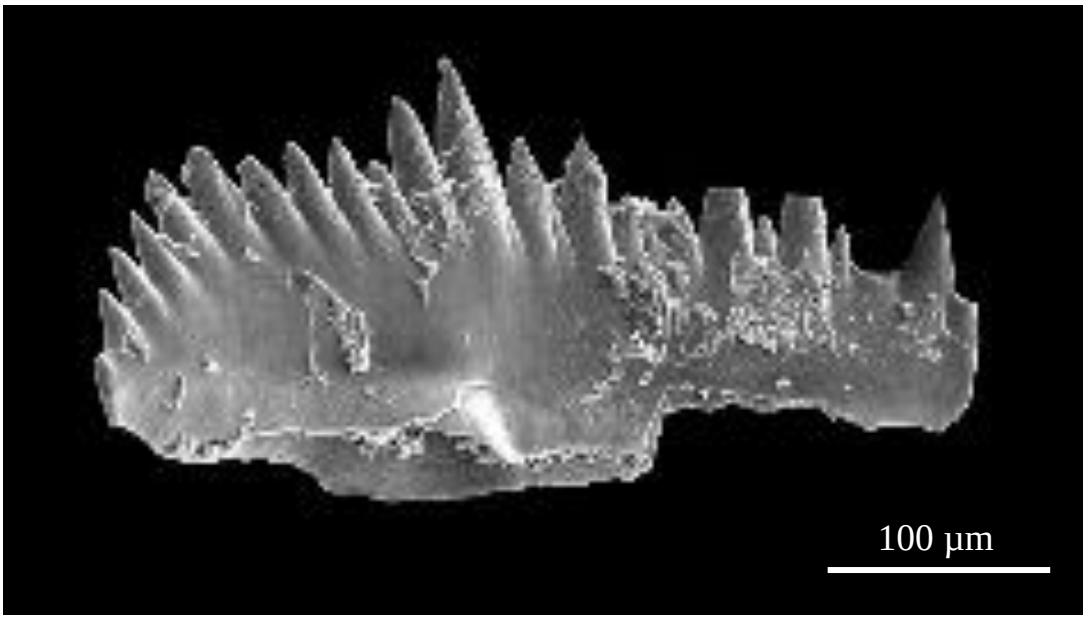

Figure 23. SEM image of *Vogelgnathus campbelli*, recovered from the Adkisson 1-33 several feet above the bottom of the fourth (uppermost) third order depositional sequence boundary. *V. campbelli* is characteristic of the basal-lower Chesterian in the Oklahoma basin (e.g., Godwin, 2017).

Figure 24. SEM image of *Rhachistognathus minutus minutus,* recovered from the Doberman 1-25 several feet above the bottom of the fourth (uppermost) third order depositional sequence boundary. *R. minutus minutus* is characteristic of the uppermost Chesterian (Visean) (e.g., Bahrami et al., 2014).

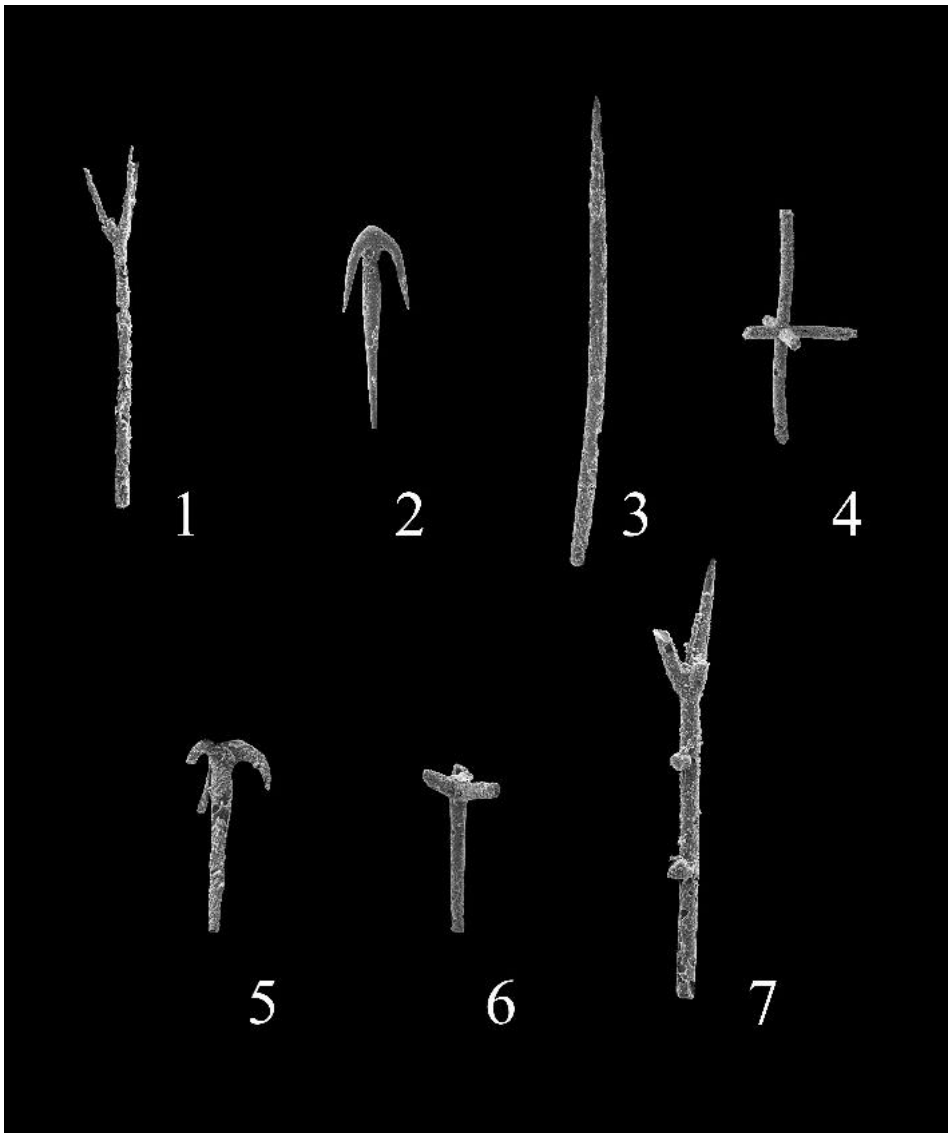

Figure 25. SEM images of a representative sample of siliceous sponge spicules in the third (from the base) third order depositional sequence of the Adkisson 1-33 (figs. 2-7) and Winney 1-8 (fig. 1). Figs. 1-2, 4-7: Triaxon forms; Fig. 3: Monaxon form. Osagean spicules are dominantly monaxon, while Chesterian forms are dominantly triaxon and tetraxon (Franseen, 2006, table 4 and references therein).

Table 2. Data table showing the similarity of relative abundance and distribution of fossil groups noted by the author during whole-rock processing in each third order depositional sequence of the study cores as initially correlated by LeBlanc (2014) and Hill (2017). The similarly between fossil groups and their relative abundances as described below in each correlated sequence suggests a genetic relationship does exist between them.

3rd order sequence	**Adkisson 1-33**	**Winney 1-8**	**Elinore 1-18**	**Doberman 1-25 (Sequences 1 and 2 coeval w/3 and 4 of the other cores, respectively)**
4	CR-rich; some BR & SP	CR-rich; some BR & SP	CR- and BR-rich; some SP	
3	SP-rich; minor CR at base	SP-rich; minor CR at base	SP-rich; some CR	
2	SP-rich; minor CR and BR	CR- and SP-rich; minor BR	CR- and SP-rich	BR at top; SP-rich
1	CR- & BR-rich base and SP-rich top	Some CR; BR-rich base & SP-rich top	Some CR; BR-rich base & SP-rich top	CR-rich base; SP-rich top

Comparison of Biostratigraphic Results with the Chemostratigraphic Record

Dupont (2016) constructed chemostratigraphic curves for the Adkisson 1-33, Winney 1-8, and Elinore 1-18 based on carbon isotope data. She then scaled her results with other carbon isotopic curves published for the Mississippian interval in select parts of the United States (Mii et al., 1999; Saltzman, 2002, 2003; Batt et al., 2007; Koch et al., 2014), basing her correlations on matching the shape and signal strength of her curves with the other data sets (Dupont, 2016). Figure 26 summarizes the author's reinterpretation of the chemostratigraphic curves constructed by Dupont (2016) in the Adkisson 1-33, Winney 1-8, and Elinore 1-18 based on the new conodont biostratigraphic evidence. The author's reinterpretation of the chemostratigraphic results is most interesting in that it strongly suggests the entire Meramecian interval is represented in the study cores and that the positive excursions in the mid-Osagean and basal Chesterian most closely match the results of Saltzman (2002, 2003) and Batt et al. (2007), indicating that the climatic drivers associated with these excursions probably affected Oklahoma basin deposition as well.

The author rescaled Dupont's (2016) chemostratigraphic data set by matching the core depths at which newly age-dating information was obtained with the same core depths from the chemostratigraphic data set and then resizing the chemostratigraphic curve to achieve a best fit among all the data sets available. Of note, the uppermost boundary for the chemostratigraphic curve in the Adkisson 1-33 was assigned below the Visean-Superkovian contact, as no conodonts characteristic of the Superkovian were identified in this study.

During the reinterpretation process, the author was less concerned about precisely matching the signal strength of carbon isotopic excursions, since they vary significantly among all the data sets presented, and focused more on fitting the general shape of the data with the other ones, while also honoring the biostratigraphic evidence. It is important to note that the curve-fitting process altered the 1:1 scale of the isotopic results as they were originally collected by their core depth; however, this is an expected and acceptable modification to the data set, since the isotopic data are meant to represent changes in the carbon isotopic signature with time and not depth. Significantly, this means that some data points appear condensed or stretched after the original data set, indicating there is potential to relate the condensing or stretching data points to relative changes in the rate of sediment deposition in the cores, especially if the data set had more biostratigraphic control points.

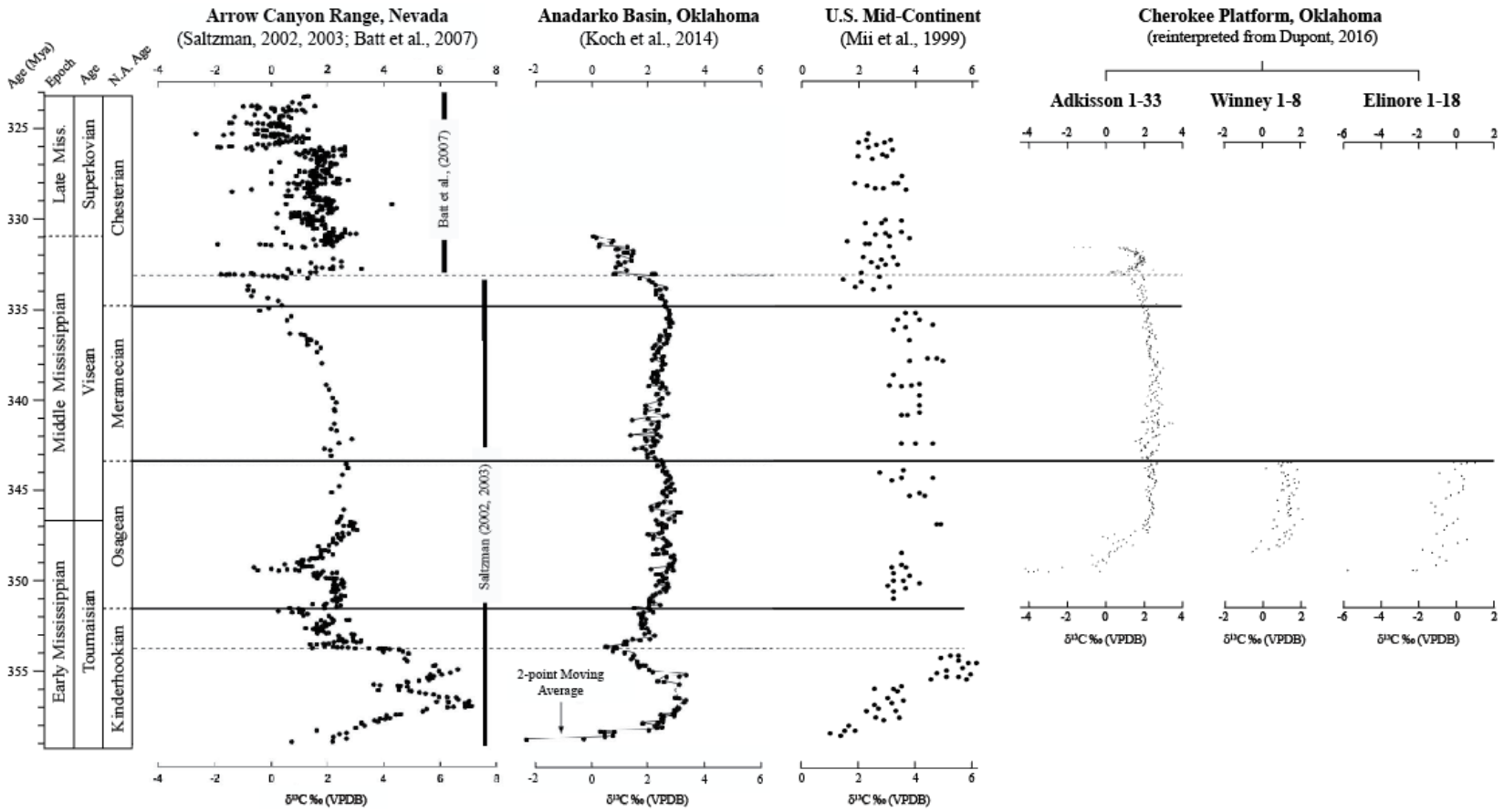

Figure 26. Summary of chemostratigraphic work showing carbon isotope data for the "Mississippian Limestone" in North America compiled by Mii et al. (1999), Saltzman (2002, 2003), Batt et al. (2007), Koch et al. (2014) and Dupont (2016). Dupont's (2016) isotopic data have been rescaled using the conodont biostratigraphic results of this study to demonstrate that the "Mississippian Limestone" interval over the area studied ranges from middle Osagean to late Chesterian in age.

Conodont Element Recovery and Preservation

A total of 689 highly-fragmented to well-preserved conodont elements were recovered from approximately 523 lb. (237 kg) of core, for an average of about 2 elements collected per 2.2 lb. (1 kg) whole-rock sample. Almost all conodont elements recovered were too poorly preserved for use as biostratigraphic markers. Based on light microscopy, just 40 conodont specimens between all the cores were well preserved enough for imaging with the SEM and about 30 specimens were identified to the species level. In total, 7 genera and 15 species types were identified.

The author attributes the low recoveries and poor preservation quality of conodont elements to three contributing factors: (1) prior studies have shown that conodont recoveries of southern Kansas, northern Oklahoma, and in places of the adjacent tristate region are expected overall to be low; (2) this study was conducted in core and not outcrop; and (3) the sampling methodology applied in this study largely biased collection sites to the mid-ramp and outer-ramp environments of the Oklahoma basin in north-central Oklahoma. A discussion of the first two of these factors follows, while the third factor is further addressed later in the chapter.

There is an overall lack of biostratigraphic work published on the "Mississippian Limestone" in south-central Kansas and north-central Oklahoma. This is not surprising since the interval does not outcrop anywhere over the region, making it less convenient to study from a biostratigraphic perspective. Prior attempts to conduct biostratigraphic analyses in the subsurface "Mississippian Limestone" over south-central Kansas and north-central Oklahoma have been made (Selk and Ciriacks, 1968; Mazzullo et al., 2009), but these studies yielded limited to unusable results. For example, Selk and Ciriacks

(1968) provided their interpretation of how Mississippian strata correlate to one another in logs in north-central Oklahoma based on conodont data they collected from some cored Mississippian wells over their area of interest. However, the authors reported they had sparse recoveries and did not include their methods for their biostratigraphic analysis or any images of the conodont elements they recovered (Selk and Ciriacks, 1968). Mazzullo et al. (2009) later attempted to constrain the age of the "Cowley" facies of the "Mississippian Limestone" across southern Kansas and northern Oklahoma, again using conodont elements recovered from core. The authors of that study reported that their recoveries and preservation quality of conodont elements were not satisfactory for use in relating them to the biostratigraphic record (Mazzullo et al., 2009).

Neither Selk and Ciriacks (1968) or Mazzullo et al. (2009) provided an explanation for why they had difficulty recovering useful conodont specimens from their cores; however, it is generally understood among conodont biostratigraphers that working from core can be difficult because (1) the amount of rock sample is very limited; (2) beds which contain high abundances of conodont elements cannot be resampled; and (3) rock samples cannot be obtained along a continuous lateral stratigraphic section for getting rock volumes that better represent later shifts in lithofacies and which may preferentially contain higher abundances of conodont elements. Experts in conodont biostratigraphy, such as Dr. Phil Heckel at the University of Iowa (personal communication, 2017) and Dr. Scott Ritter at Brigham Young University–Provo (personal communication, 2017), have also indicated during private conversations with the author that in cored Pennsylvanian and Permian intervals of the Anadarko Basin, where conodonts are generally more abundant per unit of rock volume to undergo analysis, sometimes very

little useful biostratigraphic evidence is recovered (e.g., Janousek, 2017) for reasons that are not well understood. Therefore, even though past studies and this one may collectively suggest that depositional and/or preservation conditions may not have been ideal for conodont elements throughout much of the Oklahoma basin, the relatively small number of cores analyzed to date indicates there is potential in the region for additional core(s) to yield better recoveries of well-preserved conodont elements. Another important point is that the results show that having even just a few age-diagnostic conodont specimens throughout the Mississippian interval provides valuable high-resolution time-stratigraphic information that no other age-dating method has been able to provide to date for the Oklahoma basin.

In contrast to prior conodont biostratigraphic studies conducted in core, studies conducted in "Mississippian Limestone" outcrops in the Oklahoma-Missouri-Arkansas tristate region have generally reported relatively high recoveries of conodont elements, with hundreds of conodont elements collected per pound or kilogram of rock sample in some cases (e.g., Boardman et al., 2013; Godwin, 2017). Other studies conducted within the same tristate region have reported recoveries that more closely compare with the results of this study (e.g., Shoeia, 2012; Miller, 2015). Miller (2015), for example, attributed his low recoveries from his outcrop work in the Ozarks to oversampling from coarse-grained carbonate facies, which he argued contained fewer conodonts per volume of rock because of the sediment dilution factor and the tendency of conodont elements to be fragmented or destroyed in relatively high-energy environments. Table 3 summarizes the recovery distribution of conodont elements by lithotype in each of the cores, and it generally supports the argument by Miller (2015) but not always. For example, this study

found decent recoveries from grainstone facies in the Adkisson 1-33 and Doberman 1-25, and that was with a facies bias applied against sampling from grainstone beds.

The “hit-or-miss” pattern of recovering conodont elements from Mississippian rocks over the U.S. Mid-Continent region, even in outcrop, suggests it is not just the “Mississippian Limestone” of south-central Kansas and north-central Oklahoma that bears sparse age-dating information and that it may be a problem basin wide; therefore, it requires a broader explanation for why conodont element recoveries and preservation quality within the basin are typically so poor. Interestingly, Godwin (2017) recently noted a similar basin wide recovery pattern in his doctoral research on Meramecian and Chesterian strata across northeastern Oklahoma and into the adjacent tristate region. He observed that it is generally difficult to recover conodont elements for the Meramecian and Chesterian compared with Kinderhookian and Osagean strata (Godwin, 2017).

Table 3. Charts showing how many and what relative percent of conodont elements came from each of the facies types in each of the cores. Note that columns labeled "n" represent the number of samples from the same facies type for each of the cores. Refer to figure 3ab for a reminder of what each facies number (type) means.

ADKISSON 1-33

Facies	Elements	n	avg. # of elements/facies	% elements in facies/total elements
5	1	5	0	1
4, 5	16	1	16	80
4	0	7	0	0
3, 5	0	4	0	0
3, 4	0	2	0	0
3	11	55	0	1
2, 4	0	1	0	0
2, 3	34	13	3	13
2	26	31	1	4
1	1	4	0	1
TOTAL:	89	123		100

ELINORE 1-18

Facies	Elements	n	avg. # of elements/facies	% elements in facies/total elements
5	0	8	0	0
4	0	3	0	0
3, 5	0	1	0	0
3	78	28	3	3
2, 4	0	1	0	0
2, 3	24	2	12	11
2	145	21	7	7
1, 3	33	1	33	32
1	98	2	49	47
TOTAL:	378	67		100

WINNEY 1-8

Facies	Elements	n	avg. # of elements/facies	% elements in facies/total elements
5	1	30	0	0
4, 5	0	3	0	0
4	3	8	0	4
3, 5	0	2	0	0
3, 4, 5	0	1	0	0
3, 4	0	1	0	0
3	19	62	0	3
2, 4	0	1	0	0
2, 3	28	18	2	16
2, 5	5	4	1	13
2	11	12	1	9
1, 3	7	2	4	35
1	2	1	2	20
TOTAL:	76	145		100

DOBERMAN 1-25

Facies	Elements	n	avg. # of elements/facies	% elements in facies/total elements
6	0	2	0	0
5	33	5	7	27
4	6	1	6	25
3	8	3	3	11
2,4	0	1	0	0
2,3	7	4	2	7
2	90	17	5	22
1	2	1	2	8
TOTAL:	146	34		100

Geologic Processes that Affected Conodont Elements

Just under 75% of the conodont elements obtained from the Mississippian interval in the cores were fragmented prior to their recovery. Evidence for the post-depositional fragmentation of conodont elements include (1) fractured surfaces displaying some type of mineralization (i.e., thin pyrite or vivianite coating, or iron oxide staining) that would require geologic time to form; and (2) sediment (mud) cemented to fractured surfaces, demonstrating that fractures existed prior to the processing of the whole-rock sample (Figure 27). In lieu of the observation that most of the elements were fragmented and weathered beyond identification prior to this study, the author considered three major post-depositional processes to explain why the elements were so poorly preserved in the geologic record. They are (1) sediment compaction; (2) bioerosion; and (3) reworking during storm events. In the following paragraphs, the first two of these factors are addressed, after which the third factor is discussed in greater detail in the next section.

LeBlanc (2014) examined more than 100 thin sections and described core in the Adkisson 1-33, Winney 1-8, and Elinore 1-18 but observed little evidence for differential compaction in either her thin section work or core descriptions. Similarly, Hill (2017) did not focus on describing the effects of compaction in the Doberman 1-25. As such, it is difficult to estimate the degree to which conodont elements and other fossil evidence, such as brachiopods, bryozoans, or crinoids were impacted by compaction. However, the author noted during whole-rock processing that whole specimens of thin-shelled brachiopods were sometimes preserved with two or three vertical to sub-vertical fractures running through them. Presumably, the brachiopod shells had to be deposited, then buried for them to be preserved in-situ and were later fragmented as the sediments around them

compacted from overburden stresses. More often, brachiopod shells were collections of fragmented material (shell hash) that overlapped one another along a bedding plane, indicating that the whole specimens were fragmented and transported prior to their burial. Prior studies have shown that conodont elements may also show signs of compaction in SEM work (e.g., von Bitter and Purnell, 2005). Compacted conodont elements display characteristic fracture patterns (Purnell and Jones, 2012), none of which were deterministically observed in this study. Therefore, while compaction may help to explain the low preservation quality of the conodont elements and may have influenced the data set, the author is not convinced that compaction fully explains the overall poor preservation quality of the conodont elements, since most of the brachiopod shells and conodont elements analyzed did not display convincing evidence for compaction features. In addition, it is well known that carbonate sediments cement early after their deposition (Grammer et al., 1993; 1999), which could have reasonably provided a way for the conodont elements to resist fragmentation by their becoming cemented before the sediments were significantly buried and compacted.

As the author indicated earlier, bioerosion may be another contributing factor to the poor preservation quality of conodont elements. Bioturbated zones are evident in each of the cores described by LeBlanc (2014) and Hill (2017), especially in muddier facies. However, the author noted that poorly preserved collections of conodont elements did not occur preferentially within burrowed or bioturbated zones, indicating that some other process much more geographic and stratigraphically extensive contributed to the degradation of the elements in all the cores. Evidence for borings, or teeth marks, or anything else which directly indicated the conodont elements recovered from this study

underwent any bioerosion was not observed. Therefore, it is possible that burrowed and bioturbated zones contributed to the degradation of conodont elements, but it is unlikely to be the central reason for the low preservation quality of conodont elements in this data set. Therefore, the author turns to another process to explain the preservation of conodonts: reworking of the conodont elements during frequent storm events.

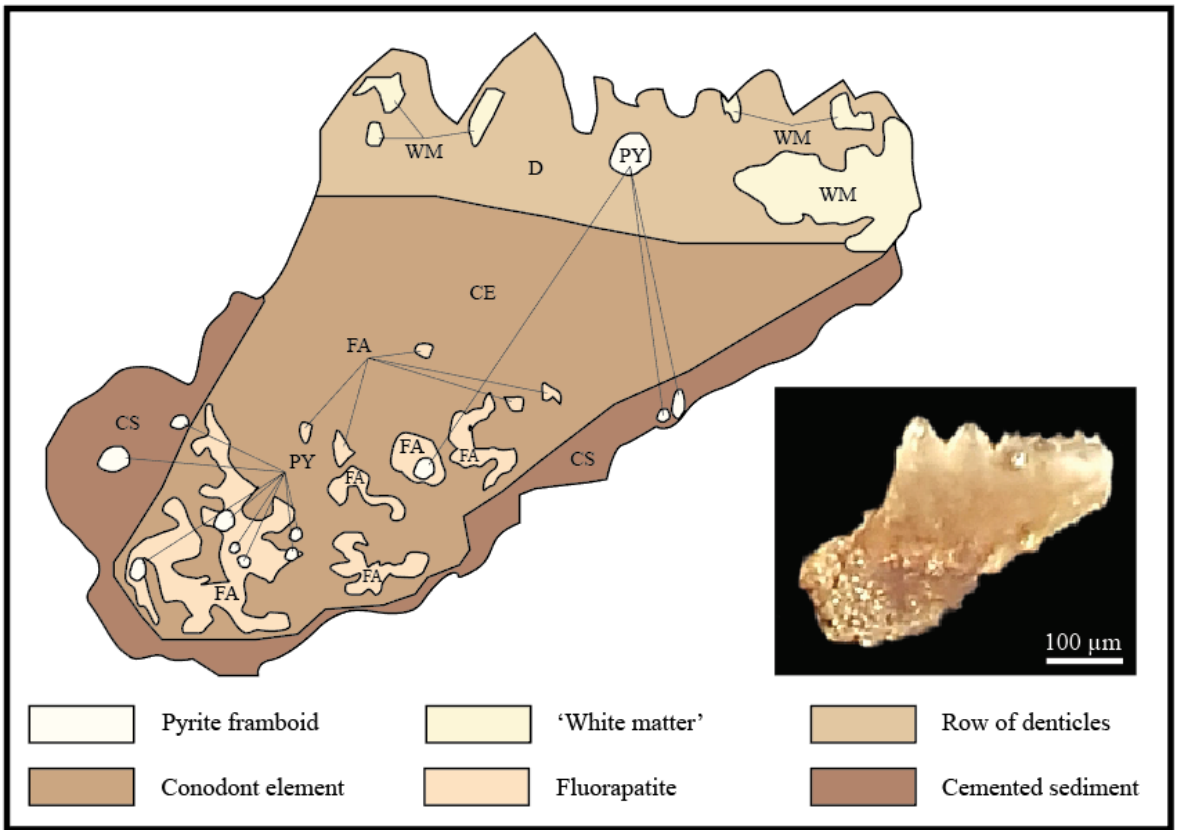

Figure 27. Schematic drawing of a typical conodont element recovered from core created from making observations of actual evidence (element pictured in the black background). Note how the conodont element displays evidence of cemented sediment around its edges and fractured surfaces as well as the mineralization (in this case pyritization) that is also present.

Reworked Storm Intervals

A clear definition of what is meant by the term "reworked storm intervals" does not exist in the literature, though it is used most frequently by biostratigraphers and in this thesis to indicate that a bed has been disturbed in some way by a storm or storm events sometime after it was deposited up to the point at which it reached burial depths beyond the influence of storms. Reworked storm intervals and storm deposits (tempestites) in general are common components on carbonate ramps, specifically within the mid-ramp and outer-ramp environments during periods of geologic history that lacked major reef-building organisms, such as during the Mississippian Subperiod (Figure 29). Evidence that the carbonate ramp of the Oklahoma basin is storm-dominated include frequent occurrences of swaley and hummocky cross-stratification in beds throughout the Mississippian interval in the study cores; dominance of high-energy facies and linear sand belts oriented across strike in the mid-ramp and outer-ramp environments in the study cores, indicating high-energy, wave-dominated (non-tidal flow) environmental conditions; and storm deposits commonly observed in the outer-ramp to distal outer-ramp facies of the study cores (LeBlanc, 2014; Hill, 2017).

Macke and Nichols (2007) observed after an extensive literature review that several authors working in Mississippian age strata over the U.S. Mid-Continent have already called on storm reworking to explain low the preservation quality of their conodont element collections, such as in the Pitkin Limestone (Chesterian), Arkansas and Mississippian interval in southern Wales of the United Kingdom (both examples are also summarized by Werner, 2004). Therefore, it should be no surprise that there was storm reworking in the Oklahoma basin, as it has already been noted to occur in places near the

study area and around the world, and it is also an expected aspect of deposition in the OSU-Industry Mississippian Consortium's depositional model.

Most often, conodont biostratigraphers identify reworked intervals by observing significantly different age conodont species within the same bed (time-averaged species) that are deposited within a suspected or known storm bed. Storm reworked intervals do not often contain such long-term and obvious changes in conodont species because they represent relatively brief moments in geologic time (i.e., hundreds to thousands of years). Therefore, the author had to use other techniques for determining if the conodont elements in the study cores were reworked by storms. To this end, the author noted that past workers have focused on using characteristics such as color, roundness, smoothness, and sorting of conodont elements to determine storm reworked intervals. The right combination of these factors differentiates a conodont element collection from having been reworked in bottom currents or storm events (e.g., sorted element collections are storm reworked while hydrodynamically concentrated element collections are bottom current reworked). Refer to Appendix A for a detailed list of where reworked intervals occur in the cores.

Observing the differences in color and texture of a conodont element is the easiest to determine whether it has been reworked by storms. Conodont elements change color and for several reasons. When conodont elements undergo diagenetic change from heating during burial, impact events, or hydrothermal fluids for example, its' color appears dull gray or white (bleached) and may have patches of dark brown, black, white, and gray left on its surfaces (Armstrong et al., 1992; Konigshof, 2003; Mason et al., 2008). Additionally, the microstructure of conodonts elements is altered during these

diagenetic processes, and these types of alteration can all be observed and differentiated in plain light and in SEM. However, if conodont elements overexposed to acids they appear a dull to opaque white, with pitted and jagged surfaces and reaction surfaces on edges of elements that look like "noise" on an analog television (Collinson, 1963; Miller, 2015). But if conodont elements are storm reworked, then they display a characteristic frosted, rounded, smoothed character on their surfaces and have a uniform pearly white color and luster to them. At that point, the level of sorting and abundance of specimens also helps determine if they were affected by storms. Therefore, to determine if conodont elements were either diagenetically altered, damaged by acid treatment, or reworked, the author conducted experiments and looked at SEM images that differentiated between the three types of effects.

A few elements that were recovered from the cores and determined to be well-preserved but have no possible biostratigraphic application were left in acid for several days. The author observed each day how these elements changed over time and compared against elements recovered from residues of whole-rock samples that were already noted to be pearly white (representative of a storm reworked conodont element). From this experiment, the author noted that conodont elements from the residues had a uniform pearly white luster and their surfaces appeared to be smoothed and their edges rounded. In contrast, conodont elements which sat in acid for prolonged periods during whole-rock processing appeared similarly white, but they lacked any luster and their surfaces became pitted, with their edges appearing jagged and displaying a relatively bright white reaction rim on surfaces where the element was thinnest. Only a handful of conodont elements recovered "as is" from the rock record displayed any evidence for having been

overexposed to acid treatment, suggesting the whitened conodont elements recovered from the residues were either reworked intervals or (possibly) the product a diagenetic alteration. However, the possibility of the elements being the product of diagenesis was ruled out because they did not fit the description of what diagenetically altered conodont elements should look like in plain view or under the SEM. Diagenesis was also ruled out because the elements have an almost ubiquitous low CAI and many of the "frosted" white specimens have organic matter preserved in the form of fluorapatite (appears blue-green), the latter of which is one of the first things removed when elements interact with diagenetic fluids. Of note, conodont elements from the upper part of the Winney 1-8 core (above 5,200 feet subsea) and in the Elinore 1-18 and Doberman 1-25 cores averaged about 1 on the CAI. In the lower part of the Winney 1-8 core (below 5,200 feet subsea) and in the Adkisson 1-33 core, conodont elements averaged about 2 on the same scale (Figure 13). These results are indicative of a relatively shallow burial history, which resulted in very minor diagenetic alternation of the conodont elements over geologic time.

Frequently, conodont specimens collected from the same whole-rock sample contained some pearly white elements while other specimens did not display any whitening. This observation is indicative of the time-average nature of storm reworked deposits, where the older specimens tend to experience more weathering affects from storms than their younger counterparts and the amount of time represented by conodont species variation is geologically insignificant (e.g.., all middle Osagean fauna). Importantly, the same conodont element collections containing specimens of white to naturally color also tended to be sorted by the type of element (e.g., M-elements only)

and size (i.e., similarly-sized fragments of conodont elements). McGoff (1991) demonstrated during his experimental lab work how conodont elements tend to fragment and sort themselves in a flow tube if a current is induced through the tube, such as what might happen if conodont elements were disturbed by a storm event. He also noted that conodont elements become hydraulically concentrated if run through a unidirectional flow tube, but they do not tend to concentrate themselves under storm-simulated conditions where the flow direction is varied (McGoff, 1991). Because the recoveries in this study were relatively low (a few to tens of specimens), the author concluded that most were not hydraulically concentrated, except for those occurring at the Mississippian-Woodford contact where they do occur in larger numbers (hundreds per kg. of whole-rock sample), probably concentrated from current flow during initial stages of flooding on the ramp.

Together, the observations for conodont elements being reworked by frequent storm events strongly support that most conodont elements were deposited within a storm-dominated environment, which led to their overall low preservation quality. Figure 28 summarizes the differences of diagenetically altered and acid-etched conodonts in general and storm reworked conodonts from this study. Because the conodont elements recovered were sampled most heavily from lithofacies interpreted to have originated on mid-ramp to outer-ramp settings that are characterized by the presence of storm deposits, it is suggested that the mid-ramp and outer-ramp are not ideal environments for preserving conodont elements in the Oklahoma basin. Conodont element recoveries and preservation quality may have also been affected to some degree by sediment compaction and bioerosion, in addition to surviving the destructive method of processing of the

whole-rock samples and experiencing minor diagenetic changes (recorded by the low CAI of all conodont elements recovered), though there is no major unifying evidence for these other processes to explain the overall preservation quality of conodonts in this study and others previously conducted within the basin (e.g., Mazzullo et al., 2009; Shoeia, 2012; Miller, 2015).

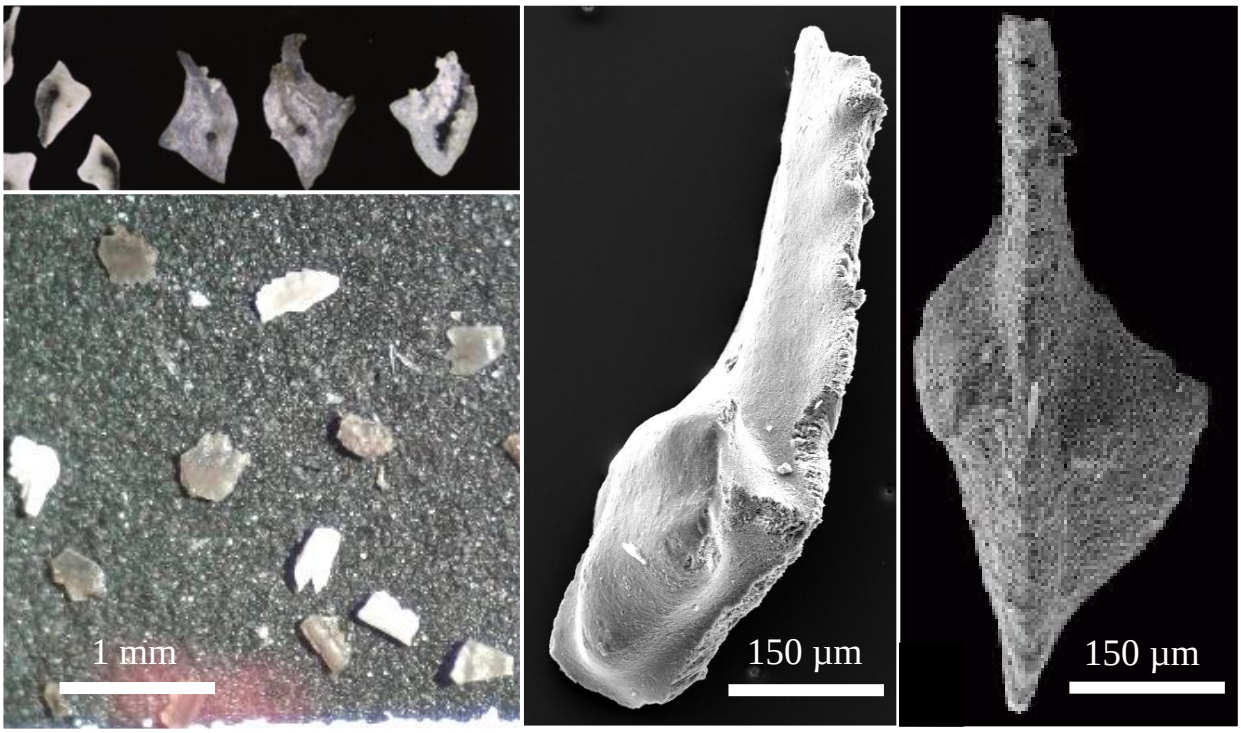

Figure 28. A) Hydrothermally altered conodonts (CAI 6.5-7.5) under normal light (Konigshof, 2003). B) Example of an interpreted storm reworked interval of the Elinore 1-18 based on conodont evidence under a light microscope (40x). Note how the elements are all similarly sized and shaped (sorted) and how some specimens appear bright white while others are not. C) Example of a storm reworked conodont under SEM from this study. Note how smooth its surfaces are, the rounding of the upper portions of the denticles along the carina. D) Example from Miller (2015) of one of his acid-etched conodont elements recovered from Mississippian outcrops along the southwestern Ozarks. Note its dull, grainy texture that resembles the "noise" of an analog television.

Stratigraphic Controls on Conodont Element Recoveries

It was suspected early in his investigation that sequence stratigraphic boundaries and major lithofacies changes, both representative of major changes in the depositional environment, might influence where abundant conodont element collections occur in the cores. Both assumptions were predicated on a study that reported where conodont elements are most recovered worldwide based on their occurrences within a time-stratigraphic framework and different lithologies (Purnell and Donoghue, 2005). The study found that on a global average, conodont element recoveries are highest in maximum flooding surfaces (condensed sections) and in mudrocks containing highly biodiverse fauna (Purnell and Donoghue, 2005).

To determine if the recovery results of this study would compare with global average recoveries, the author noted that generally, muddy facies of transgressive cycles and maximum flooding surfaces contained the highest abundances of conodonts. However, the single best predictor for determining where conodont elements are most heavily concentrated was whole-rock sampling from intervals with relatively high biodiversity. Both results are consistent with the global averages reported in Purnell and Donoghue (2005). Refer to Appendix A for a detailed list of where these "high biodiversity" intervals occurred in the cores based on the diversity of fossil specimens recovered from each whole-rock sample.

During recovery, the author noted that higher abundances of conodont elements occur in third order transgressive facies in the Adkisson 1-33, Winney 1-8, and Elinore 1-18 cores, while the highest abundances in the Doberman 1-25 occur in third order regressive facies. The author interprets this to mean that in the mid-ramp environment,

such as is best represented in the Adkisson 1-33, Winney 1-8, and Elinore 1-18 cores, conodonts are more abundant during the long-term (third order) transgressive cycles. In contrast, conodonts are more abundant in the outer-ramp and distal-outer ramp environments, such as best represented in the Doberman 1-25, during long-term regressive cycles. This recovery relationship means that during stages of third order flooding events (which characterizes the strata packages of the Oklahoma basin and represent the major events in relative sea level change), conodont populations flourished in environments that were nearer to the shore than in times of regression.

The results of Miller (2015) and Godwin (2017) are consistent with the authors interpretation of conodonts having a sequence stratigraphic control on their recoveries. Miller (2015) conducted his research in Mississippian outcrops of northwestern Arkansas that were dominantly representative of inner-ramp and mid-ramp environments and his highest recoveries were from transgressive facies. In comparison, Godwin (2017) sampled from more outer-ramp and distal environments of the "Mississippian Limestone" throughout northeastern Oklahoma and the adjacent tristate region and noted that his highest conodont element recoveries were in regressive facies. While it remains unclear what geologic processes and factors are working together to yield such a trend in collections of conodont elements from the stratigraphic record, the author predicts that a more effective strategy for sampling conodonts in the Oklahoma basin for the future is to preferentially obtain whole-rock samples from transgressive facies of third-order depositional sequences if working in an inner-ramp to mid-ramp environment, or from regressive facies of third-order depositional sequences if working in a more distal location on the ramp.

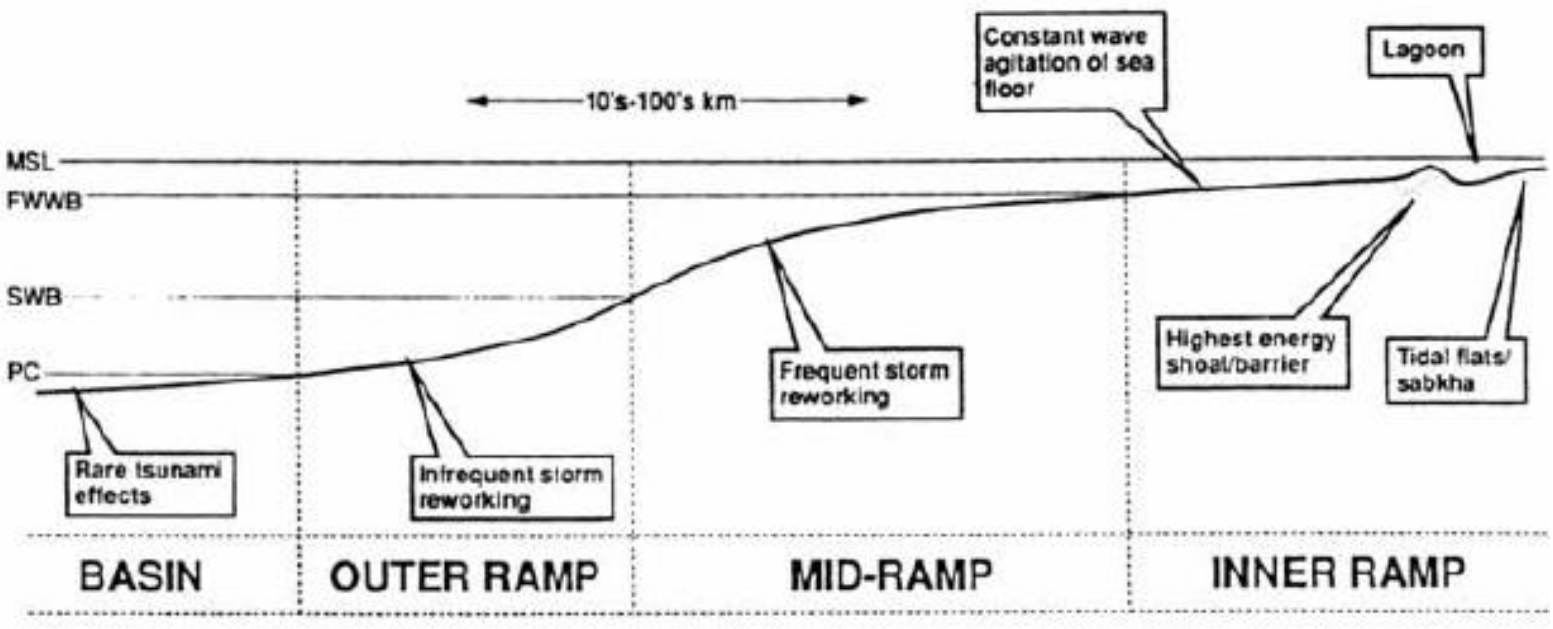

Figure 29. Generalized depositional model of a typical carbonate ramp setting. The figure shows how frequent and infrequent reworking of deposits is expected within the mid-ramp and outer-ramp environments, respectively. Figure from Burchette and Wright (1992).

CHAPTER VIII

SUMMARY AND CONCLUSIONS

Summary of Results and Answers to Major Research Questions

Conodont biostratigraphic results in combination with other lines of stratigraphic evidence have indicated that the Mississippian interval ranges from middle Osagean to late Chesterian in age. The results of this investigation support the initial hypothesis and help provide answers to the major research questions of this thesis. One important takeaway is that having even a few age diagnostic conodont species helps to greatly constrain the time-stratigraphic framework over areas that lack age-dating information in the "Mississippian Limestone" interval and provide data for better constraining depositional models of the basin and Mississippian reservoirs. What follows is a summary of answers to this study's major research questions and other major conclusions:

- Environmental conditions for the conodont animal of the Oklahoma basin over the area studied were not ideal, as indicated by the relatively low biodiversity, abundances, and preservation quality of fauna in the cores. Conditions were also not well-suited for preserving fossil evidence, as primarily indicated by the storm reworked intervals from which most of the

conodont element collections are interpreted to originate from. Most of the conodont species are indicative of deeper-water conditions on the carbonate ramp, with more moderate to shallow-water species appearing only in the upper-uppermost Chesterian

- Conodont elements in this study experienced very little diagenetic alteration, as indicated by their low CAI values and rare fluorapatite preserved on select specimens. There is also little evidence for extensive destruction of the elements because of compaction or bioerosion
- The best predictor for recovering relatively high numbers of conodont elements (in this study) was in processing whole-rock samples of muddy skeletal lithofacies with relatively high biodiversity in them. Conodont elements also appeared to occur most abundantly in transgressive facies within mid-ramp environments and more abundantly in regressive facies within outer-ramp to more distal environments
- Conodont elements recovered help constrain unconformable surfaces of the Woodford-Mississippian and Mississippian-Pennsylvanian contacts and provide evidence for a rather continual subsidence of and sedimentation rate in the Oklahoma basin, with these relative rates increasing markedly in the Chesterian. Within the stratigraphic interval, the data control points (i.e., where the biostratigraphically significant species occur in the section) help to constrain sequence stratigraphic interpretations up to third order boundary picks

- Further work is needed to apply formalized lithostratigraphic names to the Mississippian interval over the area studied, and the age-dating evidence provided should help future workers to separate the interval into its more formalized lithostratigraphic units
- The major limitations of this study are that (1) the whole-rock sampling method prevented the recovery and identification of conodonts from the entire length of each core, thereby limiting the biostratigraphic results; (2) the reinterpretation of the chemostratigraphic curve presented for three of the study cores was shown to be highly susceptible to change based on new biostratigraphic evidence, and therefore, requires additional age-constraint in future studies before it is considered well-constrained; and (3) relatively low recoveries of conodonts in this study, particularly in the Adkisson 1-33 and Winney 1-8 and lower part of the Doberman 1-25, may, may bias the biostratigraphic results and interpretation of the author, as most of the data points and interpretation are based on conodonts of the Elinore 1-18 and upper part of the Doberman 1-25 and the sequence stratigraphic framework previously established by LeBlanc (2014) and Hill (2017)
- Overall, the conodont biostratigraphic results of this study have improved the understanding of the geologic age range that is represented over the area studied within a global Carboniferous stratigraphy and provided new age-dating information to the “Mississippian Limestone” in the region that can be used in future studies conducted within the basin

Future Work

This study recommends the following future work to be conducted within the Oklahoma basin: (1) more studies on the Meramecian and Chesterian age rocks of the "Mississippian Limestone" for developing better stratigraphic and reservoir models of the Oklahoma basin and construction of a more robust paleogeographic map of Late Mississippian deposition; (2) additional conodont biostratigraphic studies over south-central Kansas and north-central Oklahoma using the sampling recommendations the author has suggested to obtain better recoveries and preservation quality of conodont elements for analysis; and more specifically (3) a conodont biostratigraphic study which compares sampling from north and south of the Kanoka Ridge for determining its effect on conodont element recoveries. It may be that conodont element recoveries have been historically better in Kansas, Missouri, and northern Arkansas because of this structural feature, which on its north flank would have provided some relief from severe storm events, leading to the proliferation of life and better preservation quality of conodont elements, versus its southern flank where the ramp environment was overall less protected from storm surges.

REFERENCES

Aldridge, R.J. and Briggs, D.E.G., 2009, The discovery of conodont anatomy and its importance for understanding the early history of vertebrates, *in* Sepkoski, D. and Ruse, M., eds., The Paleobiological Revolution–Essays on the Growth of Modern Paleontology: Chicago, University of Chicago Press, p. 73-88, doi: 10.7208/chicago/9780226748597.003. 0005.

Andrews, R.D. and Holland, A., 2015, Statement on Oklahoma seismicity: Oklahoma Geological Survey, http://wichita.ogs.ou.edu/documents/OGS_Statement-Earthquakes-4-21-15.pdf (accessed September 2017).

Appleseth, C.J., 2017, High-resolution sequence stratigraphy and reservoir characterization of Mississippian strata in central and eastern Oklahoma: American Association of Petroleum Geologists 2017 Mid-Continent Section Meeting Poster Presentation, 2 October, Oklahoma City, Oklahoma.

Armstrong, A.K., Mamet, B.L., and Repetski, J.E., 1992, Stratigraphy of the Mississippian System, south-central Colorado and north-central New Mexico, *in* Armstrong A.K., ed., Evolution of Sedimentary Basins–Uinta and Piceance Basins: United States Geological Survey Bulletin 1787-EE, 30 p.

Ausich, W.I., Kammer, T.W., and Baumiller, T.K., 1994, Demise of the Middle Paleozoic crinoid fauna–a single extinction event or rapid faunal turnover?: Paleobiology, v. 20, p. 345-361.

Bahrami, A., Boncheva, I., Konigshof, P., Yazdi, M., and Ebrahimi Khan-Abadi, A., 2014, Conodonts of the Mississippian/Pennsylvanian boundary interval in central Iran: Journal of Asian Earth Sciences, v. 92, p. 187-200.

Barham, M., 2015, Comprehending conodonts: Geology Today, v. 31, p. 74-80, doi: 10.1111/gto.12092.

Barrick, J.E., 2001, Microscopic marvels of the Paleozoic–conodonts: Barrick Lab, http://barricklab.org/twiki/ pub/Lab/LinkList/Barrick_Conodonts.pdf (accessed December, 2015).

Baesemann, J.F. and Lane, H.R., 1985, Taxonomy of the genus *Rhachistognathus* Dunn (Conodonta–Late Mississippian to Early Pennsylvanian), *in* Lane, H.R. and Ziegler, W., eds., Toward a Boundary in the Middle of the Carboniferous–Stratigraphy and Paleontology: Courier Forschungsinstitut Senckenberg 74, p. 93-115.

Bassler, R.S., 1925, Classification and stratigraphic use of the conodonts: Geological Society of America Bulletin, v. 36, p. 218-220.

Bateson, W., 1886, The ancestry of the chordata: Quarterly Journal of Microscopy Science, v. 26, p. 535–571.

Batt, L.S., Montanez, I.P., Isaacson, P., Pope, M.C., Butts, S.H., Abplanalp, J., 2007, Multi-carbonate component reconstruction of mid-Carboniferous (Chesterian)

seawater $\delta^{13}C$: Paleogeography, Paleoclimatology, Paleoecology, v. 256, p. 298-318, doi: 10.1016/j.palaeo.2007.02.049.

Bertalott, J.R., 2014, Core- and log-based stratigraphic framework of Mississippian limestone in portions of north-central Oklahoma [M.S. Thesis]: Stillwater, Oklahoma State University, 144 p.

Blakely, R., 2017, North American key time slices: Deep Time Maps, http://deeptimemaps.com/wp-content/uploads/2016/05/NAM_key-345Ma_EMiss.png (accessed March 2017).

Boardman, D.R., Mazzullo, S.J., Wilhite, B.W., Puckette, J.O., Thompson, T.L., and Woolsey, I.W., 2010, Diachronous prograding carbonate wedges from the Burlington Shelf to the southern distal shelf/basin in the southern flanks of the Ozarks: Abstracts with Programs, North-Central and South-Central Meeting Geological Society of America, v. 42, p. 41.

Boardman D.R., Mazzullo, S.J., Wilhite, B.W., Godwin, C.J., and Bryan, M., 2011, Lower Mississippian Burlington shelf derived diachronous prograding carbonate wedges, the western flanks of the Ozarks: Midcontinent Section Meeting American Association of Petroleum Geologists, 1-4 October, Oklahoma City, Oklahoma.

Boardman, D.R., Thompson, T.L., Godwin, C.J., Mazzullo, S.J., Wilhite, B.W., and Morris, B.T., 2013, High-resolution conodont zonation for Kinderhookian (middle Tournaisian) and Osagean (upper Tournaisian-lower Visean) strata of the western edge of the Ozark Plateau, North America: Oklahoma City Geological Society Shale Shaker, v. 64, p. 98-151.

Branch, J.N.H., 1988, Conodonts from the Welden Limestone (Osagean, Mississippian) south-central Oklahoma [M.S. Thesis]: Lubbock, Texas Tech University, 126 p.

Branson, C.C., 1959, Mississippian boundaries and subdivisions in Mid-Continent: Tulsa Geological Society Digest, v. 27, p. 85-89.

Branson, E.B. and Mehl, M.G., 1933, A study of Hinde's types of conodonts preserved in the British Museum, *in* Conodont Studies no. 2: Missouri University Studies, v. 8, p. 133-167.

Branson E. B. and Mehl, M.G., 1938, Conodonts from the Lower Mississippian of Missouri, *in* Branson, E.B., ed., Stratigraphy and Paleontology of the Lower Mississippian of Missouri, part 2: Missouri University Studies, v. 13, p. 128-206.

Branson, E.B. and Mehl, M.G., 1941a, New and little-known Carboniferous conodont genera: Journal of Paleontology, v. 15, p. 97-106.

Branson, E.B. and Mehl, M.G., 1941b, Conodonts from the Keokuk Formation: Journal of the Scientific Laboratories of Denison University, v. 35, p. 179-188.

Briggs, D.E.G., Clarkson, E.N.K., and Aldridge, R.J., 1983, The conodont animal: Lethaia, v. 16, p. 1-14, doi:10.1111/j.1502-3931.1983.tb01993.x.

Buggisch, W., Joachimski, M.M., Sevastopulo, G., Morrow, J.R., 2008, Mississippian $\delta^{13}C$ and conodont apatite $\delta^{18}O$ records–their relation to the Late Palaeozoic Glaciation: Palaeogeography, Palaeoclimatology, Palaeoecology, v. 268, p.273 292.

Burchette, T.P. and Wright, V.P., 1992, Carbonate ramp depositional systems: Sedimentary Geology, v. 79, p. 3-57.

Butler, M., 1973, Lower Carboniferous conodont faunas from the eastern Mendips, England: Paleontology, v. 16, p. 477-517.

Cahill, T., 2014, Subsurface sequence stratigraphy and reservoir characterization of the Mississippian limestone (Kinderhookian to Meramecian, south-central Kansas and north-central Oklahoma [M.S. Thesis]: Fayetteville, University of Arkansas, 86 p.

Campbell, J.A. and Northcutt, R.A., 2000, Petroleum systems of sedimentary basins in Oklahoma, *in* Merriam, D.F. and Johnson, K.S., eds., Petroleum Systems of Sedimentary Basins in the Southern Midcontinent Symposium: Oklahoma Geological Survey Circular 106, 196 p.

Canis, W.F., 1968, Conodonts and biostratigraphy of the Lower Mississippian of Missouri: Journal of Paleontology, v. 42, p. 525-555.

Charpentier, R.R., Klett, T.R., Obuch, R.C., and Brewton, J.D., compilers, 1996, Tabular data, text, and graphical images in support of the 1995 National Assessment of United States Oil and Gas Resources: United States Geological Survey Digital Data Series DDS-36, one CD-ROM.

Childress, M.N., 2015, High-resolution sequence stratigraphic architecture of a Mid-Continent Mississippian outcrop in southwest Missouri [M.S. Thesis]: Stillwater, Oklahoma State University, 272 p.

Collinson, C., Scott, A.J., and Rexroad, C.B., 1962, Six charts showing biostratigraphic zones, and correlations based on conodonts from the Devonian and Mississippian rocks of the upper Mississippi Valley: Illinois State Geological Survey Circular 328, 32 p.

Collinson, C., 1963, Collection and preparation of conodonts through mass production techniques: Illinois State Geological Survey Circular 343, 20 p.

Collinson, C., Rexroad, C.B., and Thompson, T.L., 1970, Conodont zonation of the North American Mississippian: Geological Society of America Memoir 127, p. 353-394, doi: 10.1130/MEM127-p353.

Cooper, C.L., 1947, Upper Kinkaid (Mississippian) microfauna from Johnson County, Illinois: Journal of Paleontology, v. 21, p. 81-94.

Curtis, D.M. and Champlin, S.C., 1959, Depositional environments of Mississippian limestones of Oklahoma, part 3: Symposium of the Mississippian of Oklahoma and Kansas Tulsa Geological Digest, v. 27, p. 90-103.

Deep Time Maps, 2017, Deep Time Maps Homepage, http://deeptimemaps.com/ (accessed March 2017).

Doll, P.L., 2015, Determining structural influence on depositional sequences in carbonates using core-calibrated wireline logs–Mississippian aged carbonates, Mid-Continent, USA [M.S. Thesis]: Stillwater, Oklahoma State University, 167 p.

Donoghue, P.C.J., Forey, P.L., and Aldridge, R.J., 2000, Conodont affinity and chordate phylogeny: Biological Reviews of the Cambridge Philosophical Society, v. 75, p. 191-251.

Dowdell, B.L., 2013, Pre-stack seismic analysis of a Mississippi lime resource play in the Midcontinent, U.S.A. [M.S. Thesis]: Norman, Oklahoma University, 168 p.

Dunn, D.L., 1965, Late Mississippian conodonts from the Bird Spring Formation in Nevada: Journal of Paleontology, v. 39, p. 1145-1150.

Dunn, D.L., 1966, New Pennsylvanian platform conodonts from southwestern United States: Journal of Paleontology, v. 40, p. 1294-1303.

Dunn, D.L., 1970, Middle Carboniferous conodonts from western United States and phylogeny of the platform group: Journal of Paleontology, v. 44, p. 312-342.

Dupont, A.M., 2016, High-resolution chemostratigraphy in the "Mississippian Limestone" of north-central Oklahoma [M.S. Thesis]: Stillwater, Oklahoma State University, 147 p.

Dzik, J., 1976, Remarks on the evolution of Ordovician conodonts: Acta Paleontologica Poloncia, v. 21, p. 395-460.

Dzik, J., 2000, The origin of the mineral skeleton in chordates, *in* Hecht, M.K., Macintyre, R.J., and Clegg, M.T., eds., Evolutionary Biology, v. 31, p. 105-154, doi: 10.1007/978-1-4615-4185-1_3.

Elium, E., 2017, Combining sequence stratigraphy with artificial neural networks to enhance regional correlation and determination of reservoir quality in the "Mississippian Limestone" of the Mid-Continent, USA: American Association of Petroleum Geologists Mid-Continent Section Meeting Poster Presentation, 2 October, Oklahoma City, Oklahoma.

Epstein, A.G., Epstein, J.B., and Harris, L.D., 1977, Conodont color alteration–an index to organic metamorphism: United States Geological Survey Professional Paper 995, 26 p.

Evans, K.R., Jackson, J.S., Mickus, K.L., Miller, J.F., and Cruz, D., 2011, Enigmas and anomalies of the Lower Mississippian subsystem in southwestern Missouri:

American Association of Petroleum Geologists Search and Discovery Article #50406, 47 p.

Farzaneh, S., 2012, Integrated paleomagnetic and diagenetic study of the Mississippian limestone in northern Oklahoma [M.S. Thesis]: Norman, University of Oklahoma, 87 p.

Flinton, K.C., 2016, The effects of high-frequency cyclicity on reservoir characteristics of the "Mississippian Limestone", Anadarko Basin, Kingfisher County, Oklahoma [M.S. Thesis]: Stillwater, Oklahoma State University, 414 p.

Franseen E.K., 2006, Mississippian (Osagean) shallow-water, mid-latitude siliceous sponge spicule and heterozoan carbonate facies – an example from Kansas with implications for regional controls and distribution of potential reservoir facies: Earth Sciences Bulletin 252, part 1, 23 p.

Friess, J.P., 2005, The southern terminus of the Nemaha tectonic zone, Garvin County, Oklahoma: Oklahoma City Geological Society Shale Shaker, v. 56, p. 55-67.

Gao, Z. and Wang, Y., 2017, Sequence stratigraphic architecture and reservoir characteristics of the unconventional "Mississippian Limestone" Play, north-central Oklahoma, *in* Proceedings, Society of Petroleum Engineers/American Association of Petroleum Geologists/Society of Exploration Geologists Unconventional Resources Technology Conference Article #2670748, 15 p., 24-26 July, Austin, Texas.

Gay, P.S., 2003a, The Nemaha Trend–a system of compressional thrust-fold strike-slip structural features in Kansas and Oklahoma, part 1: Oklahoma City Geological Society Shale Shaker, v. 54, p. 9-17.

Gay, P.S., 2003b, The Nemaha Trend–a system of compressional thrust-fold strike-slip structural features in Kansas and Oklahoma, part 2: Oklahoma City Geological Society Shale Shaker, v. 54, p. 37-49.

Godwin, C.J., 2017, Lithostratigraphy and conodont biostratigraphy of the upper Boone Group and Mayes Group in the southwestern Ozarks of Oklahoma, Missouri, Kansas, and Arkansas [Ph.D. Dissertation]: Stillwater, Oklahoma State University, 402 p.

Golonka, J., Ross, M.I., and Scotese, C.R., 1994, Phanerozoic paleogeographic and paleoclimatic modeling maps, *in* Embry, A.F., Beauchamp, B., and Glass, D.J., eds., Pangea: Global Environments and Resources: Canadian Society of Petroleum Geologists Memoir 17, p. 1–47.

Gradstein, F.M., Ogg, J.G., and Ogg, G.M., eds., 2012, A Concise Geologic Time Scale: Elsevier, p. 99-113, doi: 10.1016/B978-0-444-59467-9.00009-1.

Grammer, G.M., Ginsburg, R.N., Swart, P.K., McNeill, D.F., Jull, A.J.T., and Prezbindowski, D.R., 1993, Rapid growth rates of syndepositional marine aragonite cements in steep marginal slope deposits, Bahamas and Belize: Journal of Sedimentary Research, v. 63, p. 983-989, doi: 10.1306/D4267C62-11D7-8648000102C1865D.

Grammer, G.M., Crescini, C.M., McNeill, D.F., and Taylor, L.H., 1999, Quantifying rates of syndepositional marine cementation in deeper platform environments–new insight into a fundamental process: Journal of Sedimentary Research, v. 69, p. 202-207.

Gunnell, F.H., 1931, Conodonts from the Fort Scott Limestone of Missouri: Journal of Paleontology, v. 5, p. 244–252.

Gunnell, F.M., 1933, Conodonts and fish remains from the Cherokee, Kansas City, and Wabaunsee groups of Missouri and Kansas: Journal of Paleontology, v. 7, p. 261-297.

Gutschick, R.C. and Sandberg, C., 1983, Mississippian continental margins of the conterminous United States: Society of Economic Paleontologists and Mineralogists, v. 33, p. 79-96.

Gutschick, R.C., Weiner, J.L., and Young, L., 1961, Lower Mississippian arenaceous foraminifera from Oklahoma, Texas, and Montana: Journal of Paleontology, v. 35, p. 1193-1221.

Handford, C.R., 1986, Facies and Bedding Sequences in shelf storm-deposited carbonates–Fayetteville Shale and Pitkin Limestone (Mississippian), Arkansas: Journal of Sedimentary Research, v. 56, p. 123-137.

Handford, C.R., 1995, Baselap patterns and the recognition of lowstand exposure and drowning–a Mississippian ramp example and its seismic signature: Journal of Sedimentary Research, v. 65, p. 323-337.

Harris, A.G., 1979, Conodont color alteration–an organic mineral metamorphic index and its application to Appalachian Basin geology, *in* Scholle, P.A. and Schluger, P.R., eds., Aspects of Diagenesis: Society of Economic Paleontologists and Mineralogists, v. 26, p. 3-16, doi: 10.1306/07060909014.

Harris, S.A., 1975, Hydrocarbon accumulation in the “Meramec-Osage” (Mississippian) rocks, Sooner Trend, northwest-central Oklahoma: American Association of Petroleum Geologists Bulletin, v. 59, p. 633-664.

Hass, W.H., 1959, Conodonts from the Chappel Limestone of Texas: United States Geological Survey Professional Paper 294-J, p. 365-399.

Haq, B.U. and Schutter, S.R., 2008, A chronology of Paleozoic sea-level changes: Science, v. 322, p. 64-68.

Haynes, J., 2013, Diagenesis within the Mississippian limestone – north central Oklahoma [M.S. Thesis]: Norman, University of Oklahoma, 80 p.

Higgins, A.C. and Bouckaert, J., 1968, Conodont stratigraphy and paleontology of the Namurian of Belgium: Service Géologique de Belgique Mémoire no. 10, 64 p.

Hill, E., 2017, Core- and wireline log-based, shelf to basin stratigraphic framework of Mississippian strata, east-central Oklahoma [M.S. Thesis]: Stillwater, Oklahoma State University, 305 p.

Hinde, G.J., 1879, On conodonts from the Chazy and Cincinnati group of the Cambro-Silurian and from the Hamilton and Genesee shale divisions of the Devonian in Canada and the United States: Geological Society of London Quarterly Journal, v. 35, pt. 3, p. 351-369.

Jaeckel, L., 2016, High-resolution sequence stratigraphy and reservoir characterization of Mid-Continent Mississippian carbonates in north-central Oklahoma and south-central Kansas [M.S. Thesis]: Stillwater, Oklahoma State University, 368 p.

Janousek, T., Conodont biostratigraphy of the Wolfcamp D, Midland Basin, Texas [M.S. Thesis]: Stillwater, Oklahoma State University, 47 p.

Jarochowska, E., Tonarová, P., Munnecke, A., Ferrová, L., Sklenář, J., and Vodrážková, S., 2013, An acid-free method of microfossil extraction from clay-rich lithologies using the surfactant Rewoquat: Paleontologia Electronica, v. 16, 16 p.

Jennings, C.J., 2014, Mechanical stratigraphy of the Mississippian in Osage County, Oklahoma [M.S. Thesis]: Fayetteville, University of Arkansas, 82 p.

Jeppsson, L., Anehus, R., and Fredholm, D., 1999, The optimal acetate buffered acetic acid technique for extracting phosphatic fossils: Journal of Paleontology, v. 73, p. 964-972.

Jeppsson, L. and Anehus, R., 1995, A buffered formic acid technique for conodont extraction: Journal of Paleontology v. 69, p. 790-794.

Johnson, K.S., 2008, Geologic history of Oklahoma: Oklahoma Geological Survey Educational Publication 9, 21 p.

Jones, D., Evans, A.R., Rayfield, E.J., Siu, K.K.W., and Donoghue, P.C.J., 2012, Testing microstructural adaption in the earliest dental tools: Biology Letters, v. 8, p. 952-955, doi: 10.1098/rsbl.2012.0487.

Kerans, C. and Tinker, S.W., 1997, Sequence stratigraphy and characterization of carbonate reservoirs: Society of Economic Paleontologists and Mineralogists Short Course Notes No. 40, p. 1-130.

Knell, S.J., 2012, The great fossil enigma–the search for the conodont animal: Bloomington, Indiana University Press, 440 p.

Koch, J.T., Frank, T.D., and Bulling, T.P., 2014, Stable-isotope chemostratigraphy as a tool to correlate complex Mississippian marine carbonate facies of the Anadarko

shelf, Oklahoma and Kansas: American Association of Petroleum Geologists Bulletin, v. 98, p. 1071-1090, doi: 10.1306/10031313070.

Konigshof, P., 2003, Conodont deformation patterns and textural alteration in Paleozoic conodonts–examples from Germany and France: Senckenbergiana Lethaea, v. 83, p. 149-156.

Krumhardt, A.P., Harris, A.G., and Watts, K.F., 1996, Lithostratigraphy, microlithofacies, and conodont biostratigraphy and biofacies of the Wahoo Limestone (Carboniferous), eastern Sadlerochit Mountains, Northeast Brooks Range, Alaska: United States Geological Survey Professional Paper 1568, 88 p.

Lane, H.R. and Brenkle, P.L., 2005, Type Mississippian subdivisions and biostratigraphic succession, *in* Heckel, P.H., ed., Stratigraphic and Biostratigraphy of the Mississippian Subsystem (Carboniferous System) in its Type Region, the Mississippi River Valley of Illinois, Missouri, and Iowa: International Union of Geological Sciences Subcomission on Carboniferous Stratigraphy, Guidebook for Field Conference, St. Louis, Missouri, 8-13 September 2001: Champaign, Illinois, Illinois State Geological Survey Guidebook 34, p. 83-107.

Lane, H.R. and DeKeyser, T.L., 1980, Paleogeography of the late Early Mississippian (Tournaisian 3) in the central and southwestern United States, *in* Fouch, T.D., and Magathan, E.R., eds., Paleozoic Paleogeography of west-central United States: Rocky Mountain Paleogeography Symposium 1 Society of Economic Paleontologists and Mineralogists, p. 149-162.

Lane, H.R., 1967, Uppermost Mississippian and Lower Pennsylvanian conodonts from the type Morrowan region, Arkansas: Journal of Paleontology, v. 41, p. 920-942.

Lane, H.R. 1974, Mississippian of southeastern New Mexico and west Texas–a wedge-on-wedge relation: American Association of Petroleum Geologists Bulletin v. 58, p. 269-282.

Lane, H.R., 1978, The Burlington Shelf (Mississippian, north-central United States): Geologica et Palaeontologica, v. 12, p. 165-176.

Lane, H.R., Sandberg, C.H., and Ziegler, W., 1980, Taxonomy and phylogeny of some Lower Carboniferous conodonts and preliminary standard post–Siphonodella zonation: Journal of Paleontology, v.14, p. 117–164.

Lane, H.R. and Straka, J.J., 1974, Late Mississippian and Early Pennsylvanian conodonts Arkansas and Oklahoma: Geological Society of America Special Papers 152, 138 p., doi: 10.1130/SPE152-p1.

Laudon, L.R., 1948, Osage-Meramec contact: The Journal of Geology, v. 56, p. 288-302.

LeBlanc, S.L., 2014, High-resolution sequence stratigraphy and reservoir characterization of the "Mississippian Limestone" in north-central Oklahoma [M.S. Thesis]: Stillwater, Oklahoma State University, 443 p.

Macke, D.L. and Nichols, K.M., 2007, Conodonts viewed as evolving heavy-mineral grains, *in* Lucas, S.G. and Spielmann, J.A., eds., The Gobal Triassic: New Mexico Museum of Natural History and Science Bulletin 41, p. 262-267.

Manger, W. L., 2012, Lower Mississippian sequence stratigraphy and depositional dynamics–further insights from the outcrops, northwestern Arkansas and southwestern Missouri: Mississippian and Arbuckle Workshop Oklahoma Geological Survey, 31 October, Norman, University of Oklahoma.

Manger, W.L., 2014, Tripolitic chert development in the Mississippian Lime–new insights from SEM: American Association of Petroleum Geologists Search and Discovery Article #50957, 39 p.

Marshall, C.P. and Marshall, A.O., 2014, Examining enameloid chemistry in lower vertebrates to determine conodont taxonomic affinity: 11 Annual GeoRaman International Conference 15-19 June, St. Louis, Missouri.

Martin, J., 2015, A geomechanical approach to evaluate brittleness using well logs–Mississippian limestone, northern Oklahoma [M.S. Thesis]: Arlington, University of Texas, 56 p.

Martínez, C.P., Rayfield, E.J., Purnell, M.A., and Donoghue, P.C.J., 2014, Finite element, occlusal, microwear and microstructural analyses indicate that conodont microstructure is adapted to dental function: Paleontology, v. 57, p. 1059-1066, doi: 10.1111/pala.12102.

Mason, C.E., Repetski, J.E., Smith, W.C., Lindgren, P., Parnell, J., and Lee, P., 2008, Thermal and hydrothermal alteration of conodonts from target bedrock and impact breccias from the Aughton impact structure, Devon Island, Nunavut, Canada: Lunar and Planetary Science, v. 39, p. 2551-2552.

Matson, S.E., 2013, Mississippi Lime play from outcrop to subsurface–the evolution of a play: American Association of Petroleum Geologists Search and Discovery Article #110170, 64 p.

Mazzullo, S.J., Wilhite, B.W., and Woolsey, I.W., 2009, Petroleum reservoirs within a spiculite-dominated depositional sequence–Cowley Formation (Mississippian:

Lower Carboniferous), south-central Kansas: American Association of Petroleum Geologists Bulletin, v. 93, p. 1649-1689.

Mazzullo, S.J., Wilhite, B.W., and Boardman, D.R., 2011a, Lithostratigraphic architecture of the Mississippian Reeds Spring Formation (middle Osagean) in southwest Missouri, northwest Arkansas, and northeast Oklahoma–outcrop analog of subsurface petroleum reservoirs: Oklahoma City Geological Society Shale Shaker, v. 61, p. 254-269.

Mazzullo, S.J., Wilhite, B.W., Boardman, D.R., Morris, B., Turner, R., and Godwin, C.J., 2011b, Lithostratigraphy and conodont biostratigraphy of the Kinderhookian to Osagean series on the western flank of the Ozark Uplift: Tulsa Geological Field Trip Guide Book, 48 p.

Mazzullo, S.J., Boardman, D.R., Wilhite, B.W., and Morris, B.T., 2013, Revisions of outcrop lithostratigraphic nomenclature in the Lower to Middle Mississippian subsystem (Kinderhookian to basal Meramecian series) along the shelf-edge in southwest Missouri, northwest Arkansas, and northeast Oklahoma: Oklahoma City Geological Society Shale Shaker, v. 63, p. 414-452.

Mazzullo, S.J., Wilhite, B.W., Boardman, D.R., Morris, B.T., and Godwin, C.J., 2016, Stratigraphic architecture and petroleum reservoirs in Lower to Middle Mississippian strata (Kinderhookian to basal Meramecian) in subsurface central to southern Kansas and northern Oklahoma: Oklahoma City Geological Society Shale Shaker, v. 67, p. 20-49.

McBee, W.J., 2003, Nemaha strike-slip Fault Zone: American Association of Petroleum Geologists Search and Discovery Article #10055, 14 p.

McCarthy, K., Rojas, K., Niemann, M., Palmowski, D., Peters, K., and Stankiewics, A., 2011, Basic petroleum geochemistry for source rock evaluation: Oilfield Review, v. 23, p. 32-43.

McDuffie, R.H., 1959, Lithologic basis for correlation of Mississippian rocks in the subsurface between Kansas and north central Oklahoma, *in* Proceedings, Oklahoma Academy of Sciences, Geological Sciences, 1958, v. 39, p. 133-135.

McGoff, J.H., 1991, The hydrodynamics of conodont elements: Lethaia, v. 24, p. 235-247, doi: 10.1111/j.1502-3931.1991.tb01472.x.

McMahon, T., 2015, Historical crude oil prices: InflationData.com, http://inflationdata.com /Inflation/Inflation_Rate/Historical_Oil_Prices_Table.asp (accessed August, 2016).

Mehl, M.G. and Thomas, L.A., 1947, Conodonts from the Fern Glen of Missouri: Journal of the Scientific Laboratories of Denison University, v. 40, p. 3-20.

Miall, A.D., 2013, The geology of stratigraphic sequences: New York, Springer-Verlag Berlin Heidelberg, 435 p.

Mii, H., Grossman, E.L., and Yancey, T.E., 1999, Carboniferous isotope stratigraphies of North America–implications for Carboniferous paleoceanography and Mississippian glaciation: Geological Society of America Bulletin, v. 111, p. 960-973.

Milam, K., 2013, OSU-industry consortium eyes Mississippian: American Association of Petroleum Geologists Explorer Article #2317, http://www.aapg.org/Publications/News/Ex plorer/Details/ArticleID/2317/OSU-Industry-Consortium-Eyes-Mississippian (accessed September, 2015).

Miller, J.D., 2015, Conodont biostratigraphy of the upper Osagean (lower Visean) Ozark Uplift, Southern Midcontinent, USA [M.S. Thesis]: Stillwater, Oklahoma State University, 149 p.

Monies, P., 2016, Energy companies want federal earthquake lawsuit dismissed: The Oklahoman, http://www.newsok.com/article/5501878 (accessed June 2016).

Morrow, J.R. and Webster, G.D., 1991, Carbonate microfacies and related conodont biofacies, Mississippian-Pennsylvanian boundary strata, Granite Mountain, west-central Utah, *in* Kowallis, B.J. and Seely, K., eds., Brigham Young University Geology Studies v. 37: Department of Geology, Brigham Young University, p. 99-124.

Murdock, D.J.E., Dong, X., Repetski, J.E., Marone, F., Stampanoni, M., and Donoghue, P.C.J., 2013, The origin of conodonts and of vertebrate mineralized skeletons: Nature, v. 502, p. 546-549, doi: 10.1038/nature12645.

Nemyrovska, T.I., 2005, Late Visean-early Serpukhovian conodont succession from the Triollo section, Palencia (Cantabrian Mountains, Spain): Scripta Geologica, v, 129, p. 13-89.

Noble, P.J., 1993, Paleoceanographic and tectonic implications of a regionally extensive Early Mississippian hiatus in the Ouachita system, southern mid-continental United States: Geology, v. 21, p. 315-318.

Norby, R.D., 1976, Conodont apparatuses from Chesterian (Mississippian) strata of Montana and Illinois [Ph. D. Dissertation]: Champaign, University of Illinois, 295 p.

Norby, R.D. and Rexroad, C.B., 1985, *Vogelgnathus*, a new Mississippian conodont genus: Indiana Department of Natural Resources and Geological Survey Paper 50, 14 p.

Northcutt, R.A. and Campbell, J.A., 1996, Geologic Provinces of Oklahoma: Oklahoma City Geological Survey Shale Shaker, v. 46, p. 99-103.

Oklahoma Corporation Commission, 2017, Earthquake response summary: Oklahoma Corporation Commission, http://www.occeweb.com/News/2017/02-24-17EARTHQUAKE%20ACTION%20SUMMARY.pdf (accessed March 2017).

Oklahoma Corporation Commission Imaging, 2015, Well logs: Oklahoma Corporation Commission Web Application, http://imaging.occeweb.com/imaging/OGWellLog.aspx (accessed December, 2015).

Pander, C.H., 1856, Monographie der fossilen Fische der Silurischen systems der Russisch Baltischen Gouvernements: Obersilurische Fische, Buchdruckerei Kaiserlichen Akademie des Wissenschaften, St. Petersburg, 91 p.

Peppe, D.J. and Reiners, P.W., 2007, Conodont (U-Th)/He thermochronology–initial results, potential, and problems: Earth and Planetary Science Letters, v. 258, p. 569-580.

Parrish, J.T., 1982, Upwelling and petroleum source beds, with reference to the Paleozoic: American Association of Petroleum Geologists Bulletin, v. 66, p. 750–774.

Perri, M.C. and Spaletta, C., 1998, Conodont distribution at the Tournaisian/Visean boundary in the Carnic Alps (Southern Alps, Italy), *in* Szaniawski, H., ed.,

Proceedings of the Sixth European Conodont Symposium: Paleontologica Polonica, v. 58, p. 225-245.

Perry, M.J., 2014, Chart of the day–the great American energy boom: American Enterprise Institute, https://www.aei.org/publication/chart-of-the-day-the-great-american-energy-boom/print/ (accessed March 2017).

Pinney, R.I., 1962, The paleontology and stratigraphy of the Meppen Formation in Western Illinois and Eastern Missouri: Athens, Ohio University, M. S. Thesis.

Poole, F.G. and Sandberg, C.A., 1991, Mississippian paleogeography and conodont biostratigraphy of the Western United States, *in* Cooper, J.D. and Stevens, C.H., eds., Paleozoic Paleogeography of the Western United States, part 2: Pacific Section Society of Economic Paleontologists and Mineralogists, v. 67, p. 107-136.

Price, B.J., 2014, High-resolution sequence stratigraphic architecture and reservoir characterization of the Mississippian Burlington/Keokuk Formation, northwestern Arkansas [M.S. Thesis]: Stillwater, Oklahoma State University, 144 p.

Purnell, M.A., 1994, Skeletal ontogeny and feeding mechanisms in conodonts: Lethaia, v. 27, p. 129-138, doi: 10.1111/j.1502-3931.1994.tb01567.x.

Purnell, M.A. and Donoghue, P.C.J., 1997, Architecture and functional morphology of the skeletal apparatus of the ozarkodinid conodonts: Biological Sciences, v. 352, p. 1545-1564, doi: 10.1098/rstb.1997.0141.

Purnell, M.A. and Jones, D., 2012, Quantitative analysis of conodont tooth wear and damage as a test of ecological and functional hypotheses: Paleobiology, v. 38, p. 605-626.

Ray, M., 2016, Alternative to deep-well injection of oil/gas wastewater discussed during public forum at state capitol: The Oklahoma Welcome News, http://okwnews.com /112069/alternative-to-deep-well-injection-of-oil-gas-wastewater-discussed-during-public-forum-at-state-capitol.html (accessed July 2016).

Read, J.F., 1982, Carbonate platforms of passive (extensional) continental margins–types, characteristics and evolution: Tectonophysics, v. 81, p. 195-212.

Read, J.F., 1985, Carbonate platform facies models: American Association of Petroleum Geologists Bulletin, v. 69, p. 1-21.

Repetski, J.E. and Henry, T.W., 1983, A Late Mississippian conodont faunule from area of proposed Pennyslvanian System stratotype, eastern Appalachians: Fossils and Strata no. 15, v. 12, p. 169-170.

Rexroad, C.B., 1957, Conodonts from the Chester Series in the type areas of southwestern Illinois: Illinois Geological Survey Report of Investigation 199, 43 p.

Rexroad, C.B., and Burton, R.C., 1961, Conodonts from the Kinkaid Formation (Chester) in Illinois: Journal of Paleontology, v. 35, p. 1143-1158.

Rexroad, C.B. and Furnish, W.M., 1964, Conodonts from the Pella Formation (Mississippian) south-central Iowa: Journal of Paleontology, v. 38, p. 667-676.

Rexroad, C.B. and Horowitz, A.S., 1990, Conodont paleoecology and multielement associations of the Beaver Bend Limestone (Chesterian) in Indiana: Courier Forschungsinstitut Senckenberg, v. 118, p. 493-537.

Rhodes, F.H.T., Austin, R.L., and Druce, E.C., 1969, British Avonian (Carboniferous) conodont faunas, and their value in local and intercontinental correlation: Bulletin of the British Museum (National History) Geology Supplement 5, 313 p.

Rogers, S. M., 2001, Deposition and diagenesis of Mississippian chat reservoirs, north-central Oklahoma: American Association of Petroleum Geologists Bulletin, v. 85, p. 115-129.

Ross, C.A. and Ross, J.R.P., 1987a, Biostratigraphic zonation of Late Paleozoic depositional sequences, *in* Ross, C.A. and Haman, D., eds., Timing and Depositional History of Eustatic Sequences–Constraints on Seismic Stratigraphy: Cushman Foundation for Foraminiferal Research, Special Publication 24, p. 151-168.

Ross, C.A. and Ross, J.R.P., 1987b, Late Paleozoic sea levels and depositional sequences, *in* Ross, C.A. and Haman, D., eds., Timing and Depositional History of Eustatic Sequences–Constraints on Seismic Stratigraphy: Cushman Foundation for Foraminiferal Research Special Publication 24, p. 137-150.

Roundy, P.V., 1926, The microfauna of Mississippian formations of San Saba County, Texas: United States Geological Survey Professional Paper 146, p. 5–17.

Rowland, T.L., 1964, Mississippian rocks in the subsurface of the Kingfisher-Guthrie area, Oklahoma: Oklahoma City Geological Society Shale Shaker, v. 9, p. 145-162.

Rowley, D.B., Raymond, A., Parrish, J.T., Lottes, A.L., Scotese, C.R., and Ziegler, A.M., 1985, Carboniferous paleogeographic, phytogeographic, and paleoclimatic reconstructions: International Journal of Coal Geology, v. 5, p. 7-42.

Russell, M.P., 2013, Echinoderm responses to variation in salinity: Advances in Marine Biology, v. 66, p. 171-212.

Saltzman, M.R., 2002, Carbon and oxygen isotope stratigraphy of the Lower Mississippian (Kinderhookian to lower Osagean), western United States–implications for seawater chemistry and glaciation: Geological Society of America Bulletin, v. 114, p. 96-108.

Saltzman, M.R., 2003, Late Paleozoic ice age–Oceanic gateway or pCO_2?: Geology, v. 31, p.151-154.

Scotese, C.R., 1997, PALEOMAP Paleogegraphic atlas, PALEOMAP progress report 90-0497: Department of Geology, University of Texas at Airlington, 37 p.

Scott, H.W., 1942, Conodont assemblages from the Heath Formation, Montana: Journal of Paleontology, v. 16, p. 293-300.

Selk, E.L. and Ciriacks, K.W., 1968, Mississippian stratigraphy in Southern Kansas and Northern Oklahoma, based on conodont fauna: Kansas Geological Survey Open-file Report 68-3, 5 p.

Shale Daily, 2015, Information on the Mississippian lime: Natural Gas Intelligence, http://www.naturalgasintel.com/misslimeinfo (accessed March 2017).

Shelley, S.A., 2016, Outcrop-based sequence stratigraphy and reservoir characterization of an Upper Mississippian mixed carbonate-siliciclastic ramp, Mayes County, Oklahoma [M.S. Thesis]: Stillwater, Oklahoma State University, 92 p.

Shoeia, O.O., 2012, High-resolution stratigraphy of Lower Mississippian strata near Jane, Missouri [M.S. Thesis]: Stillwater, Oklahoma State University, 262 p.

Singh, M.K., 2007, Correlation and biostratigraphy of surface and shallow subsurface sections of the Barnett Shale, Llano Uplift, south-central Texas [M.S. Thesis]: Stillwater, Oklahoma State University, 92 p.

Sloss, L.L., 1963, Sequences in the cratonic interior of North America: Geological Society of America Bulletin, v. 74, p. 93-114.

Snedden, J.W. and Liu, C., 2010, A compilation of Phanerozoic sea-level change, coastal onlaps and recommended sequence designations: American Association of Petroleum Geologists Search and Discovery Article #40594, 3 p.

Snedden, J.W. and Liu, C., 2011, Recommendations for a uniform chronostratigraphic desgination system for Phanerozoic depositional sequences: American Association of Petroleum Geologists Bulletin, v. 95, p. 1095-1122.

Steen, J.T., 2017, Structural geometry and kinematics of the Nemaha Uplift, north-central Oklahoma [M.S. Thesis]: Stillwater, Oklahoma State University, 201 p.

Steinmann, J., Riedinder, N., Brunner, B., and Grammer, G.M., Assessing novel chemostratigraphic correlation tools in carbonate reservoir rocks–a Mississippian limestone Case Study: American Association of Petroleum Geologists Search and Discovery Article #90291, 3 p.

Stone, J., 2001, Heavy liquid mineral separation: University of Washington, http://webcache.googleusercontent.com/search? q=cache:X4-suFw-m9MJ:faculty.washington.edu/kate1/Facilities_files/HvyMinSepSOP.doc+&cd=2&hl=en&ct=clnk&gl=us (accessed December 2015).

Suneson, N.H., 2012, Arkoma Basin petroleum past, present, and future–a geologic journey through the Wichitas, Black Mesa basalt, and much more: Oklahoma City Geological Society Shale Shaker, v. 63, p. 37-71.

Sweet, W.C. and Cooper, B.J., 2008, C.H. Pander's introduction to conodonts, 1856: Episodes, v. 31, p. 429-432.

Terrill, D.F., 2015, Examination of conodont ontogeny, phylogeny, and experimental diagenesis utilizing field emission scanning electron microscopy and strontium isotope analysis [M.S. Thesis]: Alberta, University of Calgary, 76 p.

Thompson, T.L., 1967, Conodont zonation of lower Osagean rocks (Lower Mississippian) of southwestern Missouri: Missouri Geological Survey and Water Resources Report 39, 88 p.

Thompson, T.L. and Fellows, L.D., 1970, Stratigraphy and conodont biostratigraphy of Kinderhookian and Osagean (lower Mississippian) rocks of southwestern Missouri and adjacent states: Missouri Geological Survey and Water Resources Report of Investigations 45, 263 p.

Thompson, T.L. and Goebel, E.D., 1963, Preliminary report on conodonts of the Meramecian Stage (Upper Mississippian) from the subsurface of Western Kansas: Kansas Geological Survey Bulletin 165, part 1, 19 p.

Thompson, T.L. and Goebel, E.D., 1968, Conodonts and stratigraphy of the Meramecian Stage (Upper Mississippian) in Kansas: Kansas Geological Survey Bulletin 192, 56 p.

Thornton, W.D., 1958, Mississippian rocks in the subsurface of Alfalfa and northwestern Oklahoma [M.S. Thesis]: Norman, University of Oklahoma, 114 p.

Tubbs, P.K., 1986, Conodonts and stratigraphy of the Meramecian Stage (Upper Mississippian) in Kansas: Kansas Geological Survey Bulletin, v. 192, p. 1-56.

Ulrich, E.O. and Bassler, R.S., 1926, A classification of the toothlike fossils, conodonts, with descriptions of American Devonian and Mississippian species: Proceedings of the United States National Museum, v. 68, p.1-63.

Unrast, M.A., 2013, Composition and classification of Mississippian carbonate mounds in the Ozark region, North America: Oklahoma City Geological Society Shale Shaker, v. 63, p. 254-273.

U.S. Energy Information Administration, 2016, Annual energy outlook 2016 reference case: United States Energy Information Administration, https://www.eia.gov/energyexplained/index.cfm?page=natural_gas_where (accessed March 2017).

Uyeda, J.C., Hansen, T.F., Arnold, S.J., Pienaar, J., 2011, The million-year wait for macroevolutionary bursts: Proceedings of the National Academy of Sciences, www.pnas.org/cgi/doi/10.1073/pnas.1014503108u (accessed September 2017).

von Bitter, P.H. and Purnell, M.A., 2005, An experimental investigation of post-depositional taphonomic bias in conodonts: Special Papers in Paleontology, v. 73, p. 39-56.

Watney, W. L., 2015, A maturing Mississippian Lime play in the Midcontinent – A perspective on what we know and what we need to know: American Association of Petroleum Geologists Search and Discovery Article #80445, 77 p.

Weller, J.M. et al., 1948, Correlation of the Mississippian formations of North America: Geological Society of America Bulletin, v. 59, p. 91-196.

Wenzel, B., Lécuyer, C., Joachimski, M.M., 2000, Comparing calcite and phosphate oxygen isotope paleothermometers–$\delta^{18}O$ of Silurian brachiopods and conodonts: Geochimica et Cosmochimica Acta, v. 64, p. 1859–1872.

Werner, M., 2004, Carbonate ramp depositional environments: Freiberg Mining Academy and Technical University, http://www.geo.tu-freiberg.de/oberseminar/os03_04/mirco_werner.pdf (Accessed September 2017).

Wertz, J., 2016, Oil companies ask judge to toss federal earthquake lawsuit: National Public Radio, https://stateimpact.npr.org/oklahoma/2016/06/03/oil-companies-ask-judge-to-toss-federal-earthquake-lawsuit/ (accessed July 2016).

Wickström, L.M. and Donoghue, P.C.J., 2005, Cladograms, phylogenies, and the veracity of the conodont fossil record, *in* Purnell, M.A. and Donoghue, P.C.J., eds., Conodont Biology and Phylogeny–Interpreting the Fossil Record, Special Papers in Paleontology 73, p. 185-218.

Wilhite, B.W., Mazzullo, S.J., Morris, B.T., and Boardman D.R., 2011, Syndepositional tectonism and its effects on Mississippian (Kinderhookian to Osagean) lithostratigraphic architecture, part 1–based on exposures in the Midcontinent USA: American Association of Petroleum Geologists Search and Discovery Article #30207, 43 p.

Witzke, B.J., 1990, Paleoclimatic constraints for Paleozoic paleoaltitudes of Laurentia and Euamerica: The Geological Society of London Memoirs, v. 12, p. 57-73.

Youngquist, W., Miller, A.K., and Downs, H.R., 1950, Burlington conodonts from Iowa: Journal of Paleontology, v. 24, p. 525-530.

Youngquist, W. and Miller, A.K., 1949, Conodonts from the Pella beds of south-central Iowa: Journal of Paleontology, v. 23, p. 617-622.

Zeller, D.E., ed., 1968, Stratigraphic succession in Kansas: Geological Survey Bulletin 189, http://www.kgs.ku.edu/Publications/Bulletins/189/index.html (accessed March 2017).

APPENDICES

APPENDIX A: WHOLE-ROCK SAMPLE DATA

Datasheets

This section is meant to provide the reader with the raw data sheets that were used in the collection, processing, analyzing, and calculating of data during this study.

An explanation for the abbreviations as presented in the "Notes" and "Microscope Notes" sections of the datasheets is provided below:

ABBREVIATION	MEANING
AP	Apatite crystal
AZ	Azurite crystal
BLU/BRN CHRT	Blue/Brown chert
BRAC or BRACH	Brachiopod shell
CHRT	Chert fragment
CRIN	Crinoid stem
DOL	Dolomite grain
FELD	Feldspar grain
GLAUC	Glauconite grain
IO	Iron Oxide staining
MAR or MARC	Marcasite crystal
PY or (micro)PY	Pyrite crystal (framboidal or euhedral)
QTZ	Quartz (angular to sub-angular) grains
(Reworked)	Reworked interval
RND or DIT QTZ	Rounded or detrital quartz grain
SPIC	Sponge spicule
VIV	Vivianite crystal
WF SH	Woodford Shale

ADKISSON 1-33 Core

ADKISSON #1-33 SWD core
Logan County, Oklahoma
Depth Interval CD/LD: 5496'-5820'

121 samples analyzed of 123 taken

~324 ft. thick section

3rd Order Sequence	Core Depth* (ft)	Footage (ft)	Sample Type	Approx. Whole-rock Weight (kg)	Approx. Sample Weight (kg)	Facies	XRD	Stain	Start Date	End Date	Type	# baths	Residue Weight (kg)	Conodonts	# conodonts useful w/SEM	Processor	Notes
4	5517.0-5517.75	0.75	core	0.75	0.38	5	no	no	05/17/16	05/26/16	S, 5A	6	0.040	0	0	JEH	PY, MAR, CHERT
4	5518.0-5518.7	0.70	core	0.70	0.35	5	no	no	05/17/16	05/26/16	S, 5A	6	0.006	1	0	JEH	PY
			residue						n/a	n/a	n/a	n/a	0.002	0	0	JDM	n/a
4	5518.7-5519.2	0.50	big core	0.50	0.25	4	no	no	05/17/16	05/26/16	S, 5A	6	0.045	0	0	JEH	PY, IO, SPIC
4	5519.2-5520.0	0.80	core	0.80	0.40	4, 5	no	yes	05/26/16	06/02/16	S, 3A	4	0.014	16	1	JEH	PY, MAR, IO, SPIC, CRIN
			residue						n/a	n/a	n/a	n/a	0.003	0	0	JDM	n/a
4	5522.0-5522.7	0.70	small core	0.70	0.35	4	no	yes	n/a	n/a	n/a	n/a	0.003	0	0	JDM	n/a
4	5522.7-5523.3	0.60	core	0.60	0.30	4	no	no	03/14/17	03/16/17	2A	2	0.006	0	0	JEH	PY
			residue						n/a	n/a	n/a	n/a	0.001	0	0	JDM	n/a
4	5523.3-5524.0	0.70	small core	0.70	0.35	3	no	no	n/a	n/a	n/a	n/a	0.002	0	0	JDM	n/a
4	5524.0-5524.7	0.70	core	0.70	0.35	3, 4	yes	no	03/14/17	03/16/17	P, 2A	3	0.021	0	0	JEH	IO
			residue						n/a	n/a	n/a	n/a	0.002	0	0	JDM	n/a
4	5524.0-5525.3	1.3	core	1.3	0.65	3	yes	no	02/17/17	02/19/17	P, 2A	3	0.062	4	0	JEH	PY, BRACH, CRIN, SPIC
4	5525.3-5526.0	0.70	core	0.70	0.35	3	no	no	02/17/17	02/19/17	2A	2	0.010	0	0	JEH	PY, MARC, IO
			residue						n/a	n/a	n/a	n/a	0.002	0	0	JDM	n/a
4	5567.0-5567.5	0.50	core	0.50	0.25	3	no	no	02/17/17	02/19/17	2A	2	0.025	0	0	JEH	PY, MARC, CRIN
			residue						n/a	n/a	n/a	n/a	0.002	0	0	JDM	n/a
4	5567.5-5568.5	1.0	small core	1.0	0.50	3	no	no	n/a	n/a	n/a	n/a	0.003	0	0	JDM	n/a
4	5568.5-5569.0	0.50	core	0.50	0.25	3	no	no	02/14/17	02/17/17	3A	3	0.014	0	0	JEH	IO, BRACH, BLU CHRT
			residue						n/a	n/a	n/a	n/a	0.002	0	0	JDM	n/a
4	5569.0 (repeat)	n/a	core	n/a	n/a	2	no	no	n/a	n/a	n/a	n/a	n/a	n/a	n/a	n/a	repeat section
4	5569.0-5570.0	1.0	core	1.0	0.50	2	yes	no	02/14/17	02/17/17	P, 3A	4	0.014	0	0	JEH	PY, BRACH
			residue						n/a	n/a	n/a	n/a	0.001	0	0	JDM	n/a
4	5570.0-5571.0	1.0	core	1.0	0.50	2	no	no	02/17/17	02/19/17	2A	2	0.022	2	0	JEH	PY, IO
			residue						n/a	n/a	n/a	n/a	0.002	0	0	JDM	n/a
4	5571.0-5571.5	0.50	small core	0.50	0.25	2	no	no	02/17/17	02/19/17	2A	2	0.003	0	0	JEH	PY
			residue						n/a	n/a	n/a	n/a	0.002	0	0	JDM	n/a
4	5571.5-5572.5	1.0	small core	1.0	0.50	2	no	no	02/14/17	02/17/17	3A	3	0.003	1	0	JEH	PY, BRACH
			residue						n/a	n/a	n/a	n/a	0.002	0	0	JDM	n/a
4	5572.5-5573.0	0.50	core	0.50	0.25	2	no	no	02/14/17	02/17/17	3A	3	0.015	0	0	JEH	PY, IO, CRIN
			residue						n/a	n/a	n/a	n/a	0.002	0	0	JDM	n/a
4	5573.0-5573.5	0.50	core	0.50	0.25	2	no	no	02/17/17	02/19/17	2A	2	0.025	1	0	JEH	PY, MARC, SPIC
			residue						n/a	n/a	n/a	n/a	0.002	0	0	JDM	n/a
4	5573.5-5574.5	1.0	small core	1.0	0.50	2	yes	no	n/a	n/a	n/a	n/a	0.002	0	0	JDM	n/a
4	5574.5-5575.0	0.50	small core	0.50	0.25	2	no	no	n/a	n/a	n/a	n/a	0.002	0	0	JDM	n/a
4	5575.0-5575.5	0.50	core	0.50	0.25	2	no	no	02/17/17	02/19/17	2A	2	0.076	5	0	JEH	PY
4	5575.5-5576.5	1.0	core	1.0	0.50	2	no	no	02/17/17	02/19/17	2A	2	0.084	0	0	JEH	
4	5576.5-5577.0	0.50	core	0.50	0.25	2	no	no	02/17/17	02/19/17	2A	2	0.015	3	1	JEH	PY, BRACH, CRIN, SPIC
4	5577.0-5577.5	0.50	core	0.50	0.25	2	no	no	02/14/17	02/17/17	3A	3	0.021	1	0	JEH	PY, CRIN
			residue						n/a	n/a	n/a	n/a	0.002	0	0	JDM	n/a
4	5577.5-5578.5	1.0	core	1.0	0.50	2	no	no	02/14/17	02/17/17	3A	3	0.065	0	0	JEH	PY
			residue						n/a	n/a	n/a	n/a	0.002	0	0	JDM	n/a
4	5578.5-5579.0	0.50	core	0.50	0.25	2	no	no	02/17/17	02/19/17	P, 2A	3	0.083	1	0	JEH	PY, VIV
4	5579.0-5579.5	0.50	core	0.50	0.25	2	no	no	03/14/17	03/16/17	2A	2	0.066	11	0	JEH	PY, BRACH, CRIN, SPIC
			residue						n/a	n/a	n/a	n/a	0.002	0	0	JDM	n/a
4	5579.5-5580.5	1.0	residue	1.0	0.50	2	no	no	n/a	n/a	n/a	n/a	0.002	0	0	JDM	n/a
4	5580.5-5581.0	0.50	small core	0.50	0.25	2	no	no	02/14/17	02/17/17	3A	3	0.077	0	0	JEH	PY
			residue						n/a	n/a	n/a	n/a	0.003	0	0	JDM	n/a
4	5581.0-5581.55	0.55	small core	0.55	0.28	2, 3	yes	no	n/a	n/a	n/a	n/a	0.002	0	0	JDM	n/a
4	5581.8-5582.5	0.50	small core	0.50	0.25	2, 3	yes	no	06/02/16	06/09/16	P, S, 4A	4	0.016	33	0	JEH	PY, MARC, SPIC (Reworked)
4	5581.55-5582.5	0.95	residue	0.95	0.48	2,3	yes	no	n/a	n/a	n/a	n/a	0.002	0	0	JDM	n/a
4	5582.5-5583.0	0.50	core	0.50	0.25	2, 3	no	no	02/14/17	02/17/17	3A	3	0.008	0	0	JEH	
			residue						n/a	n/a	n/a	n/a	0.002	0	0	JDM	n/a
4	5583.0-5583.5	0.50	residue	0.50	0.25	2,3	no	no	n/a	n/a	n/a	n/a	0.001	0	0	JDM	n/a
4	5583.5-5584.5	1.0	core	1.0	0.50	2, 3	no	no	05/26/16	06/02/16	S, 3A	4	0.010	1	0	JEH	SPIC, RND QTZ, CRIN, CHRT (Reworked)
			residue						n/a	n/a	n/a	n/a	0.002	0	0	JDM	n/a
4	5585.0-5585.5	0.50	small core	0.50	0.25	2, 4	no	no	n/a	n/a	n/a	n/a	n/a	n/a	n/a	n/a	not enough core
			residue						n/a	n/a	n/a	n/a	0.002	0	0	JDM	n/a
3rd Order Sequence Boundary (CD: 5585')																	
3	5585.5-5586.0	0.50	core	0.50	0.25	4	no	no	06/02/16	06/09/16	S, 3A	4	0.006	0	0	JEH	PY, MARC, SPIC, FISH TOOTH/FOSSIL?

3	5586.2 (repeat)	n/a	core	n/a	n/a	4	no	no	n/a	n/a	n/a	n/a	n/a	n/a	n/a	n/a	repeat section
3	5586.2-5587.0	0.80	core	0.80	0.40	3, 4	no	no	02/14/17	02/17/17	2A	2	0.003	0	0	JEH	PY
			residue						n/a	n/a	n/a	n/a	0.005	0	0	JDM	n/a
3	5587.0-5587.5	0.50	big core	0.50	0.25	3	no	no	06/09/16	06/16/16	4A	4	0.062	0	0	JEH	PY, MARC, SPIC
3	5587.5-5588.5	0.50	core	0.50	0.25	3	no	no	03/14/17	03/16/17	2A	2	0.015	0	0	JEH	CHRT
			residue						n/a	n/a	n/a	n/a	0.001	0	0	JDM	n/a
3	5588.5-5589.0	0.50	big core	0.50	0.25	2, 3	no	no	03/14/17	03/16/17	2A	2	0.066	0	0	JEH	SPIC
3	5589.0-5589.5	0.50	small core	0.50	0.25	2	no	no	n/a	n/a	n/a	n/a	n/a	n/a	n/a	n/a	not enough core
			residue						n/a	n/a	n/a	n/a	0.002	0	0	JDM	n/a
3	5589.5-5590.5	1.0	core	1.0	0.50	2	no	no	03/14/17	03/16/17	2A	2	0.011	0	0	JEH	PY, SPIC, RND QTZ
			residue						n/a	n/a	n/a	n/a	0.001	0	0	JDM	n/a
3	5590.5-5591.0	0.50	core	0.50	0.25	2, 3	no	no	03/14/17	03/16/17	2A	2	0.001	0	0	JEH	PY, MARC, IO, SPIC, RND QTZ
			residue						n/a	n/a	n/a	n/a	0.003	0	0	JDM	n/a
3	5591.0-5591.5	0.50	disaggregate	0.50	0.25	3	no	no	n/a	n/a	n/a	n/a	0.004	0	0	JDM	n/a
3	5591.5-5592.5	1.0	core	1.0	0.50	3, 5	no	no	n/a	n/a	n/a	n/a	0.003	0	0	JDM	n/a
3	5592.5-5593.0	0.50	disaggregate	0.50	0.25	5	yes	no	n/a	n/a	n/a	n/a	0.006	0	0	JDM	n/a
3	5617.0-5618.0**	1.0	residue	1.0	0.50	5	no	yes	n/a	n/a	n/a	n/a	0.027	0	0	JDM	n/a
3	5629.0-5629.3	0.30	small core	0.30	0.15	4	no	no	n/a	n/a	n/a	n/a	0.003	0	0	JDM	n/a
3	5629.3-5630.0	0.70	core	0.70	0.35	4	no	no	n/a	n/a	n/a	n/a	0.003	0	0	JDM	n/a
3	5630.0-5630.6	0.60	core	0.60	0.30	3	no	no	03/14/17	03/16/17	2A	2	0.032	0	0	JEH	SPIC
3	5630.6-5631.0	0.40	small core	0.40	0.20	3	yes	no	n/a	n/a	n/a	n/a	0.002	0	0	JDM	n/a
3	5631.0-5632.0	1.0	core	1.0	0.50	3	no	no	03/14/17	03/16/17	2A	2	0.007	0	0	JEH	PY, MARC, IO, SPIC
			residue						n/a	n/a	n/a	n/a	0.001	0	0	JDM	n/a
3	5632.0-5632.5	0.50	disaggregate	0.50	0.25	3	no	no	04/24/15	04/25/15	n/a	n/a	0.003	0	0	JDM	n/a
3	5632.5-5633.0	0.50	core	0.50	0.25	3	no	no	02/17/17	02/19/17	2A	2	0.002	0	0	JEH	SPIC
			residue						n/a	n/a	n/a	n/a	0.002	0	0	JDM	n/a
3	5633.0-5633.7	0.70	core	0.70	0.35	3	no	no	03/14/17	03/16/17	2A	2	0.004	0	0	JEH	SPIC
			residue						n/a	n/a	n/a	n/a	0.002	0	0	JDM	CRIN
3	5633.7-5634.7	1.0	big core	1.0	0.50	3	no	yes	03/14/17	03/16/17	2A	2	0.003	0	0	JEH	PY, IO, SPIC
3	5634.0-5634.4	0.40	core	0.40	0.20	3	no	yes	06/09/16	06/16/16	P, 3A	4	0.015	0	0	JEH	PY
			residue						n/a	n/a	n/a	n/a	0.008	0	0	JDM	n/a
3	5634.4-5635.0	0.60	core	0.60	0.30	3	yes	yes	06/09/16	06/16/16	P, 3A	4	0.004	0	0	JEH	SPIC, CRIN
			residue						n/a	n/a	n/a	n/a	0.002	0	0	JDM	n/a
3rd Order Sequence Boundary (CD: 5634.5')																		
2	5635.0-5635.9**	0.90	big core	0.90	0.45	4	no	no	n/a	n/a	n/a	n/a	0.045	0	0	TMQ	n/a
2	5655.0-5655.5	0.50	small core	0.50	0.25	3	no	no	03/16/17	03/18/17	2A	2	0.003	0	0	JEH	SPIC
			residue						n/a	n/a	n/a	n/a	0.002	0	0	JDM	n/a
2	5655.5-5656.0	0.50	core	0.50	0.25	3	no	no	03/16/17	03/18/17	2A	2	0.004	0	0	JEH	MARC, IO
2	5656.0-5656.35	0.35	small core	0.35	0.18	3	no	no	03/16/17	03/18/17	2A	2	0.001	0	0	JEH	PY, MARC, SPIC
			residue						n/a	n/a	n/a	n/a	0.002	0	0	JDM	n/a
2	5658.0-5658.5	0.50	small core	0.50	0.25	3	no	no	03/16/17	03/18/17	2A	2	0.002	0	0	JEH	PY, IO, BRACH, SPIC
2	5658.5-5659.0	0.50	big core	0.50	0.25	3	no	no	03/16/17	03/18/17	2A	2	0.003	0	0	JEH	PY, MARC, IO, BRACH
			residue						n/a	n/a	n/a	n/a	0.002	0	0	JDM	n/a
2	5659.0-5660.0	1.0	big core	1.0	0.50	3	no	no	03/16/17	03/18/17	2A	2	0.007	0	0	JEH	PY, MARC, IO, SPIC, VIV
2	5697.0-5698.0	1.0	core	1.0	0.50	3	no	no	03/16/17	03/18/17	2A	2	0.031	0	0	JEH	SPIC, BRACH
2	5698.0-5698.5	0.50	core	0.50	0.25	3	no	no	03/16/17	03/18/17	2A	2	0.018	0	0	JEH	PY
			residue						n/a	n/a	n/a	n/a	0.002	0	0	JDM	n/a
2	5698.5-5699.2	0.70	disaggregate	0.70	0.35	3	no	no	n/a	n/a	n/a	n/a	0.002	0	0	JDM	n/a
2	5699.2-5700.0	0.80	disaggregate	0.80	0.40	3	no	no	n/a	n/a	n/a	n/a	0.004	0	0	JDM	n/a
2	5700.0-5700.7	0.70	core	0.70	0.35	3	no	no	03/16/17	03/18/17	2A	2	0.004	1	0	JEH	PY, MARC, SPIC
			residue						n/a	n/a	n/a	n/a	0.005	0	0	JDM	n/a
2	5700.7-5701.3	0.60	small core	0.60	0.30	2	yes	no	03/16/17	03/18/17	2A	2	0.008	1	0	JEH	PY, CRIN, SPIC, VIV, FISH TOOTH/FOSSIL?
			residue						n/a	n/a	n/a	n/a	0.002	0	0	JDM	n/a
2	5701.55-5702.0	0.45	core	0.45	0.23	2	yes	no	03/16/17	03/18/17	2A	2	0.003	0	0	JEH	PY, SPIC
			residue						n/a	n/a	n/a	n/a	0.002	0	0	JDM	n/a
3rd Order Sequence Boundary (CD: 5702.5')																		
1	5714.0-5714.5	0.50	big core	0.50	0.25	3, 5	no	no	n/a	n/a	n/a	n/a	0.002	0	0	JDM	n/a
1	5714.5-5715.5	1.0	core	1.0	0.50	3, 5	no	no	03/20/17	03/22/17	2A	2	0.007	0	0	JEH	WAVY STEM-LIKE FOSSIL
			residue						n/a	n/a	n/a	n/a	0.002	0	0	JDM	n/a
1	5715.5-5716.0	0.50	small core	0.50	0.25	2, 3	no	no	n/a	n/a	n/a	n/a	0.002	0	0	JDM	n/a
1	5716.0-5716.3	0.30	small core	0.30	0.15	2	no	no	n/a	n/a	n/a	n/a	0.002	0	0	JDM	n/a
1	5716.3-5716.5	0.20	core	0.20	0.10	2	no	no	03/22/17	03/24/17	2A	2	0.042	0	0	JEH	PY
1	5716.5-5717.5	1.0	core	1.0	0.50	2, 3	yes	no	03/20/17	03/22/17	2A	2	0.028	0	0	JEH	PY
			residue						n/a	n/a	n/a	n/a	0.010	0	0	JDM	n/a
1	5717.5-5718.0	0.50	small core	0.50	0.25	3	yes	no	n/a	n/a	n/a	n/a	n/a	n/a	n/a	n/a	not enough core
			residue						n/a	n/a	n/a	n/a	0.004	0	0	JDM	n/a
1	5720.0-5720.5	0.50	core	0.50	0.25	3	no	no	03/20/17	03/22/17	2A	2	0.006	0	0	JEH	

1	5720.5-5721.5	1.0	small core	1.0	0.50	2, 3	no	no	n/a	n/a	n/a	n/a	n/a	n/a		n/a	not enough core
			residue						n/a	n/a	n/a	n/a	0.006	0	0	JDM	n/a
1	5721.5-5722.0	0.50	core	0.50	0.25	2	yes	no	03/20/17	03/22/17	2A	2	0.018	0	0	JEH	
1	5728.0-5729.0	1.0	core	1.0	0.50	2	yes	yes	n/a	n/a	n/a	n/a	n/a	0	0	TMQ	n/a
			residue						n/a	n/a	n/a	n/a	0.005	0	0	JDM	SPIC
1	5729.0-5730.0	1.0	core	1.0	0.50	3	no	no	03/20/17	03/22/17	2A	2	0.002	0	0	JEH	MARC, IO
			residue						n/a	n/a	n/a	n/a	0.003	0	0	JDM	n/a
1	5731.6-5732.0	0.4	core	0.40	0.20	3	no		03/20/17	03/22/17	2A	2	0.002	0	0	JEH	PY, MARC, IO, SPIC, RND QTZ, VIV, AZ
1	5732.0-5732.8	0.80	small core	0.80	0.40	2	no	no	n/a	n/a	n/a	n/a	n/a	n/a	n/a	n/a	not enough core
			residue						n/a	n/a	n/a	n/a	0.003	0	0	JDM	n/a
1	5732.8-5733.5	0.70	small core	0.70	0.35	2	no	no	n/a	n/a	n/a	n/a	0.002	0	0	JDM	n/a
1	5733.0 (repeat)	n/a	core	n/a	n/a	2	no	no	n/a	n/a	n/a	n/a	n/a	n/a	n/a	n/a	repeat section
1	5733.5-5734.0	0.50	core	0.50	0.25	2	no	no	n/a	n/a	n/a	n/a	0.002	0	0	JDM	n/a
1	5738.0-5738.5	0.50	core	n/a	n/a	3	no	no	n/a	n/a	n/a	n/a	n/a	n/a	n/a	n/a	not processed
1	5738.5-5739.5	1.0	big core	1.0	0.50	2, 3	no	no	03/21/17	03/23/17	2A	2	0.009	0	0	JEH	PY
1	5739.5-5740.0	0.50	core	0.50	0.25	2	no	no	03/22/17	03/24/17	2A	2	0.004	0	0	JEH	PY, SPIC
1	5740.0-5740.8	0.80	big core	0.80	0.40	2	no	no	03/22/17	03/24/17	2A	2	0.005	0	0	JEH	PY, MARC, SPIC
1	5740.8-5742.0	1.2	core	1.2	0.60	2	no	no	03/22/17	03/24/17	2A	2	0.011	0	0	JEH	PY, IO, SPIC, QTZ
1	5742.0-5742.5	0.50	small core	0.50	0.25	3	no	no	n/a	n/a	n/a	n/a	0.003	0	0	JDM	n/a
1	5742.5-5743.5	1.0	core	1.0	0.50	3	no	no	03/22/17	03/24/17	2A	2	0.002	0	0	JEH	MARC, SPIC
1	5743.5-5744.0	0.50	big core	0.50	0.25	3	no	no	03/22/17	03/24/17	2A	2	0.002	0	0	JEH	MARC, SPIC
1	5746.0-5747.0**	1.0	big core	1.0	0.50	3	no	no	n/a	n/a	n/a	n/a	0.014	0	0	JDM	n/a
1	5747.0-5747.6**	0.60	big core	0.60	0.30	3	no	no	n/a	n/a	n/a	n/a	0.010	0	0	JDM	n/a
1	5747.6-5748.0	0.40	core	0.40	0.20	3	no	no	03/20/17	03/22/17	2A	2	0.001	1	0	JEH	PY, MARC, IO, CRIN, SPIC
1	5748.0-5748.5	0.50	small core	0.50	0.25	2, 3	no	no	n/a	n/a	n/a	n/a	n/a	n/a	n/a	n/a	not enough core
			residue						n/a	n/a	n/a	n/a	0.001	0	0	JDM	n/a
1	5748.5-5749.0	0.50	small core	0.50	0.25	3	no	no	n/a	n/a	n/a	n/a	n/a	n/a	n/a	n/a	not enough core
			residue						n/a	n/a	n/a	n/a	0.003	0	0	JDM	n/a
1	5749.0-5750.0	1.0	core	1.0	0.50	3	no	no	03/20/17	03/22/17	2A	2	0.004	0	0	JEH	PY, MARC, IO
			residue						n/a	n/a	n/a	n/a	0.002	0	0	JDM	n/a
1	5758.0-5758.5	0.50	small core	0.50	0.25	3	no	no	n/a	n/a	n/a	n/a	n/a	n/a	n/a	n/a	not enough core
			residue						n/a	n/a	n/a	n/a	0.001	1	0	JDM	CRIN
1	5758.5-5759.5	1.0	small core	1.0	0.50	3	no	no	n/a	n/a	n/a	n/a	n/a	n/a	n/a	n/a	not enough core
			residue						n/a	n/a	n/a	n/a	0.001	0	0	JDM	n/a
1	5759.5-5760.0	0.50	residue	0.50	0.25	3	no	no	04/24/15	04/25/15	n/a	n/a	0.012	0	0	JDM	n/a
1	5762.0-5762.8	0.80	core	0.80	0.40	3	no	no	03/22/17	03/24/17	2A	2	0.003	0	0	JEH	PY
			residue						n/a	n/a	n/a	n/a	0.002	0	0	JDM	n/a
1	5763.5-5764.0	0.50	small core	0.50	0.25	3	no	no	n/a	n/a	n/a	n/a	0.002	0	0	JDM	n/a
1	5764.0-5764.5	0.50	small core	0.50	0.25	3	no	no	n/a	n/a	n/a	n/a	0.004	0	0	JDM	n/a
1	5764.5-5765.0	0.50	small core	0.50	0.25	3	no	no	n/a	n/a	n/a	n/a	n/a	n/a	n/a	n/a	not enough core
			residue						n/a	n/a	n/a	n/a	0.002	0	0	JDM	n/a
1	5765.0-5766.0**	1.0	big core	1.0	0.50	3	no	no	n/a	n/a	n/a	n/a	0.006	0	0	JDM	n/a
1	5799.0-5799.5	0.50	core	0.50	0.25	5	no	no	03/20/17	03/22/17	2A	2	0.003	0	0	JEH	IO, CRIN, VIV
1	5799.5-5800.0	0.50	core	0.50	0.25	3, 5	no	no	n/a	n/a	n/a	n/a	n/a	n/a	0	TMQ	n/a
			residue						n/a	n/a	n/a	n/a	0.002	0	0	JDM	n/a
1	5800.0-5801.0	1.0	core	1.0	0.50	3	no	no	03/20/17	03/22/17	2A	2	0.004	0	0	JEH	PY, MARC
			residue						n/a	n/a	n/a	n/a	0.002	0	0	JDM	n/a
1	5801.0-5801.5	0.50	core	0.50	0.25	3	no	no	03/20/17	03/22/17	2A	2	0.003	1	0	JEH	MARC, BRACH, CRIN, VIV, QTZ, GLAUC, AP
			residue						n/a	n/a	n/a	n/a	0.002	0	0	JDM	n/a
1	5801.5-5802.0	0.50	residue	0.50	0.25	3	no	no	n/a	n/a	n/a	n/a	0.002	0	0	JDM	n/a
1	5801.5-5802.5	1.0	core	1.0	0.50	3	no	no	03/22/17	03/24/17	2A	2	0.001	0	0	JEH	BRACH, CRIN
			residue						n/a	n/a	n/a	n/a	0.002	0	0	JDM	n/a
1	5802.5-5803.0	0.50	core	0.50	0.25	3	no	no	03/22/17	03/24/17	2A	2	0.001	0	0	JEH	BRACH, CRIN
1	5815.0-5815.5	0.50	core	0.50	0.25	3	no	no	04/07/16	05/13/16	S, 5A	6	0.004	3	0	JEH	PY, MARC, IO, DOL, VIV, RND QTZ (Reworked)
1	5815.5-5816.5	1.0	core	1.0	0.50	1	no	no	05/16/16	05/25/16	5A	5	0.007	0	0	JEH	PY, MAR, SPIC, VIV, WF SH
1	5816.5-5817.1	0.60	core	0.60	0.30	1	no	no	04/07/16	05/09/16	4A	4	0.005	1	0	JEH	PY, BRACH, IO, WF SH, RND QTZ (Reworked)
1	5817.1-5817.5	0.40	disaggregate	0.40	0.20	1	no	no	05/09/16	05/18/16	6A	6	0.012	0	0	JEH	PY, MAR, BRACH, WF SH
1	5817.5-5818.5	1.0	core	n/a	n/a	1	no	no	n/a	n/a	n/a	n/a	n/a	n/a	n/a	n/a	not processed
1	5818.5-5819.0	0.50	residue	0.50	0.25	1	no	no	n/a	n/a	n/a	n/a	0.002	0	0	JDM	n/a
	TOTALS:	82		82	41								1.67	89	2		

*No difference between core depth and log depth

**Residues not saved

WINNEY 1-8 Core

WINNEY #1-8 SWD core — 145 samples analyzed of 145 taken
Payne County, Oklahoma
Depth Interval 5120'-5316' — ~190 ft. thick section

3rd Order Sequence	Core Depth* (ft)	Footage (ft)	Sample Type	Approx. Whole-rock Weight (kg)	Approx. Sample Weight (kg)	Facies	XRD	Stain	Start Date	End Date	Type	# baths	Residue Weight (kg)	Conodonts	# conodonts useful w/SEM	Processor	Microscope Notes
4	5133.0-5133.5	0.50	core	0.50	0.25	2, 5	N	N	05/26/16	06/02/16	4A	4	0.031	5	0	JEH	PY, MARC, CHRT, BRACH
			residue						04/24/15	04/25/15	n/a	n/a	0.001	0	0	JDM	AP
4	5133.5-5134.5	1.0	core	1.0	0.50	2, 4	Y	Y	05/26/16	06/02/16	4A	4	0.017	0	0	JEH	PY, MARC, IO, CHRT, SPIC, BRACH
4	5134.5-5135	0.50	core	0.50	0.25	4	Y	Y	04/19/17	04/21/17	2A	2	0.045	1	0	JEH	PY, MARC, BRACH
4	5143.0-5143.5	0.50	core	0.50	0.25	2, 5	N	N	04/19/17	04/21/17	2A	2	0.024	0	0	JEH	PY, SPIC
4	5143.5-5144.5	1.0	core	1.0	0.50	2	Y	N	04/19/17	04/21/17	2A	2	0.012	3	0	JEH	PY, SPIC
4	5144.5-5145.0**	0.50	core	0.50	0.25	2	Y	N	05/09/16	05/11/16	2A	2	0.031	0	0	JEH	SPIC
4	5145.0-5145.66**	0.66	core	0.66	0.33	2	Y	N	05/09/16	05/11/16	2A	2	0.024	0	0	JEH	
4	5145.66-5146.33	0.67	core	0.67	0.34	2, 5	N	N	04/19/17	04/21/17	2A	2	0.042	0	0	JEH	PY
4	5146.33-5147.0**	0.67	core	0.67	0.34	5	N	N	05/09/16	05/11/16	2A	2	0.009	0	0	JEH	MARC, CHRT
4	5151.0-5152.2	1.2	core	1.2	0.60	4	N	N	04/19/17	04/21/17	2A	2	0.012	0	0	JEH	SPIC
4	5152.2-5153.0**	0.80	core	0.80	0.40	2, 3	Y	N	05/09/16	05/11/16	2A	2	0.013	0	0	JEH	CRIN, VIV
4	5153.0-5153.3**	0.30	core	0.30	0.15	2	N	N	05/09/16	05/11/16	2A	2	0.007	0	0	JEH	
4	5153.3-5153.7**	0.40	core	0.40	0.20	2	N	N	05/09/16	05/11/16	2A	2	0.008	0	0	JEH	VIV
4	5154.0-5154.3	0.30	core	0.30	0.15	2	Y	N	04/19/17	04/21/17	2A	2	0.016	1	0	JEH	PY, SPIC, BRACH, CRIN
4	5154.3-5155.0**	0.70	core	0.70	0.35	2, 3	N	N	05/09/16	05/11/16	2A	2	0.009	0	0	JEH	RND QTZ
4	5155.0-5155.5**	0.50	core	0.50	0.25	3	N	N	05/09/16	05/11/16	2A	2	0.006	0	0	JEH	
4	5155.5-5156.5**	1.0	core	1.0	0.50	3	Y	N	05/09/16	05/11/16	2A	2	0.002	0	0	JEH	
4	5156.5-5157.0**	0.50	core	0.50	0.25	3	N	N	05/09/16	05/11/16	2A	2	0.013	0	0	JEH	PY, VIV
4	5157.0-5157.6	0.60	core	0.60	0.30	3	Y	N	04/19/17	04/21/17	2A	2	0.020	0	0	JEH	MARC
4	5157.6-5158.1	0.50	core	0.50	0.25	3	N	N	04/19/17	04/21/17	2A	2	0.012	1	0	JEH	PY, MARC, BRACH, CRIN
4	5158.1-5158.7**	0.60	core	0.60	0.30	3	Y	N	05/09/16	05/11/16	2A	2	0.005	0	0	JEH	RND QTZ
4	5158.9-5159.0**	0.10	core	0.10	0.05	3	Y	N	05/09/16	05/11/16	2A	2	0.008	0	0	JEH	PY
4	5159.0-5159.8**	0.80	core	0.80	0.40	3	Y	N	05/09/16	05/11/16	2A	2	0.005	0	0	JEH	PY, SPIC
4	5159.8-5160.6	0.80	residue	0.80	0.40	2, 3	N	N	04/24/15	04/25/15	n/a	n/a	0.005	0	0	JDM	AP
4	5160.6-5161.0**	0.40	core	0.40	0.20	2	N	N	05/11/16	05/13/16	2A	2	0.022	0	0	JEH	PY, IO, BRACH, SPIC, VIV
4	5161.0-5161.5	0.50	core	0.50	0.25	2, 3	N	N	04/19/17	04/21/17	2A	2	0.013	0	0	JEH	SPIC
4	5161.3 (repeat)	n/a	core	n/a	n/a	2	N	N	n/a	n/a	n/a	n/a	n/a	n/a	n/a	n/a	repeat section
4	5261.5-5162.5**	1.0	big core	1.0	0.50	3	Y	N	05/11/16	05/13/16	2A	2	0.007	0	0	JEH	PY, IO, CRIN, SPIC
4	5162.5-5163.0**	0.50	core	0.50	0.25	3	N	N	05/11/16	05/13/16	2A	2	0.006	0	0	JEH	PY, MARC, CRIN
4	5163.0-5163.7	0.70	core	0.70	0.35	3	N	N	05/26/16	06/02/16	4A	4	0.045	0	0	JEH	PY, MARC, SPIC
4	5163.7-5164.0	0.30	core	0.30	0.15	3	N	N	05/26/16	06/02/16	4A	4	0.011	2	0	JEH	MARC, SPIC, VIV (Reworked)
4	5164.0-5165.0	1.0	core	1.0	0.50	3	N	N	05/26/16	06/02/16	P, 3A	4	0.008	1	0	JEH	PY, MARC, SPIC, CRIN, VIV (Reworked)
									3rd Order Sequence Boundary (CD: 5168')								
3	5171.0-5171.5	0.50	core	0.50	0.25	4, 5	N	Y	06/02/16	06/09/16	4A	4	0.008	0	0	JEH	MARC, SPIC, CHRT
3	5171.5-5172.5	1.0	core	1.0	0.50	5	N	Y	06/02/16	06/08/16	3A	3	0.004	0	0	JEH	MAR, IO, SPIC
3	5172.3 (repeat)	n/a	core	n/a	n/a	5	N	N	n/a	n/a	n/a	n/a	n/a	n/a	n/a	n/a	repeat section
3	5172.5-5173.0	0.50	core	0.50	0.25	5	N	Y	06/02/16	06/08/16	3A	3	0.003	1	0	JEH	IO, SPIC
3	5174.0-5174.9**	0.90	core	0.90	0.45	3	N	N	05/11/16	05/13/16	2A	2	0.017	0	0	JEH	FISH SCALE?
3	5181.0-5181.9**	0.90	core	0.90	0.45	3, 4, 5	N	Y	05/17/16	05/19/16	2A	2	0.016	0	0	JEH	PY
3	5181.9-5182.4**	0.50	core	0.50	0.25	3, 5	N	N	05/17/16	05/19/16	2A	2	0.004	0	0	JEH	MARC
3	5182.4-5283.0**	0.60	core	0.60	0.30	5	Y	Y	05/17/16	05/19/16	2A	2	0.004	0	0	JEH	SPIC
3	5183.0-5184.0**	1.0	core	1.0	0.50	4, 5	N	Y	05/11/16	05/13/16	2A	2	0.032	0	0	JEH	
3	5184.0-5185.0**	1.0	core	1.0	0.50	5	Y	Y	05/17/16	05/19/16	2A	2	0.005	0	0	JEH	PY
3	5185.0-5185.9**	0.90	core	0.90	0.45	4, 5	N	Y	05/11/16	05/13/16	2A	2	0.016	0	0	JEH	
3	5185.9-5187.0**	1.1	core	1.1	0.55	5	Y	N	05/17/16	05/19/16	2A	2	0.005	0	0	JEH	SPIC
3	5187.0-5187.5**	0.50	core	0.50	0.25	5	N	N	05/19/16	05/21/16	2A	2	0.007	0	0	JEH	PY, MARC
3	5187.5-5188.5**	1.0	core	1.0	0.50	5	Y	Y	05/19/16	05/21/16	2A	2	0.007	0	0	JEH	PY, SPIC
3	5188.5 (repeat)	n/a	big core	n/a	n/a	5	N	N	n/a	n/a	n/a	n/a	n/a	n/a	n/a	n/a	repeat section
3	5188.5-5189.0**	0.50	core	0.50	0.25	5	N	N	05/19/16	05/21/16	2A	2	0.003	0	0	JEH	PY
3	5189.0-5189.5**	0.50	core	0.50	0.25	4	N	Y	05/19/16	05/21/16	2A	2	0.031	0	0	JEH	SPIC
3	5189.5-5190.0**	0.50	core	0.50	0.25	4	N	Y	05/19/16	05/21/16	2A	2	0.022	0	0	JEH	PY
3	5190.0-5190.75**	0.75	core	0.75	0.38	5	Y	N	05/19/16	05/21/16	2A	2	0.021	0	0	JEH	
3	5190.95-5191.7**	0.75	core	0.75	0.38	5	N	Y	05/19/16	05/21/16	2A	2	0.010	0	0	JEH	SPIC
3	5191.7-5192.4**	0.70	core	0.70	0.35	5	N	Y	05/21/16	05/23/16	2A	2	0.005	0	0	JEH	PY, MARC, IO
3	5192.4-5193.0**	0.60	core	0.60	0.30	5	N	Y	05/21/16	05/23/16	2A	2	0.006	0	0	JEH	
3	5193.0-5193.5**	0.50	core	0.50	0.25	5	N	Y	05/21/16	05/23/16	2A	2	0.005	0	0	JEH	SPIC
3	5193.5-5194.4**	0.90	core	0.90	0.45	5	N	Y	05/21/16	05/23/16	2A	2	0.011	0	0	JEH	SPIC
3	5194.5-5195.0**	0.50	core	0.50	0.25	5	N	Y	05/21/16	05/23/16	2A	2	0.004	0	0	JEH	
3	5195.0-5195.5**	0.50	core	0.50	0.25	5	N	Y	05/21/16	05/23/16	2A	2	0.002	0	0	JEH	PY, IO

3	5195.5-5196.5**	1.0	core	1.0	0.50	5	N	Y	04/19/17	04/21/17	2A	2	0.007	0	0	JEH	
3	5196.5-5197.0**	0.50	core	0.50	0.25	5	N	Y	05/19/16	05/21/16	2A	2	0.004	0	0	JEH	
3	5197.0-5197.6**	0.60	core	0.60	0.30	5	N	Y	04/19/17	04/21/17	2A	2	0.005	0	0	JEH	
3	5197.6-5198.4	0.80	core	0.80	0.40	5	N	Y	06/08/16	06/16/16	P, 4A	5	0.031	0	0	JEH	PY, SPIC
3	5198.4-5199.0	0.60	core	0.60	0.30	5	Y	Y	06/08/16	06/16/16	P, 4A	5	0.012	0	0	JEH	PY, MARC, IO, SPIC, CRIN
3	5205.0-5205.3**	0.30	core	0.30	0.20	5	Y	N	05/11/16	05/13/16	2A	2	0.006	0	0	JEH	
									n/a	n/a	n/a	n/a	n/a	0	0	TMQ	n/a
3rd Order Sequence Boundary (CD: ~5204')																	
2	5207.0-5207.5**	0.50	core	0.50	0.25	5	Y	N	05/11/16	05/13/16	2A	2	0.003	0	0	JEH	SPIC
									n/a	n/a	n/a	n/a	n/a	0	0	TMQ	n/a
2	5207.5 (repeat)	n/a	core	n/a	n/a	5	Y	N	n/a	n/a	n/a	n/a	n/a	n/a	n/a	n/a	repeat section
2	5208.0-5209.5**	1.5	core	1.5	0.75	2, 5	N	N	05/11/16	05/13/16	2A	2	0.002	0	0	JEH	SPIC
2	5233.0-5233.9**	1.5	core	1.5	0.75	4	Y	N	05/11/16	05/13/16	2A	2	0.021	0	0	JEH	IO
2	5235.0-5235.9**	1.5	small core	1.5	0.75	5	N	Y	05/11/16	05/13/16	2A	2	0.001	0	0	JEH	PY, SPIC
2	5236.0-5236.5**	0.50	core	0.50	0.25	5	N	Y	05/11/16	05/13/16	2A	2	0.012	0	0	JEH	PY, FISH FOSSIL?
2	5236.5-5237.5**	1.0	core	1.0	0.50	5	N	Y	05/11/16	05/13/16	2A	2	0.006	0	0	JEH	PY, IO
2	5237.5-5238.0**	0.50	core	0.50	0.25	5	N	Y	05/02/16	05/04/16	2A	2	0.005	0	0	JEH	SPIC, BRACH
2	5243.0-5243.5**	0.50	core	0.50	0.25	4	Y	N	05/02/16	05/04/16	2A	2	0.022	0	0	JEH	PY, CRIN, VIV
2	5247.2-5248.0**	0.50	core	0.50	0.25	5	N	N	05/02/16	05/04/16	2A	2	0.016	0	0	JEH	PY, MARC
2	5248.0-5248.8**	0.80	core	0.80	0.40	3, 5	N	N	05/02/16	05/04/16	2A	2	0.016	0	0	JEH	SPIC, BRACH
2	5248.8-5249.2**	0.40	core	0.40	0.20	3	N	N	05/02/16	05/04/16	2A	2	0.009	0	0	JEH	PY, MARC
2	5249.2 (repeat)	n/a	core	n/a	n/a	3	N	N	n/a	n/a	n/a	n/a	n/a	n/a	n/a	n/a	repeat section
2	5249.0-5250.0**	1.0	big core	1.0	0.50	3	Y	N	05/02/16	05/04/16	2A	2	0.015	0	0	JEH	PY, SPIC
2	5250.0-5250.5**	0.50	core	0.50	0.25	2, 3	N	N	05/02/16	05/04/16	2A	2	0.014	0	0	JEH	PY
2	5250.5-5251.0**	0.50	core	0.50	0.25	2, 3	N	N	05/02/16	05/04/16	2A	2	0.018	0	0	JEH	SPIC
2	5251.0-5251.5**	0.50	core	0.50	0.25	3	N	N	05/02/16	05/04/16	2A	2	0.018	0	0	JEH	MARC
2	5251.5-5252.5**	1.0	core	1.00	0.50	3	N	N	05/02/16	05/04/16	2A	2	0.009	4	0	JEH	IO, BRACH, CRIN, VIV
2	5252.5-5253.0**	0.50	core	0.50	0.25	3	N	N	05/02/16	05/04/16	2A	2	0.005	0	0	JEH	PY, SPIC, CRIN
2	5253.0-5253.5**	0.50	core	0.50	0.25	3	N	N	05/02/16	05/04/16	2A	2	0.002	1	0	JEH	
2	5254.5-5255.0**	0.50	core	0.50	0.25	3	N	N	05/02/16	05/04/16	2A	2	0.003	0	0	JEH	PY
2	5255.0-5255.5**	0.50	core	0.50	0.25	3	N	N	04/25/16	04/27/16	2A	2	0.006	0	0	JEH	RND QTZ
2	5255.5-5256.5**	1.0	disaggregate	1.0	0.50	3	N	N	04/24/15	04/25/15	n/a	n/a	0.001	0	0	JDM	n/a
2	5256.5-5257.0**	0.50	core	0.50	0.25	3	N	N	04/25/16	04/27/16	2A	2	0.007	1	0	JEH	
3rd Order Sequence Boundary (CD: 5256')																	
1	5257.0-5257.5**	0.50	core	0.50	0.25	3	N	N	04/25/16	04/27/16	2A	2	0.020	4	0	JEH	SPIC, CRIN
1	5258.5-5259.0	0.50	residue	0.50	0.25	4	Y	Y	04/24/15	04/25/15	n/a	n/a	0.012	2	0	JDM	n/a
1	5262.0-5262.3**	0.3	core	0.30	0.15	3	Y	N	04/25/16	04/27/16	2A	2	0.003	0	0	JEH	IO
									n/a	n/a	n/a	n/a	n/a	0	0	TMQ	n/a
1	5263.0-5263.8**	0.80	core	0.80	0.40	5	N	Y	04/25/16	04/27/16	2A	2	0.005	0	0	JEH	
1	5270.0-5270.5**	0.50	core	0.50	0.25	2, 3	Y	N	04/25/16	04/27/16	2A	2	0.004	0	0	JEH	PY
1	5270.5 (repeat)	n/a	core	n/a	n/a	2, 3	Y	N	n/a	n/a	n/a	n/a	n/a	n/a	n/a	n/a	repeat section
1	5270.9-5271.4**	0.50	core	0.5	0.25	2, 3	N	N	04/25/16	04/27/16	2A	2	0.016	0	0	JEH	MARC
1	5271.4 (repeat)	n/a	big core	n/a	n/a	3	N	N	n/a	n/a	n/a	n/a	n/a	n/a	n/a	n/a	repeat section
1	5271.6-5272.0**	0.40	core	0.40	0.20	2	N	N	04/25/16	04/27/16	2A	2	0.017	0	0	JEH	MARC
1	5272.0-5272.5**	0.50	core	0.50	0.25	3	N	N	04/25/16	04/27/16	2A	2	0.046	0	0	JEH	PY
1	5272.5-5273.0**	0.50	core	0.50	0.25	3	N	N	04/25/16	04/27/16	2A	2	0.016	0	0	JEH	PY
1	5273.0-5274.0**	1.0	core	1.0	0.50	3	N	N	04/25/16	04/27/16	2A	2	0.012	0	0	JEH	
1	5274.0-5274.5	0.50	residue	0.50	0.25	4	N	N	04/24/15	04/25/15	n/a	n/a	0.010	0	0	JDM	n/a
1	5274.5-5275.5**	1.0	core	1.0	0.50	3, 4	Y	N	04/25/16	04/27/16	2A	2	0.009	0	0	JEH	
1	5275.5-5276.0**	0.50	core	0.50	0.25	3	N	N	04/25/16	04/27/16	2A	2	0.002	2	0	JEH	PY, CRIN
1	5276.0-5276.8**	0.80	core	0.80	0.40	3	N	N	04/27/16	04/29/16	2A	2	0.003	1	0	JEH	
1	5276.8-5277.2**	0.40	core	0.40	0.20	3	N	N	04/27/16	04/29/16	2A	2	0.008	0	0	JEH	SPIC
1	5277.2-5278.0**	0.80	core	0.80	0.40	3	N	N	04/27/16	04/29/16	2A	2	0.006	0	0	JEH	SPIC
1	5278.0-5278.3**	0.30	core	0.30	0.15	3	N	N	04/27/16	04/29/16	2A	2	0.004	0	0	JEH	MARC
1	5278.3-5279.3	1.0	residue	1.0	0.50	3	N	N	04/24/15	04/25/15	n/a	n/a	0.009	0	0	JDM	n/a
1	5279.3-5279.9**	0.60	core	0.60	0.30	3	Y	N	04/27/16	04/29/16	2A	2	0.018	0	0	JEH	PY
1	5279.9-5280.5**	0.60	core	0.60	0.30	2, 3	N	N	04/27/16	04/29/16	2A	2	0.034	0	0	JEH	PY, IO
1	5280.5-5281.0**	0.50	core	0.50	0.25	2	N	N	04/27/16	04/29/16	2A	2	0.043	0	0	JEH	PY
1	5281.0-5281.9**	0.90	core	0.90	0.45	2	N	N	04/27/16	04/29/16	2A	2	0.002	0	0	JEH	
1	5281.9-5282.8**	0.90	core	0.90	0.45	2, 3	Y	N	04/27/16	04/29/16	2A	2	0.004	0	0	JEH	
1	5282.8 (repeat)	n/a	core	n/a	n/a	3	Y	N	n/a	n/a	n/a	n/a	n/a	n/a	n/a	n/a	repeat section
1	5283.0-5283.5**	0.50	core	0.50	0.25	3	N	N	04/27/16	04/29/16	2A	2	0.004	0	0	JEH	
1	5283.5-5284.5**	1.0	core	1.0	0.50	3	N	N	04/27/16	04/29/16	2A	2	0.004	0	0	JEH	
1	5284.5-5285.0**	0.50	core	0.50	0.25	3	N	N	04/27/16	04/29/16	2A	2	0.007	0	0	JEH	SPIC
1	5285.0-5285.5**	0.50	core	0.50	0.25	2, 3	N	N	04/27/16	04/29/16	2A	2	0.011	0	0	JEH	SPIC
1	5285.5-5286.5**	1.0	core	1.0	0.50	2, 3	Y	N	04/18/16	04/20/16	2A	2	0.012	0	0	JEH	PY, MARC, IO
1	5286.5-5287.0**	0.50	core	0.50	0.25	3	N	N	04/18/16	04/20/16	2A	2	0.005	0	0	JEH	

1	5287.0-5287.8**	0.80	core	0.80	0.40	3	N	N	04/18/16	04/20/16	2A	2	0.008	0	0	JEH	
1	5287.8 (repeat)	n/a	big core	n/a	n/a	3	N	N	n/a	n/a	n/a	n/a	n/a	n/a	n/a	n/a	repeat section
1	5288.0-5289.05**	1.05	core	1.1	0.53	3	N	N	04/18/16	04/20/16	2A	2	0.012	0	0	JEH	PY
1	5289.5-5290.5**	1.0	core	1.0	0.50	2, 3	Y	N	04/18/16	04/20/16	2A	2	0.025	0	0	JEH	MARC, IO
1	5290.5 (repeat)	n/a	core	n/a	n/a	2	N	N	n/a	n/a	n/a	n/a	n/a	n/a	n/a	n/a	repeat section
1	5290.5-5291.0**	0.50	core	0.50	0.25	2	N	N	04/18/16	04/20/16	2A	2	0.034	6	0	JEH	PY, MARC, IO
1	5291.0-5291.5**	0.50	core	0.50	0.25	2	N	N	04/18/16	04/20/16	2A	2	0.055	1	0	JEH	SPIC, CRIN
1	5292.5-5293.0**	0.50	core	0.50	0.25	1, 3	Y	N	04/18/16	04/20/16	P, 2A	3	0.003	0	0	JEH	PY, RND QTZ, CHRT
1	5293.0-5293.4**	0.40	core	0.40	0.20	3	N	N	04/18/16	04/20/16	2A	2	0.001	0	0	JEH	
1	5293.4-5294.4**	1.0	core	1.0	0.50	3	N	N	04/18/16	04/20/16	2A	2	0.004	0	0	JEH	CHRT
1	5294.4-5295.0**	0.60	core	0.60	0.30	3	N	N	04/18/16	04/20/16	2A	2	0.003	0	0	JEH	PY, IO
1	5295.0-5295.5**	0.50	core	0.50	0.25	3	N	N	04/18/16	04/20/16	2A	2	0.002	0	0	JEH	PY, MARC
1	5295.5-5296.0**	0.50	core	0.50	0.25	3	N	N	04/18/16	04/20/16	2A	2	0.006	0	0	JEH	
1	5295.7 (repeat)	n/a	core	n/a	n/a	3	N	N	n/a	n/a	n/a	n/a	n/a	n/a	n/a	n/a	repeat section
1	5296.0-5297.0**	1.0	core	1.0	0.50	3	N	N	04/20/16	04/22/16	2A	2	0.013	0	0	JEH	PY, SPIC
1	5297.0-5297.6**	0.60	core	0.60	0.30	3	N	N	04/20/16	04/22/16	2A	2	0.010	0	0	JEH	PY
1	5297.6-5298.3**	0.60	core	0.60	0.30	2, 3	N	N	04/20/16	04/22/16	2A	2	0.050	0	0	JEH	PY
1	5298.3-5299.2**	0.90	core	0.90	0.45	2, 3	Y	N	04/20/16	04/22/16	2A	2	0.023	17	0	JEH	PY, SPIC, CRIN, BRACH
1	5299.2-5300.0**	0.80	core	0.80	0.40	3	N	N	04/20/16	04/22/16	2A	2	0.034	0	0	JEH	PY, MARC
1	5302.0-5302.7**	0.70	core	0.70	0.35	3	N	N	04/20/16	04/22/16	2A	2	0.045	0	0	JEH	IO
1	5302.7-5303.3**	0.60	core	0.60	0.30	3	N	N	04/20/16	04/22/16	2A	2	0.012	0	0	JEH	IO
1	5303.3-5304.0**	0.70	core	0.70	0.35	3	N	N	04/20/16	04/22/16	2A	2	0.015	0	0	JEH	PY, MARC
1	5304.0-5304.5**	0.50	core	0.50	0.25	3	N	Y	04/20/16	04/22/16	2A	2	0.005	0	0	JEH	PY
1	5304.5-5305.5**	1.0	core	1.0	0.50	3	Y	Y	04/20/16	04/22/16	2A	2	0.007	0	0	JEH	
1	5305.5-5306.0	0.50	residue	0.50	0.25	3	N	Y	04/24/15	04/25/15	n/a	n/a	0.011	0	0	JDM	n/a
1	5306.0-5306.8**	0.80	core	0.80	0.40	2, 3	N	N	04/20/16	04/22/16	2A	2	0.008	0	0	JEH	PY, SPIC
1	5306.8-5307.6**	0.80	core	0.80	0.40	3	N	Y	04/20/16	04/22/16	2A	2	0.062	0	0	JEH	CRIN
1	5307.6-5308.0**	0.40	core	0.40	0.20	3	N	Y	04/20/16	04/22/16	2A	2	0.004	0	0	JEH	CRIN, VIV
1	5308.0-5308.7**	0.70	core	0.70	0.35	2, 3	N	N	05/16/16	05/18/16	2A	2	0.031	11	0	JEH	PY, MARC, BRACH, CRIN
1	5308.7-5309.3	0.60	residue	0.60	0.30	2, 3	N	N	04/24/15	04/25/15	n/a	n/a	0.001	0	0	JDM	n/a
1	5309.3-5309.7**	0.40	core	0.40	0.20	3	Y	N	05/16/16	05/18/16	2A	2	0.004	0	0	JEH	
1	5309.7-5310.2**	0.50	core	0.50	0.25	3	N	N	05/16/16	05/18/16	2A	2	0.005	0	0	JEH	PY, MARC, IO
1	5310.2-5311.0**	0.80	core	0.80	0.40	3	N	N	05/16/16	05/18/16	2A	2	0.007	0	0	JEH	PY, MARC, CRIN, BRACH
1	5311.0-5311.7	0.70	core	0.70	0.35	3	N	N	05/16/16	05/25/16	2P, 4A	6	0.011	2	0	JEH	PY, SPIC, CRIN (Reworked)
1	5311.7-5312.8	1.1	core	1.1	0.55	1, 3	Y	N	05/04/16	05/17/16	S, P, 4A	6	0.005	7	0	JEH	PY, MAR, SPIC, CRIN, BRACH, WF SH (Reworked)
1	5312.95-5313.0	0.050	core	0.050	0.025	1	N	N	05/04/16	05/13/16	S, 4A	5	0.007	2	0	JEH	PY, MAR, SPIC, CRIN, BRACH, WF SH (Reworked)
	TOTALS:	97		97	49								1.88	76	0		

*Core depths are ~10 ft stratigraphically higher on logs

**Residues not saved

ELINORE 1-18 Core

ELINORE #1-18 SWD core
Payne County, Oklahoma
Depth Interval LD: 4333'-4476'; CD: 4339'-4482'

67 samples analyzed of 67 taken

~143 ft. thick section

3rd Order Sequence	Core Depth* (ft)	Footage (ft)	Sample Type	Approx. Whole-rock Weight (kg)	Approx. Sample Weight (kg)	Facies	XRD	Stain	Start Date	End Date	Type	# baths	Residue Weight (kg)	Conodonts	# conodonts useful w/SEM	Processor	Microscope Notes
4	4338.5-4339.0	0.50	core	0.50	0.25	5	N	N	06/02/16	06/09/16	4A	4	0.024	0	0	JEH	PY, BRAC
4	4340.6-4341.0	0.40	core	0.40	0.20	5	N	Y	06/02/16	06/09/16	P,3A	4	0.018	0	0	JEH	VIV
4	4345.5-4346.0	0.50	core	0.50	0.25	4	N	Y	06/27/16	07/05/16	P,4A	5	0.013	0	0	JEH	PY
4	4362.0-4362.5	0.50	disaggregate	0.50	0.25	4	Y	N	06/27/16	07/05/16	4A	4	0.042	0	0	JEH	PY, CHRT, SPIC, CRIN
			residue						09/29/14	09/30/14	n/a	n/a	0.032	0	0	JDM	n/a
4	4362.5-4363.5	1.0	residue	1.0	0.50	2, 4	N	N	06/27/16	07/01/16	4A	4	0.035	0	0	JEH	IO, BRACH, VIV
			residue						09/30/14	10/01/14	n/a	n/a	0.006	0	0	JDM	n/a
4	4363.5-4364.0	0.50	residue	0.50	0.25	2	N	N	07/18/16	07/21/16	3A	3	0.014	0	0	JEH	IO, BRACH
			residue						09/30/14	10/01/14	n/a	n/a	0.010	0	0	JDM	n/a
4	4364.0-4364.7	0.70	core	0.70	0.35	2	N	N	07/26/16	07/29/16	3A	3	0.032	0	0	JEH	IO
4	4364.7-4365.3	0.60	residue	0.60	0.30	2	N	N	06/27/16	07/01/16	4A	4	0.018	0	0	JEH	PY, BRACH, CRIN
			residue						09/23/14	09/24/14	n/a	n/a	0.026	0	0	JDM	n/a
4	4365.3-4365.6	0.30	residue	0.30	0.15	2	N	N	06/27/16	07/01/16	4A	4	0.014	1	0	JEH	BRACH
			residue						09/29/14	09/30/14	n/a	n/a	0.004	0	0	JDM	n/a
4	4365.6-4366.0	0.40	core	0.40	0.20	2	N	N	07/26/16	07/29/16	3A	3	0.025	0	0	JEH	PY, BRACH
4	4366.0-4366.5	0.50	core	0.50	0.25	2	N	N	07/27/16	08/02/16	3A	3	0.031	15	0	JEH	PY, CHRT, SPIC, BRACH (Reworked)
4	4366.5-4367.5	1.0	core	1.0	0.50	2	N	N	07/26/16	07/29/16	3A	3	0.042	9	0	JEH	PY, SPIC, BRACH, CRIN, VIV
4	4367.5-4368.0	0.50	core	0.50	0.25	2, 3	N	N	07/26/16	07/29/16	3A	3	0.054	24	4	JEH	PY
4	4369.55-4370.0	0.45	core	0.45	0.23	3	N	N	07/25/16	07/27/16	3A	3	0.007	27	2	JEH	BRACH (Reworked)
4	4370.0-4370.5	0.50	core	0.50	0.25	2	N	N	06/09/16	06/16/16	4A	4	0.065	70	0	JEH	PY, MAR, IO, SPIC, BRAC, VIV (Reworked)
4	4370.5-4371.0	0.50	core	0.50	0.25	2	N	N	06/09/16	06/16/16	5A	5	0.014	3	0	JEH	PY, MAR, VIV
3rd Order Sequence Boundary (CD: 4371')																	
3	4376.0-4376.5	0.50	core	0.50	0.25	4	N	Y	06/27/16	07/05/16	P, 4A	5	0.008	0	0	JEH	SPIC, VIV
3	4391.0-4391.5	0.50	core	0.50	0.25	2	N	N	06/27/16	07/01/16	4A	4	0.022	0	0	JEH	MAR, CRIN, VIV
3	4391.5-4392.5	1.0	residue	1.0	0.50	2	N	N	06/20/16	06/24/16	5A	5	0.027	0	0	JEH	PY, MAR, CHRT, SPIC, BRAC, CRIN
			residue						09/29/14	09/30/14	n/a	n/a	0.007	0	0	JDM	n/a
3	4392.5-4393.0	0.50	residue	0.50	0.25	2	N	N	06/20/16	06/24/16	5A	5	0.026	1	0	JEH	PY, MAR, IO, SPIC, CHRT, VIV (Reworked)
			residue						09/29/14	09/30/14	n/a	n/a	0.007	0	0	JDM	n/a
3rd Order Sequence Boundary (CD: 4393')																	
2	4395.0-4395.5	0.50	core	0.50	0.25	5	N	Y	07/27/16	08/02/16	P, 2A	3	0.007	0	0	JEH	SPIC, CRIN
2	4401.05-4401.5**	0.45	core	0.45	0.23	5	N	N	07/27/16	08/02/16	3A	3	0.011	0	0	JEH	SPIC
2	4401.5-4402.5**	1.0	core	1.0	0.50	5	N	N	07/27/16	08/02/16	3A	3	0.016	0	0	JEH	CRIN
2	4402.5-4403.0	0.50	residue	0.50	0.25	3	N	N	07/05/16	07/09/16	5A	5	0.004	0	0	JEH	PY, MAR, IO
2	4402.8 (repeat)	n/a	core	n/a	n/a	3	N	N	n/a	n/a	n/a	n/a	n/a	n/a	n/a	n/a	repeat section
2	4402.0-4403.0	1.0	residue	1.0	0.50	3	N	N	09/23/14	09/24/14	n/a	n/a	0.006	0	0	JDM	n/a
			residue						09/23/14	09/24/14	n/a	n/a	0.003	0	0	JDM	n/a
2	4407.7-4408.2**	0.50	core	0.50	0.25	5	N	N	08/01/16	08/04/16	3A	3	0.020	0	0	JEH	SPIC
2	4414.4-4415.4**	1.0	core	1.0	0.50	5	N	N	08/01/16	08/04/16	3A	3	0.035	0	0	JEH	PY, SPIC, BRACH
2	4427.74428.7**	1.0	core	1.0	0.50	5	N	Y	08/01/16	08/04/16	P, 2A	3	0.041	0	0	JEH	PY
2	4449.5-4450.5**	1.0	core	1.0	0.50	3, 5	N	N	08/01/16	08/04/16	3A	3	0.017	0	0	JEH	PY, MAR
2	4450.5-4451.0**	0.50	core	0.50	0.25	3	N	N	08/02/16	08/05/16	3A	3	0.034	0	0	JEH	SPIC
2	4451.0-4451.5**	0.50	core	0.50	0.25	3	N	N	08/02/16	8/5/'6	3A	3	0.025	0	0	JEH	PY
2	4451.5-4452.5	1.0	residue	1.0	0.50	2	N	N	06/16/16	06/24/16	S, 5A	6	0.047	12	0	JEH	PY, MAR, SPIC, CRIN, VIV (Reworked)
			residue						09/23/14	09/24/14	n/a	n/a	0.017	0	0	JDM	n/a
2	4452.5-4453.0	0.50	core	0.50	0.25	2	N	N	08/02/16	8/5/'6	3A	3	0.043	1	0	JEH	MAR
2	4453.0-4453.5	0.50	residue	0.50	0.25	2	N	N	06/16/16	06/24/16	S, 5A	6	0.009	0	0	JEH	SPIC, CRIN
			residue						09/23/14	09/24/14	n/a	n/a	0.004	0	0	JDM	n/a
2	4453.5-4454.5	1.0	residue	1.0	0.50	2, 3	N	N	06/16/16	06/24/16	S, 5A	6	0.014	0	0	JEH	PY, MAR, IO, SPIC, BRAC, CRIN, VIV
			residue						09/23/14	09/24/14	n/a	n/a	0.003	0	0	JDM	n/a
3rd Order Sequence Boundary (CD: 4454')																	
1	4454.5-4455.0	0.50	core	0.50	0.25	3	N	N	07/21/16	07/27/16	4A	4	0.035	3	0	JEH	PY, SPIC
1	4455.0-4455.5	0.50	core	0.50	0.25	3	N	N	07/21/16	07/27/16	4A	4	0.039	3	0	JEH	PY, SPIC
1	4455.5-4456.5	1.0	residue	1.0	0.50	3	N	N	07/04/16	07/09/16	6A	6	0.029	0	0	JEH	PY, SPIC, CRIN
			residue						04/24/15	04/25/15	n/a	n/a	0.025	0	0	JDM	n/a
1	4456.5-4457.0	0.50	core	0.50	0.25	3	N	N	07/21/16	07/26/16	2A	2	0.019	12	1	JEH	PY
			residue						04/24/15	04/25/15	n/a	n/a	0.012	0	0	JDM	n/a

1	4457.0-4457.5	0.50	residue	0.50	0.25	3	N	N	07/18/16	07/21/16	3A	3	0.069	0	0	JEH	PY
			residue						10/21/14	10/22/14	n/a	n/a	0.021	0	0	JDM	n/a
1	4457.5-4458.5	1.0	residue	1.0	0.50	3	N	N	07/18/16	07/21/16	3A	3	0.030	0	0	JEH	PY, CRIN
			residue						10/21/14	10/22/14	n/a	n/a	0.026	0	0	JDM	n/a
1	4458.5-4459.0	0.50	residue	0.50	0.25	3	N	N	07/12/16	07/15/16	4A	4	0.030	25	2	JEH	PY, CHRT, FELD
			residue						10/21/14	10/22/14	n/a	n/a	0.020	0	0	JDM	n/a
1	4458.6 (repeat)	n/a	core	n/a	n/a	3	N	N	n/a	n/a	n/a	n/a	n/a	n/a	n/a	n/a	repeat section
1	4459.0 (repeat)	n/a	core	n/a	n/a	3	N	N	n/a	n/a	n/a	n/a	n/a	n/a	n/a	n/a	repeat section
1	4459.5-4460.0	0.50	residue	0.50	0.25	3	N	N	07/04/16	07/09/16	S, 5A	6	0.008	0	0	JEH	IO
			residue						10/21/14	10/22/14	n/a	n/a	0.009	0	0	JDM	n/a
1	4460.0-4460.5	0.50	residue	0.50	0.25	3	N	N	07/12/16	07/15/16	4A	4	0.019	0	0	JEH	PY, MAR, SPIC
			residue						10/21/14	10/22/14	n/a	n/a	0.008	0	0	JDM	n/a
1	4460.5-4461.4	0.90	residue	0.90	0.45	3	N	N	07/12/16	07/15/16	4A	4	0.027	0	0	JEH	PY, CRIN
			residue						10/21/14	10/22/14	n/a	n/a	0.009	0	0	JDM	n/a
1	4461.4-4462.0	0.60	residue	0.60	0.30	3	N	N	07/12/16	07/15/16	3A	3	0.030	0	0	JEH	PY, CRIN
			residue						10/21/14	10/22/14	n/a	n/a	0.011	0	0	JDM	n/a
1	4462.0-4462.5	0.50	residue	0.50	0.25	3	N	N	07/18/16	07/21/16	3A	3	0.027	0	0	JEH	PY, CRIN
			residue						09/30/14	10/01/14	n/a	n/a	0.007	0	0	JDM	n/a
1	4462.5-4463.5	1.0	residue	1.0	0.50	3	N	N	07/18/16	07/26/16	5A	5	0.017	1	0	JEH	PY, CRIN (Reworked?)
			residue						09/23/14	09/24/14	n/a	n/a	0.014	0	0	JDM	n/a
1	4463.5-4464.0	0.50	residue	0.50	0.25	3	N	N	07/04/16	07/09/16	S, 5A	6	0.027	0	0	JEH	PY, MAR, IO
			residue						09/23/14	09/24/14	n/a	n/a	0.010	0	0	JDM	n/a
1	4463.9 (repeat)	n/a	core	n/a	n/a	3	N	N	n/a	n/a	n/a	n/a	n/a	n/a	n/a	n/a	repeat section
1	4464.0-4464.5	0.50	residue	0.50	0.25	3	N	N	07/12/16	07/15/16	4A	4	0.008	1	1	JEH	PY
			residue						09/23/14	09/24/14	n/a	n/a	0.015	0	0	JDM	n/a
1	4464.5-4465.5	1.0	residue	1.0	0.50	3	N	N	07/18/16	07/22/16	4A	4	0.011	2	1	JEH	MARC, IO (Reworked?)
			residue						09/23/14	09/24/14	n/a	n/a	0.007	0	0	JDM	n/a
1	4465.5-4466.0	0.50	residue	0.50	0.25	3	N	N	07/04/16	07/09/16	S, 5A	6	0.015	0	0	JEH	IO
1	4466.0-4467.0	1.0	residue	1.0	0.50	3	Y	N	07/18/16	07/26/16	P, 4A	5	0.037	0	0	JEH	PY, VIV
			residue						09/23/14	09/24/14	n/a	n/a	0.043	0	0	JDM	n/a
1	4467.0-4468.0	1.0	residue	1.0	0.50	2	N	N	07/05/16	07/09/16	5A	5	0.004	0	0	JEH	PY, MARC, IO, BRACH
			residue						10/21/14	10/22/14	n/a	n/a	0.007	0	0	JDM	n/a
1	4468.0-4468.5	0.50	small core	0.50	0.25	2	N	N	07/21/16	07/27/16	4A	4	0.044	0	0	JEH	PY
1	4468.5-4469.5	1.0	residue	1.0	0.50	2	N	N	07/05/16	07/09/16	5A	5	0.024	0	0	JEH	PY, IO, CRIN
			residue						10/21/14	10/22/14	n/a	n/a	0.014	0	0	JDM	n/a
1	4469.5-4470.0	0.50	residue	0.50	0.25	2	N	N	07/12/16	07/19/16	5A	5	0.022	4	0	JEH	PY, BRACH, VIV
			residue						10/21/14	10/22/14	n/a	n/a	0.010	0	0	JDM	n/a
1	4470.0-4470.5	0.50	residue	0.50	0.25	3	N	N	07/12/16	07/15/16	4A	4	0.019	4	0	JEH	PY, BRACH, VIV
			residue						10/21/14	10/22/14	n/a	n/a	0.010	0	0	JDM	n/a
1	4470.5 (repeat)	n/a	core	n/a	n/a	3	N	N	n/a	n/a	n/a	n/a	n/a	n/a	n/a	n/a	repeat section
1	4470.5-4471.5	1.0	residue	1.0	0.50	3	Y	N	07/12/16	07/15/16	P, 3A	4	0.012	0	0	JEH	PY, BRACH, VIV
			residue						10/21/14	10/22/14	n/a	n/a	0.009	0	0	JDM	n/a
1	4471.5-4472.0	0.50	residue	0.50	0.25	3	N	N	n/a	n/a	n/a	n/a	0.003	0	0	JEH	PY, CRIN, BRACH
			residue						10/21/14	10/22/14	n/a	n/a	0.002	0	0	JDM	n/a
1	4476.0-4476.7	0.70	core	0.70	0.35	3	N	N	07/21/16	07/26/16	2A	2	0.035	0	0	JEH	PY
1	4478.0-4478.5	0.50	disaggregated	0.50	0.25	2	N	N	06/16/16	06/24/16	S, 5A	6	0.030	15	0	JEH	PY, CRIN
1	4478.5-4479.0	0.50	small core	0.50	0.25	2	N	N	06/16/16	06/24/16	S, 5A	6	0.068	14	0	JEH	PY, MAR, BRACH, CRIN (Reworked)
1	4479.0-4480.0	1.0	residue	1.0	0.50	1, 3	Y	N	05/16/16	05/25/16	S,P,4A	6	0.021	33	4	JEH	PY, MARC, IO, BRACH, CRIN, WF SH (Reworked)
1	4480.0-4481.0	1.0	disaggregated	1.0	0.50	3	Y	N	05/04/16	05/13/16	5A	5	0.005	0	0	JEH	PY, MAR, WF SH
			residue						04/24/15	04/25/15	n/a	n/a	0.002	0	0	JDM	n/a
1	4481.0-4481.7	0.70	disaggregated	0.70	0.35	1	N	N	05/04/16	05/13/16	S,P,4A	6	0.020	98	1	JEH	PY, MAR, CRIN, SPIC, BRACH, WF SH, Fish scale? (Reworked)
			residue						04/24/15	04/25/15	n/a	n/a	0.020	0	0	JDM	n/a
1	4481.7-4482.0	0.30	residue	0.30	0.15	1	N	N	04/24/15	04/25/15	n/a	n/a	0.003	0	0	JDM	n/a
	TOTALS:	44		44	22								2.08	378	16		

*Core depths are ~6 ft stratigraphically higher on logs

**Residues not saved

DOBERMAN 1-25 Core

Doberman #1-25 SWD core
Lincoln County, Oklahoma
Depth Interval LD: 4971'-5205'; CD: 4965'-5199'

34 samples analyzed of 34 taken

~234 ft. thick section

3rd Order Sequence	Core Depth* (ft)	Footage (ft)	Sample Type	Approx. Whole-rock Weight (kg)	Approx. Sample Weight (kg)	Facies	XRD	Start Date	End Date	Type	# baths	Residue Weight (kg)	Conodonts	# conodonts useful w/SEM	Processor	Microscope Notes
4	4968.0-4968.5	0.50	small core	0.50	0.25	4	N	01/26/17	01/28/17	S, 2A	3	0.020	6	0	JEH	(micro)PY, RND QTZ
4	4972.0-4972.5	0.50	small core	0.50	0.25	2	N	01/26/17	01/28/17	S, 2A	3	0.047	7	0	JEH	(micro)PY, BLU CHRT (Reworked)
4	4983.0-4983.5	0.50	small core	0.50	0.25	2	N	01/30/17	02/01/17	S, 2A	3	0.043	3	0	JEH	(Reworked)
4	4992.6-4992.8	0.20	tiny core	0.25	0.15	2	N	01/30/17	02/01/17	S, 2A	3	0.003	5	0	JEH	RND QTZ (Reworked)
4	5000.4-5000.6	0.20	tiny core	0.25	0.15	2	N	01/26/17	01/28/17	S, 2A	3	0.027	6	0	JEH	(micro)PY
4	5002.0-5002.2	0.20	tiny core	0.25	0.15	3	N	01/23/17	01/25/17	S, 2A	3	0.017	6	0	JEH	(micro)PY, VIV, DIT QTZ (?)
4	5011.9-5012.1	0.20	tiny core	0.25	0.15	2	N	01/23/17	01/25/17	S, 2A	3	0.024	0	0	JEH	
3rd Order Sequence Boundary CD: 5014'																
3	5022.0-5022.5	0.50	small core	0.50	0.25	2	N	01/30/17	02/01/17	S, 2A	3	0.023	55	4	JEH	RND QTZ, VIV, FISH TOOTH/FOSSIL?
3	5035.8-5036.0	0.20	tiny core	0.25	0.15	2	N	01/23/17	01/25/17	S, 2A	3	0.008	2	0	JEH	(micro)PY, AP
3	5044.0-5044.3	0.30	tiny core	0.25	0.15	2	N	01/30/17	02/01/17	S, 2A	3	0.006	3	0	JEH	
3	5050.0-5050.5	0.50	small core	0.50	0.25	2	N	01/30/17	02/01/17	S, 2A	3	0.042	1	0	JEH	(Reworked)
3	5052.0-5052.3	0.30	tiny core	0.25	0.15	2	N	01/23/17	01/25/17	S, 2A	3	0.065	0	0	JEH	
3	5059.0-5059.3	0.30	tiny core	0.25	0.15	2,4	N	01/30/17	02/01/17	S, 2A	3	0.002	0	0	JEH	
3	5068.0-5068.5	0.50	small core	0.50	0.25	2,3	N	01/26/17	01/28/17	S, 2A	3	0.017	0	0	JEH	(micro)PY
3	5075.7-5075.9	0.20	tiny core	0.25	0.15	2	N	01/30/17	02/01/17	S, 2A	3	0.002	3	0	JEH	(Reworked)
3	5078.5-5078.8	0.30	tiny core	0.25	0.15	3	N	01/23/17	01/25/17	S, 2A	3	0.041	0	0	JEH	(micro)PY
3	5091.0-5091.3	0.30	tiny core	0.25	0.15	2	N	01/30/17	02/01/17	S, 2A	3	0.053	3	0	JEH	BLU CHRT
3	5094.8-5095.3	0.50	small core	0.50	0.25	2	N	01/26/17	01/28/17	S, 2A	3	0.026	0	0	JEH	(micro)PY
3	5110.2-5110.4	0.20	tiny core	0.25	0.15	2,3	N	01/26/17	01/28/17	S, 2A	3	0.073	6	0	JEH	BLU CHRT
3	5112.0-5112.3	0.30	tiny core	0.25	0.15	2,3	N	01/30/17	02/01/17	S, 2A	3	0.059	1	0	JEH	
3	5117.1-5117.6	0.50	small core	0.50	0.25	3	N	01/30/17	02/01/17	S, 2A	3	0.010	2	0	JEH	(micro)PY, BLU CHRT, RND QTZ
3	5120.0-5120.3	0.30	tiny core	0.25	0.15	2	N	01/23/17	01/25/17	S, 2A	3	0.003	0	0	JEH	SPIC
3	5122.0-5122.3	0.30	tiny core	0.25	0.15	5	N	01/23/17	01/25/17	2A	2	0.017	4	0	JEH	(Reworked)
3rd Order Sequence Boundary CD: 5125'																
2	5138.0-5138.5	0.50	small core	0.50	0.25	5	N	02/03/17	02/07/17	2A	2	0.002	0	0	JEH	PY, MARC, BRACH
2	5142.0-5142.5	0.50	small core	0.50	0.25	5	N	02/03/17	02/07/17	2A	2	0.011	0	0	JEH	
2	5147.0-5147.3	0.30	tiny core	0.25	0.15	5	N	02/03/17	02/07/17	2A	2	0.070	2	0	JEH	(micro)PY, BLU/BRN CHRT
2	5156.0-5156.5	0.50	small core	0.50	0.25	2	N	02/03/17	02/07/17	S, 2A	3	0.041	2	0	JEH	(micro)PY, BLU/BRN CHRT, AP
2	5166.9-5167.2	0.30	tiny core	0.25	0.15	2	N	01/26/17	01/28/17	S, 2A	3	0.004	0	0	JEH	BLU CHRT
3rd Order Sequence Boundary CD: 5169'																
1	5171.4-5171.6	0.20	tiny core	0.25	0.15	6	N	01/26/17	01/28/17	2A	2	0.003	0	0	JEH	SPIC
1	5171.75-5172	0.25	tiny core	0.25	0.15	6	N	01/26/17	01/28/17	2A	2	0.047	0	0	JEH	SPIC
1	5184.0-5184.2	0.20	tiny core	0.25	0.15	2	N	02/03/17	02/07/17	S, 2A	3	0.008	0	0	JEH	
1	5192.0-5192.4	0.40	small core	0.50	0.25	2,3	N	01/26/17	01/28/17	S, 2A	3	0.007	0	0	JEH	(micro)PY, AP
1	5195.0-5195.7	0.20	core	0.60	0.35	5	N	02/03/17	02/07/17	2A	2	0.039	27	0	JEH	(micro)PY, BLU/BRN CHRT, VIV, CRIN
1	5199.0-5199.2	0.20	tiny core	0.25	0.15	1	N	01/23/17	01/25/17	S, 2A	3	0.003	2	0	JEH	(micro)PY, DOL (?) (Reworked)
	TOTALS:	11		12	6.5							0.863	146	4		

*Core depths must be placed ~6 feet stratigraphically higher on logs

APPENDICES

APPENDIX B: PROCESSING TECHNIQUES

Disaggregation and Acid Treatment of Whole-rock Samples

Whole-rock samples were disaggregated into 1 cm^3 "chips" with a sledge hammer and personal protective equipment at the Hazardous Reactions Laboratory at Oklahoma State University. The "chips" from a single sample were placed into a 5-gal. bucket and labeled by core (sampled) depth in quantities of about 1 kg before undergoing acid treatment. Acids were then applied to whole-rock samples and included formic acid, hydrogen peroxide, and sodium hexametaphosphate. The number and type of acid baths applied to a whole-rock sample varied, depending on its overall lithology that was determined by the author. What follows is a general description of the acids and how each of them was used to digest whole-rock samples.

Formic Acid

Formic acid (CH_2O_2) has been long used to digest carbonate rocks and isolate fossil remains, such as phosphatic conodont elements (e.g., Collinson, 1963). The mineral calcite is readily dissolved by acidic solutions, but phosphatic material resists chemical weathering in acids if exposed in relatively short intervals (~24 hrs.). Therefore, because

whole-rocks samples in the cores consisted dominantly of calcite, it was thought that formic acid would have the strongest effect on digesting the bulk of the sample from short-term exposure while also preserving any conodont elements present.

Formic acid treatments were applied to disaggregated whole-rock samples at 50% concentrations over 24 hr. periods, at which time the spent acid was decanted, residue collected, and a fresh supply of acid was applied to the remaining whole-rock sample to avoid etching conodont elements recovered from the residue. All samples underwent at least two formic acid treatments (excluding quartz-rich glauconitic intervals) and up to seven (Appendix A). Formic acid treatments tended to work most effectively on samples which had moderately high to high (>65%) carbonate content and a relatively moderate to high (>30%) mud content, presumably because this relationship promoted grains with a lot of surface area and dissolution susceptibility to digest most effectively per acid treatment. Facies 3, a bioturbated wackestone-packstone described by LeBlanc (2014) in the Adkisson 1-33, Winney 1-8, and Elinore 1-18, for example produced large amounts of residue, with some whole-rock samples being almost wholly digested in just one 24 hr. period. Facies 2, a burrowed calcareous mudstone in the same cores (LeBlanc, 2014), also generally responded very well to formic acid treatment.

Sodium Hexametaphosphate

Sodium hexametaphosphate ($[NaPO_3]_6$) is a surfactant (meaning that it reduces surface tensions between small particles, such as mud-sized grains in a whole-rock sample that allows the rock to freely disaggregate). It is sometimes used in biostratigraphic studies when acid treatment of samples in ineffective (Jeppson et al., 1995, 1999). The surfactant is also capable of removing acid rinds that may form after a

whole-rock sample has undergone multiple formic acid treatments, thus exposing a fresh surface to be digested later (Jarochowska et al., 2013). Because quartz-rich glauconitic intervals were overall unresponsive to formic acid treatments, these whole-rock samples remained largely undigested until sodium hexametaphosphate treatments were applied to them. These samples were the only ones to undergo this type of treatment. To avoid the samples developing acid rinds from overexposure to acid and disaggregate them, sodium hexametaphosphate treatments were needed. which was most effective at 55% concentrations and by heating the sample-solution. All samples were placed in the sodium hexametaphosphate solution and put in an oven set at 200°F (93.3℃) and took about 5 hrs. to become significantly to wholly disaggregated.

Hydrogen Peroxide

Hydrogen peroxide (H_2O_2) was purchased and used at 32% concentration. Hydrogen peroxide readily reacts with organic matter and minerals such as pyrite to oxidize (degrade) them. Known organic matter content in the Adkisson 1-33, Winney 1-8, and Elinore 1-18 cores is characteristically less than 1% (LeBlanc, 2014), but heavily pyritized intervals occur commonly throughout each of the cores, and they may be observed in core easily without visual aid. Therefore, hydrogen peroxide works best in whole-rock samples that had significant presence by visual inspection of pyrite and/or marcasite in them. Heavily pyritized intervals proved to be largely independent of facies type, so this type of acid treatment was applied most often just once to any sample which showed obvious evidence for pyritization upon inspection.

Heavy Liquid Density Separation

Miller (2015) recognized during his work on Mississippian conodonts from Ozark outcrops in northern Arkansas that analyzing residues for conodonts in relatively large amounts (i.e., >20 grams) is tedious work. As many of the samples in his study and in this study produced residues from individual samples that weighed more than 20 grams, Miller (personal communication, 2015) recommended applying a heavy liquid density separation technique to concentrate the conodont elements into a heavy fraction that would be easier to pick. The technique is described by Stone (2001) who used lithium metatungstate (LMT) to isolate heavy minerals from disaggregated rock samples. The procedure developed by Stone (2001) was altered slightly to best fit the needs of this study. A detailed description of the theory, justification, and procedure for using lithium metatungstate for isolating conodont elements and other heavy minerals follows.

Theory

The heavy liquids separation technique is applied for isolating relatively heavy grains and other solid constituents from their lighter weight counterparts. This is done by suspending a disaggregated sample in the LMT solution and allowing gravity to separate the heavy fraction from the lighter fraction over a short time based on differences in the densities of the solid materials. This technique is useful for concentrating certain fossil types (e.g., conodonts and pollen grains) as well as heavy minerals for their analysis, respectively. Lithium metatungstate ($Li_2O_{13}W_4$) is one commonly used heavy liquid that is stable and non-toxic at standard temperature and pressure conditions. When fully concentrated, its density is 2.95 grams per cubic centimeter. After experimental analysis, conodont elements have been shown to have densities between 2.84 and 3.14 grams per

cubic centimeter (Barrick, 2001); therefore, the LMT must be diluted to about 2.80 grams per cubic centimeter to allow the elements to fall through the solution while lighter grain types, such as quartz and calcite which have densities of 2.65 and 2.71 grams per cubic centimeter, respectively, stay in suspension.

Justification for Use

LMT is currently the heavy liquid of choice for most studies which rely on heavy liquids separation because it is generally the safest to work with of all the heavy liquids that are available. LMT requires no fume hood and minimal personal safety gear to handle (just gloves, safety glasses, and attire that protects the skin). LMT is also an attractive choice for its users because it is one of the least expensive to purchase among its competitors. Nevertheless, the cost of LMT is still not cheap for most laboratories; therefore, it is essential for anyone using this technique to apply a procedure that uses the liquid most efficiently. To that end, a robust technique for using and reusing LMT in density separation experiments has been developed.

Materials and Procedure

The following step-by-step procedure is meant to describe how to apply the LMT technique to just one sample.

(1) Set up the Experiment

On a table that is secure and clear of any mess, mount a 4-in. diameter support ring to any standard laboratory ring stand and its base. Place a 0.8 liter Nalgene-brand teardrop-shaped bottle with its cap screwed off and its stopcock closed into the 4-in.

support ring. Make sure the bottle is at least four inches away from the table's surface and adjust the ring stand and support ring as necessary.

(2) Measure the Sample

Place your disaggregated sample into a beaker large enough to contain the entire sample. Make note of its volume (or weight). For every 25 milliliters volume (25 grams by weight) of sample you must process, you will add approximately 100 milliliters of LMT to the Nalgene bottle. If your sample is greater than 150 milliliters (150 grams), meaning that it will require approximately 600 milliliters of LMT, then you will have to split the sample into multiple Nalgene bottles (and preferably equal amounts) such that the total volume of the LMT in each bottle does not exceed 600 milliliters, as you will need the leftover space for stirring your sample once you have added it and the LMT.

(3) Dilute and Measure the LMT

Before you pour the new and fully concentrated LMT into the Nalgene bottle for the first time, you will need to dilute it. LMTliquid.com has a density calculator that you may use to derive the amount of water you will need to add to dilute your concentrated LMT. Use the online calculator (that you can also download to an external drive) to derive the amount of water you will need to add to the fully concentrated LMT to lower its density to the desired value (e.g., a density of 2.80 g/cm^3 is ideal for conodont work). After adding the desired amount of water to the LMT in its original bottle to dilute it, close the container and shake it moderately for about a minute to mix its contents. Measure about 50 milliliters of it into an empty beaker and set it on a scale to make sure it is the correct density desired.

Use the following formula to check the density of the liquid:

$$\frac{1000\ mL}{amount\ of\ measured\ LMT} \times (weight\ of\ LMT\ in\ beaker - weight\ of\ beaker)$$

(4) Add the LMT

Pour the diluted LMT into a separate beaker per the amount you have already determined to need for your sample. If you had to split your sample into multiple bottles, then pour the necessary amounts (preferably equal amounts) of the LMT into each bottle according to how much of the sample you plan to add to the bottles. If splitting the sample does not apply, then pour all the measured LMT into the one Nalgene bottle you plan to use for your single sample.

(5) Add the Sample

Take a two to 3-in. diameter plastic funnel and place it on top of the bottle with the LMT in it. Pour your sample from its beaker through the funnel and into the bottle with the LMT in it. Once again, if you had to split your samples up into multiple bottles, see that you pour the right amount (preferably equal amounts) of sample into your bottles with the LMT in them. Rinse the funnel with water under one of the laboratory's faucet and dry it with a paper towel or use one of the air valves in the laboratory to blow off any sample residue. Save the funnel for additional runs.

(6) Stir the Sample

Take a glass stir rod (alternatively, a glass thermometer will do) and stir your sample that you just added to the LMT in its bottle until the entire sample is mixed well, meaning that all the sample is wet and there are no lumps in it. Take out the stir stick,

waiting for some of the larger LMT liquid to drop back into the bottle first, and move it over an empty one liter beaker once the drips have more-or-less stopped coming off the rod. Take a one liter wash bottle with deionized water in it that you got from one of the laboratory's faucets and gently wash any remaining LMT and sample residue on the rod into the empty beaker. After the stir rod has been thoroughly rinsed, dry it with a paper towel and place it to the side for use with future sample runs. Depending on how "muddy" your sample is, you may want to stir the sample again, following the same procedure as has been described to this point to ensure the sample is well-mixed and all the constituents have an equal opportunity to fall through the solution. To tell if you need to stir your sample again, wait about 30 minutes for the stirred sample to settle. If most of the particles in the bottle have returned toward the top of the bottle and the LMT solution is mostly to all clear, then you do not need to stir the sample again. If after 30 minutes the sample has not cleared and appears somewhat to severely cloudy, then consider re-stirring the sample up to two or three more times to ensure that it has been mixed well enough. Once the sample has had time enough to settle through gravity (should not need more than 24 hours), there will be a light fraction that sits on top of the solution and a heavy fraction that rests near or at the bottom of the bottle, assuming a heavy fraction is present at all. Also, note that the bottle with the settled sample in it may still not look clear with mud-rich sample you work with.

(7) Collect Heavy Fraction and Get LMT Ready for Immediate Reuse

Take a 5 L beaker and place a #200 mesh sieve over it. Place laboratory gloves (e.g., nitrile gloves) on your hands and put safety glasses over your eyes for this step and the next. Grab the Nalgene bottle with the settled heavy fraction in it and gently lift it

from its support ring. Take the bottle over to the sieve and open the stopcock to the bottle about halfway to release the heavy fraction onto the mesh sieve while also allowing the associated LMT liquid to drain through the sieve down into the beaker. When all the particulates have come out of through the bottom of the bottle and with the light fraction sample and LMT still in it, keep the stopcock to the bottle open (you may want to open it more at this point) and allow the rest of the LMT to drain until the light fraction is reached. Before the light fraction begins collecting onto the sieve, close the stopcock (for most analyses, it is okay if just a little of the lighter fraction goes through). It is helpful to begin closing the stopcock well before the light fraction is reached to slow the flow and allow more LMT to come out before it pulls the light fraction with it. Also, when collecting the heavy fraction and LMT from the bottle, you will want to lift the sieve up to angle it slightly so that the LMT pools and its drainage is focused rather than having it go toward the sides of the sieve and run down the outside edges of the 5 L beaker. Once the LMT is completely drained from the mesh sieve, walk over to the beaker which was used to put the LMT and sample residue from stirring in and use the wash bottle with the deionized water in it to gently rinse the remaining liquid contents of the sieve into the beaker, being sure not to add the heavy fraction to the beaker.

(8) Deliver Heavy Fraction for Analysis and LMT for Reuse

Put the heavy fraction from the sieve into a labeled sample bag or paper towel that has been folded into a funnel shape by washing it with a wash bottle. If using a sample bag, place a labeled and open sample bag into an empty beaker and wash the heavy fraction into the bag. The liquid contents of the bag will dry within 24 hours with no help from the oven. You can also dry the sample bag in the oven set at “3” or “4” setting if

you wish. If you are using a folded paper towel to pour into, then place the towel on a 6-in. diameter funnel that is mounted to another support ring and ring stand and wash the heavy fraction into the funnel you created. You can then place the folded paper towel with the heavy fraction in it into the oven in NRC 019 set at the "3" or "4" setting for it to dry in the next several minutes. Get the bottle that the LMT arrived in. Pour the liquid contents in the 5 L beaker into that bottle. This is the portion that does not need reconstitution and which may be reused immediately on other samples. Do not pour the contents of the 5 L beaker into the original LMT container if you are unhappy with the color (cloudiness) of the used LMT. Your sample may have contained so much silt and clay that it clouded the sample so much that it will need to be diluted to allow the small particles to fall out of suspension for the LMT to clear up. If you wish to dilute a cloudy LMT portion, then simply leave the liquid in the 5 L beaker and move on to the next step.

(9) Collect the Light Fraction and Diluted LMT

Take the Nalgene bottle with only the light fraction and used LMT in it and unscrew the lid. Add water from the wash bottle to the bottle, spraying around the sides to collect the entire sample. In general, you will need to add enough water to the bottle at this point such that there is about a quarter inch standing water above the sample and the diluted LMT. Take the bottle over to the mesh sieve again with the 5 L beaker underneath and take off the stopcock completely from the bottle. The light fraction and diluted LMT will drain into the sieve and the diluted LMT will continue into the beaker. Rinse the sieve with the light fraction with some more water from the wash bottle and then take the sieve and sample over to a sink. Using tap water, thoroughly rinse the light fraction. Get a sample bag and label it and place it in any empty beaker. Set it under the large diameter

(i.e., about six inches) funnel set on a ring stand and pour the contents of the sieve into the funnel and into the sample bag. The sample bag will air dry over the next 24 to 48 hours. Do not place this bag to dry in the oven as the high-water content leaking from the bag will cause lead to the formation of rust and hard minerals inside the oven.

(10) Reconstitute the Diluted LMT

Rinse out the empty Nalgene bottle(s) with tap water as well as the lids and stopcocks and then fully reassemble it (them) for the next run. Take the 5 L beaker with the diluted and/or muddy LMT in it and pour it into an empty beaker(s) that is (are) large enough to hold the contents. Wait 24 to 48 hours for this portion to settle and then use a syringe to collect the now clear and diluted liquid into a new beaker. Set this new beaker with the clear and diluted LMT in the oven set at "3" or "4". Do not set the oven above the "4" setting when reconstituting the LMT as the LMT liquid may become unstable and decompose to produce harmful carcinogens. You will have to check on the liquid periodically to see when it is reconstituted to your desired density. To do this, use the formula for checking the density of the LMT presented in step three of this procedure. Note that the reconstitution process usually takes three to four days. It is also largely guess and check, so you will have to be ready to calculate how much water you need to add to it if you reconstitute it above the desired value, and you will have to also be ready to wait longer for it to reconstitute itself at times. In the former of the two cases, try avoiding over-reconstitution. If too much water is driven from the LMT liquid, the LMT becomes solid (amber to white in color). If this happens, simply add water to the LMT to start the process over and stir the LMT-water mixture vigorously for periods of about 30 seconds, putting the mixture back in the oven for periods of five or ten minutes. Soon the

mixture will return to its original liquid state given enough stirring and adding water. However, if you happen to leave the LMT-water mixture and it turns sold and becomes a white-greenish to green color, you will have to throw the solid LMT out. Do not try to reconstitute the LMT at this point as it has already begun to degrade significantly.

(11) Repeat Experiment Using a New Sample

Follow steps one through ten as described in this procedure and as necessary for your samples in future runs.

APPENDICES

APPENDIX C: SYSTEMATIC PALEONTOLOGY

Phylum CHORDATA Bateson, 1886

Class CONODONTA Pander, 1856

Division PRIONIOCONTIDA Dzik, 1976

Order OZARKODINIDA Dzik, 1976

Suborder OZARKODININA Dzik, 1976

Superfamily POLYGNATHACEA Bassler, 1925

Genus ADETOGNATHUS Lane, 1967

Type Species – Cavusgnathus lautus Gunnell, 1933, p. 286, pl. 31, figs. 67-68

ADETOGNATHUS UNICORNIS (Rexroad and Burton, 1961)

pl. 1, figs. 3 and 7; pl. 2, fig. 1

1947 *Taphrognathus varians* Cooper, p. 92, pl. 20, figs. 14-16

1961 *Streptognathodus unicornis* Rexroad and Burton, p. 1157, pl. 138, figs. 1-9

1962 *Streptognathodus unicornis* Collinson et al., p. 27, charts 1 and 4

1965 *Streptognathodus unicornis* Dunn, p. 1149, pl. 140, figs. 5-6, 13, and 14

1967 *Adetoghanthus unicornis* Lane, p. 925, pl. 119, figs. 16-21

Diagnosis – Specimens are consistent with Lane's (1967) original diagnosis and look most like specimens found in Repetski and Henry (1983).

Range and Occurrence – Upper Chesterian. Recovered from the upper part of the Doberman 1-25.

Remarks – Because the specimens assigned to *Adetognathus unicornis* in this study all lack their free blades their identification is tentative at best, as they may be easily confused with other species that belong to a couple of genera with similar morphologies, such as *Taphrognathus varians* and C*avusgnathus unicornis*. However, the author is convinced that *A. unicornis* is the most proper name to give these specimens, since they are otherwise very consistent in their diagnostic morphologies described in Lane (1967) and Morrow and Webster (1991) and because of where they fit stratigraphically in relation to other conodont faunal occurrences in this study.

Specimens assigned to *A. unicornis* were recovered just below a bed bearing representatives of *Rhachistognathus* that are indicative of the uppermost Chesterian. The specimens are also stratigraphically above occurrences of *Vogelgnathus campbelli* and *Lochriea commutata*, which are indicative of the basal-lower Chesterian. Therefore, it was thought that a *Taphrognathus varians* assignment for these specimens would not be appropriate, given the fact that this species ranges only from the middle Osagean to the upper Meramecian. The specimens were also determined to most likely not belong to any

of the species in the genus *Cavusgnathus* that are easily confused with *A. unicornis* because all *Cavusgnathus* varieties that are typical for the Oklahoma basin range from the upper Meramecian to the middle Chesterian (e.g., Godwin, 2017). Therefore, while it still may be plausible for the specimens assigned to *A. unicornis* to truly represent a "look-alike" species of *Cavusgnathus* because the specimens are not wholly preserved, the fact that they occur just below uppermost Chesterian conodonts and that there is such a large section of core devoid of any conodonts from the basal-lower Chesterian to what supposedly represents the middle Chesterian, *A. unicornis* is, from a biostratigraphic perspective, the most logical species designation.

Genus GNATHODUS Pander, 1856

Type Species – *Gnathodus mosquensis* Pander, 1856, p. 33, pl. 2A, figs. 10a, b, c

Polygnathus bilineatus Roundy, 1926 (from Nemyrovska, 2005 citing Tubbs, 1986)

GNATHODUS BULBOSUS (Thompson, 1967)

pl. 1, fig. 11

1967 *Gnathodus bulbosus* Thompson, p. 66, pl. 3, figs. 7, 11, 14, 15, 18-21; p. 72, pl. 6, figs. 2 and 7

1970 *Gnathodus bulbosus* Thompson and Fellows, p. 128, pl. 1, figs. 3, 6, 8, 9, 12, 13

2013 *Gnathodus bulbosus* Boardman et al., p. 148, pl. 14, figs. 1-3, 5-11

Diagnosis – Specimen is consistent with Thompson's (1967) original diagnosis and the observations of Miller (2015).

Range and Occurrence – upper Osagean (this study). This species is also known to range throughout the Osagean. Recovered from the lower part of the Elinore 1-18.

Remarks – Free blades not readily preserved in any of the specimens recovered.

Materials – A total of six almost identical specimens assigned to *Gnathodus bulbosus* were recovered from a sample collected from the lower part of the Elinore 1-18, but only one (which had the best preservation quality) was selected for SEM work.

GNATHODUS CUNEIFORMIS (Mehl and Thomas, 1947)

pl. 2 fig. 3

1947 Gnathodus cuneiformis Mehl and Thomas, p. 10, pl. 1, fig. 2

1980 Gnathodus cuneiformis Lane et al., p. 130, pl. 4, figs. 5-13; pl. 10, fig. 7

1998 Gnathodus cuneoformis Perri and Spaletta, p. 243, pl. 1, figs. 3-4; p. 247, pl. 3, figs. 1-2

Diagnosis – Specimen is consistent with the original diagnosis of Mehl and Thomas (1947) and the observations of Perri and Spaletta (1998).

Range and Occurrence – middle to upper Osagean. Recovered from the lower part of the Adkisson 1-33.

Remarks – The specimen assigned to *Gnathodus cuneiformis* is missing most of its free blade but is otherwise well-preserved.

GNATHODUS LINGUIFORMIS (Branson and Mehl, 1941a)

pl. 1, fig. 10

1941a *Gnathodus linguiformis* Branson and Mehl, n. sp., p. 183, pl. 6, figs. 18-26

2013 *Gnathodus linguiformis* Boardman et al., pl. 15, fig. 4

Diagnosis – Specimen is consistent with Branson and Mehl's (1941a) original diagnosis and the observations of Miller (2015) and Godwin (2017).

Range and Occurrence – upper Osagean (this study). This species is also known to extend into the lower Meramecian (Godwin, 2017). Recovered from the bottom part of the Elinore 1-18.

Remarks – The outer platform and free blade of the specimen recovered is not well-preserved. Still, enough detail is preserved to determine the position of the outer platform in relation to the inner platform for its identification and it is otherwise very consistent with the descriptions of Branson and Mehl (1941a), Miller (2015), and Godwin (2017).

Refer to Miller's (2015) description of *G. linguiformis* for a description on how to differentiate this species from its closely related *G. pseudosemiglaber* and *G. texanus* forms. The species designation *G. linguiformis* has become somewhat passé among experts and was replaced with *G. pseudosemiglaber*; therefore, the distinction between *G. linguiformis* and *G. pseudosemiglaber* may be unnecessary.

GNATHODUS PSEUDOSEMIGLABER (Thompson and Fellows, 1970)

pl. 1, fig. 1

1970 *Gnathodus texanus pseudosemiglaber* Thompson and Fellows, n. ssp., p. 88, pl. 2, figs., 6, 8, 9, 11-13

1973 *Gnathodus texanus pseudosemiglaber* Butler, p. 500, pl. 56, figs. 28, 29, and 36

1980 *Gnathodus pseudosemiglaber* Lane et al., p. 132, pl. 4, figs. 15-17, and 19; p. 133, pl. 5, figs. 8-15; p. 134, pl. 6, fig. 14

2013 *Gnathodus pseudosemiglaber* Boardman et al., pl. 15, figs. 1-3, 6

Diagnosis – Specimen is consistent with Thompson and Fellows' (1970) original diagnosis and the observations of Miller (2015) and Godwin (2017).

Range and Occurrence – upper Osagean (this study). This species is known to range from the Osagean into the basal Meramecian (Godwin, 2017). Recovered from the lower part of the Elinore 1-18.

Remarks – The free blade of this specimen is not well-preserved; however, based on its co-occurrence with *G. linguiformis* and *G. texanus* and its other unique platform morphologic features that help to differentiate it between the other two species types, the specimen can be distinguished from its closely related *G. linguiformis* and *G. texanus* forms. Refer to Miller's (2015) descriptions of these species for how to differentiate between them.

GNATHODUS n. sp. 15 aff. PUNCTATUS (Boardman et al., 2013)

pl. 2, fig. 5

2013 *Gnathodus n. sp. 15 aff. punctatus* Boardman et al., pl. 15, fig. 7

2017 *Gnathodus n. sp. 15 aff. punctatus* Godwin, pl. 7, figs. A-G

Diagnosis – Specimen is consistent with the original diagnosis of Boardman et al. (2013) and the observations of Godwin (2017).

Range and Occurrence – lower Meramecian (this study and as established when this species was originally defined as new). Recovered from the lower part of the Elinore 1-18.

Remarks – Not all the free blade is preserved on this specimen, making distinction between *Gnathodus n. sp. 15 aff. punctatus* and *G. punctatus* difficult. However, given this specimen's stratigraphic position (being placed above the middle and upper Osagean

conodont fauna in this study), a *G. punctatus* assignment is not plausible, as this species ranges from the upper Kinderhookian to the lower Osagean. The specimen most closely compares with a specimen from pl. 7, fig. G in Godwin (2017).

GNATHODUS sp. A (Godwin, 2017)

pl. 2, fig. 2

1970 *Gnathodus pseudosemiglaber texanus* Thompson and Fellows, n. ssp., p. 88, pl. 2, figs. 6, 8-9, 11-13

1980 *Gnathodus pseudosemiglaber* Lane et al., pl. 4, figs. 15-17; pl. 5, figs. 8-15

1998 *Gnathodus pseudosemiglaber* Perri and Spaletta, pl. 1, fig. 14; pl. 2, fig. 12

2007 *Gnathodus bilineatus* Singh, pl. 6, figs. 5-7 (as primitive morphotype); pl. 6, fig. 4 (as transitional form)

2017 *Gnathodus sp. A* Godwin, n. sp., pl. 8, figs. A-M

Diagnosis – Specimen is consistent with the original diagnosis of Godwin (2017).

Range and Occurrence – lower Meramecian (this study and as established when originally defined as a new species). Recovered from the lower part of the Elinore 1-18.

Remarks – This specimen may be a junior form of the specimens described in Godwin (2017).

GNATHODUS TEXANUS (Roundy, 1926)

pl. 1, figs. 6, 8, 9, and 12; pl. 2, fig. 6

1926 *Gnathodus texanus* Roundy, n. sp., p. 12, pl. 2, figs. 7-8.

1980 *Ganthodus texanus* Lane et al., p. 133, pl. 6, figs. 8, 9, 11, 12, 16

Diagnosis – Specimen is consistent with the original diagnosis of Roundy (1926).

Range and Occurrence – upper Osagean. This species is known to range from the Osagean into the middle Chesterian. Recovered from the lower part of the Elinore 1-18.

Remarks – Refer to Miller's (2015) description of *G. texanus* for a description on how to differentiate this species from its closely related *G. pseudosemiglaber* and *G. linguiformis* forms. Specimens assigned to *G. texanus* in this study are occasionally tentative due to the poor preservation quality of some of the platform and free blade morphologies on select specimens.

Genus LOCHRIEA Scott, 1942

Type species – *Lochriea montanaensis* Scott, 1942, p. 295, pl. 37, figs. 1-7; p. 296, pl. 38, figs. 1-4, 6, 7, 10, and 12

Spathognathodus commutatus Branson and Mehl, 1941, p. 98, pl. 19, figs. 1-4

LOCHRIEA COMMUTATA (Branson and Mehl, 1941b)

pl. 2, fig. 7

1941b *Spathognathodus commutatus* Branson and Mehl, p. 98, pl. 19, figs. 1-4

1942 *Lochriea montanaensis* Scott, p. 295, pl. 37, figs. 1-7; p. 296, pl. 38, figs. 1-4, 6, 7, 10, and 12

1953 *Gnathodus inortatus* Hass n. sp., p. 80, pl. 14, figs. 9-11

1964 *Gnathodus commutatus* Rexroad and Furnish, p. 671

1970 *Gnathodus commutatus commutatus* Dunn, p. 318, pl. 62, figs. 11-12

1974 *Gnathodus commucatus commucatus* Lane and Straka, p. 77, pl. 37, figs. 1-9; pl. 40, figs. 15-18, 23-26

1976 *Lochriea commutatus* Norby, p. 143, pl. 13, figs, 1-3; p. 144, pl. 14, figs. 3-9

1990 *Lochriea commutata* Rexroad and Horowitz, p. 535, pl. 2, figs, 10-24

Diagnosis – Specimen is consistent with the original diagnosis of Branson and Mehl (1941b).

Range and Occurrence – basal Chesterian. This species is also known to occur throughout the Chesterian in North America. Recovered from the upper part of the Doberman 1-25.

Remarks – The two specimens recovered in this study was assigned to *Lochriea commutata* because they most closely fit with the description for the species in Godwin (2017) and because of its similarity with a specimen assigned to the same species on pl.

62, fig. 12 in Dunn (1970). However, the posterior tip of the carina of this specimen does extend a little further than what is common for *L. commutata*; therefore, its designation is tentative.

Genus POLYGNATHUS Hinde, 1879

Type Species – *Polygnathus dubius* Hinde, 1879, p. 363, pl. 16, fig. 17

POLYGNATHUS BISCHOFFI (Rhodes et al., 1969)

pl. 2 fig. 8

1969 *Polygnathus bischoffi* Rhodes et al., p. 134, pl. 2, fig. 7-17

1998 *Polygnathus bischoffi* Perri and Spaletta, p. 244, pl. 2, figs. 18 a, b

Diagnosis – Specimen is consistent with the original diagnosis of Rhodes et al. (1969).

Range and Occurrence – middle Osagean. Recovered from the lower part of the Elinore 1-18.

Remarks – The specimen assigned to *Polygnathus bischoffi* in this study is coated in a thin, pitted layer of cement and sediment, making it difficult to see some of the important morphologic for its identification. However, higher resolution SEM images (not pictured in this study but available at the Paleontology Repository at the University of Iowa)

provided the author with the ability to see past much of the pitted material covering the element and allow for this specimen's identification.

Genus RHACHISTOGNATHUS Dunn, 1965

Type Species – *Rhachistognathus prima* Dunn, 1966, p. 1301, pl. 157, figs. 1-2

RHACHISTOGNATHUS MINUTUS MINUTUS (Higgins and Bouckaert, 1968)

pl. 2, fig. 4

1968 *Idiognathoides minuta* Higgins and Bouckaert, n. sp, p. 66, pl. 6, figs. 7-12

1996 *Rhachistognathus minutus minutus* Krumhardt et al., p. pl. 7, figs. 9-13

Diagnosis – Specimen is consistent with the original diagnosis of Krumhardt et al. (1996).

Range and Occurrence – uppermost Chesterian. Recovered from the upper part of the Doberman 1-25.

RHACHISTOGNATHUS MURICATUS trans. to WEBSTERI? (Krumhardt et al., 1996)

pl. 2, fig. 5

1966 *Cavusgnathus transitoria* Dunn, p. 1299, pl. 157, fig. 9

1985 *Rhachistognathus muricatus* Baesemann and Lane, p. pl. 8, fig. 9

1996 *Rhachistognathus muricatus trans. to Websteri* Krumhardt et al., p. 79, pl. 4, fig. 16

Diagnosis – Specimen is consistent with the original diagnosis of Baesemann and Lane (1985). In addition, this species is diagnosed by observing its fused denticles which are oriented transversely to the carina and join the left and right parapets in a central location in the center part of the carina.

Range and Occurrence – uppermost Chesterian. Recovered from the upper part of the Doberman 1-25.

Remarks – This specimen may be better placed in *Rhachistognathus muricatus* because it lacks the asymmetric node on the posterior end of the platform that can help distinguish it from *R. websteri*.

Genus SPATHOGNATHODUS Branson and Mehl, 1941b

Type species – *Ctenognathus murchisoni* Pander, 1856, p. 32, pl. 4, fig. 17; pl. 6, figs. 18a, b

SPATHOGNATHODUS sp.?

pl. 1 fig. 2

Diagnosis – Specimens belonging to *Spathognathodus* have a thin platform, with a basal cavity that forms at the center of the specimen. Denticles of this genus are often fused, with the largest ones occurring toward the anterior end.

Range and Occurrence – Specimens belonging to *Spathognathodus* are known to occur throughout the Mississippian. Recovered from the upper part of the Elinore 1-18.

Remarks – The specimen assigned to *Spathognathodus* in this study was not well-preserved enough for species level identification.

Genus VOGELGNATHUS Norby and Rexroad, 1985

Type Species – *Spathognathodus campbelli* Rexroad, 1957

VOGELGNATHUS CAMPBELLI (Rexroad, 1957)

pl. 2 fig. 4

1957 *Spathognathodus campbelli* Rexroad, p. 37, pl. 3, figs. 13-15

1964 *Spathognathodus campbelli* Rexroad and Furnish, p. 674, pl. 111, figs. 23-24

1985 *Vogelgnathus campbelli* Norby and Rexroad, p. 2, pl. 2, figs. 3-10

1998 *Vogelgnathus campbelli* Perri and Spaletta, p. 245, pl. 2, fig. 15

2005 Vogelgnathus campbelli Nemyrovska, p. 46, pl. 1, figs. 1-2, 4-5, and 9

Diagnosis – Specimen is consistent with the original diagnosis of Rexroad (1957) and observations of Perri and Spaletta (1998) and Godwin (2017).

Range and Occurrence – lower Chesterian (this study). This species is also known to range from the upper Meramecian to the lower Chesterian in the Oklahoma basin (e.g., Godwin, 2017).

Remarks – This specimen is well-preserved and displays all the characteristics of *Vogelgnathus campbelli*, including the polygonal apices which cannot be easily seen in the SEM image in plate 2.

APPENDICES

APPRENDIX D: PLATES

All conodont specimens imaged with the SEM are displayed at 120X magnification and were deposited with the Paleontology Repository of the Department of Earth and Environmental Sciences at the University of Iowa, 115 Trowbridge Hall, Iowa City, IA, 52242, U.S.A. All sample depths reported herein reflect core depths.

Plate 1

Figure 1 – *Gnathodus pseudosemiglaber* (Thompson and Fellows, 1970); Elinore 1-18, sample depth: 4458.5-4459.0 ft., SUI 145079

Figure 2 – *Spathognathodus sp.?* (Branson and Mehl, 1941b); Elinore 1-18, sample depth: 4479.0-4480.0 ft., SUI 145080

Figure 3 – *Adetognathus unicornis?* (Rexroad and Burton, 1961); Doberman 1-25, sample depth: 5035.8-5536.0 ft., SUI 145081

Figure 4 – *Rhachistognathus minutus minutus* (Higgins and Bouckaert, 1968); Doberman 1-25, sample depth 4992.6-4992.8, SUI 145082

Figure 5 – *Rhachistognathus muricatus trans. to R. websteri?* (Krumhardt et al., 1996); Doberman 1-25, sample depth: 5000.4-5000.6, SUI 145083

Figure 6 – *Gnathodus aff. texanus?* (Roundy, 1926); Elinore 1-18, sample depth: 4479.0-4480.0 ft., SUI 145084

Figure 7 – *Adetognathus unicornis?* (Rexroad and Burton, 1961); Doberman 1-25, sample depth: 5035.8-5536.0 ft., SUI 145085

Figure 8 – *Gnathodus texanus* (Roundy, 1926); Elinore 1-18, sample depth: 4464.5-4465.5 ft., SUI 145086

Figure 9 – *Gnathodus texanus* (Roundy, 1926); Elinore 1-18, sample depth: 4456.6-4457.0 ft., SUI 145087

Figure 10 – *Gnathodus linguiformis* (Branson and Mehl, 1941a); Elinore 1-18, sample depth: 4458.5-4459.0 ft., SUI 145088

Figure 11 – *Gnathodus bulbosus* (Thompson, 1967); Elinore 1-18, sample depth: 4479.0-4480.0 ft., SUI 145089

Figure 12 – *Gnathodus aff. texanus?* (Roundy, 1926); Elinore 1-18, sample depth: 4479.0-4480.0 ft., SUI 145090

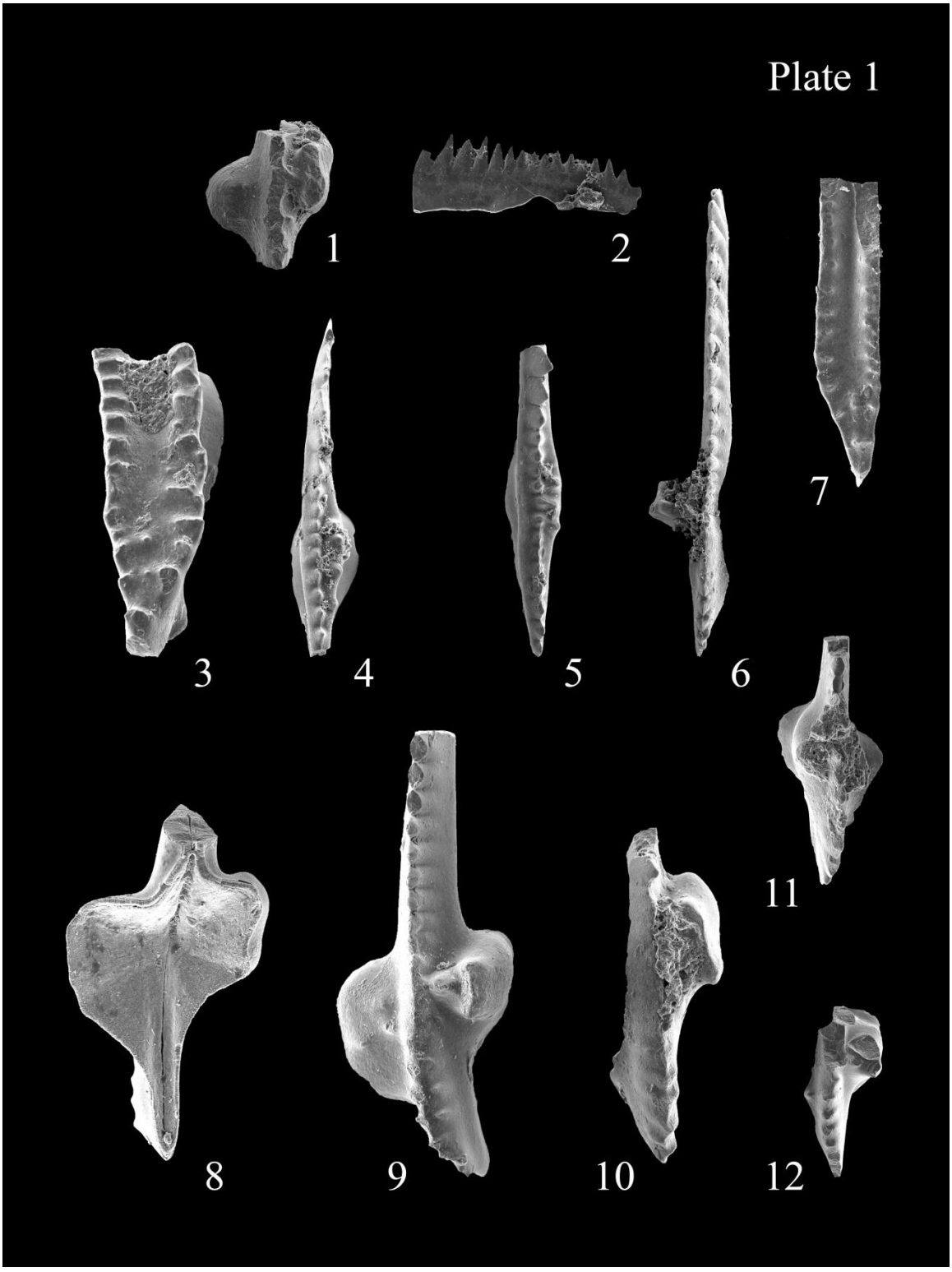
Plate 1
1
2
3
4
5
6
7
8
9
10
11
12

Plate 2

Figure 1 – *Adetognathus unicornis?* (Rexroad and Burton, 1961); Doberman 1-25, sample depth: 5022.0-5022.5 ft., SUI 145091

Figure 2 – *Gnathodus sp. A* (Thompson and Fellows, 1970); Elinore 1-18, sample depth: 4451.5-4452.5 ft., SUI 145092

Figure 3 – *Gnathodus cuneiformis* (Mehl and Thomas, 1947); Elinore 1-18, sample depth: 4458.5-4459.0 ft., SUI 145093

Figure 4 – *Vogelgnathus campbelli* (Rexroad, 1957); Adkisson 1-33, sample depth: 5570.0-5571.0 ft., SUI 145094

Figure 5 – *Gnathodus n. sp. 15 (aff. punctatus)* (Boardman et al., 2013); Elinore 1-18, sample depth: 4451.5-4452.5 ft., SUI 145095

Figure 6 – *Gnathodus texanus* (Roundy, 1926); Elinore 1-18, sample depth: 4456.5-4457.0 ft., SUI 145096

Figure 7 – *Lochriea commutata?* (Branson and Mehl, 1941b); Elinore 1-18, sample depth: 4367.5-4468.0 ft., SUI 145097

Figure 8 – *Polygnathus bischoffi* (Rhodes et al., 1969); Elinore 1-18, sample depth: 4481.0-4481.7 ft., SUI 145098

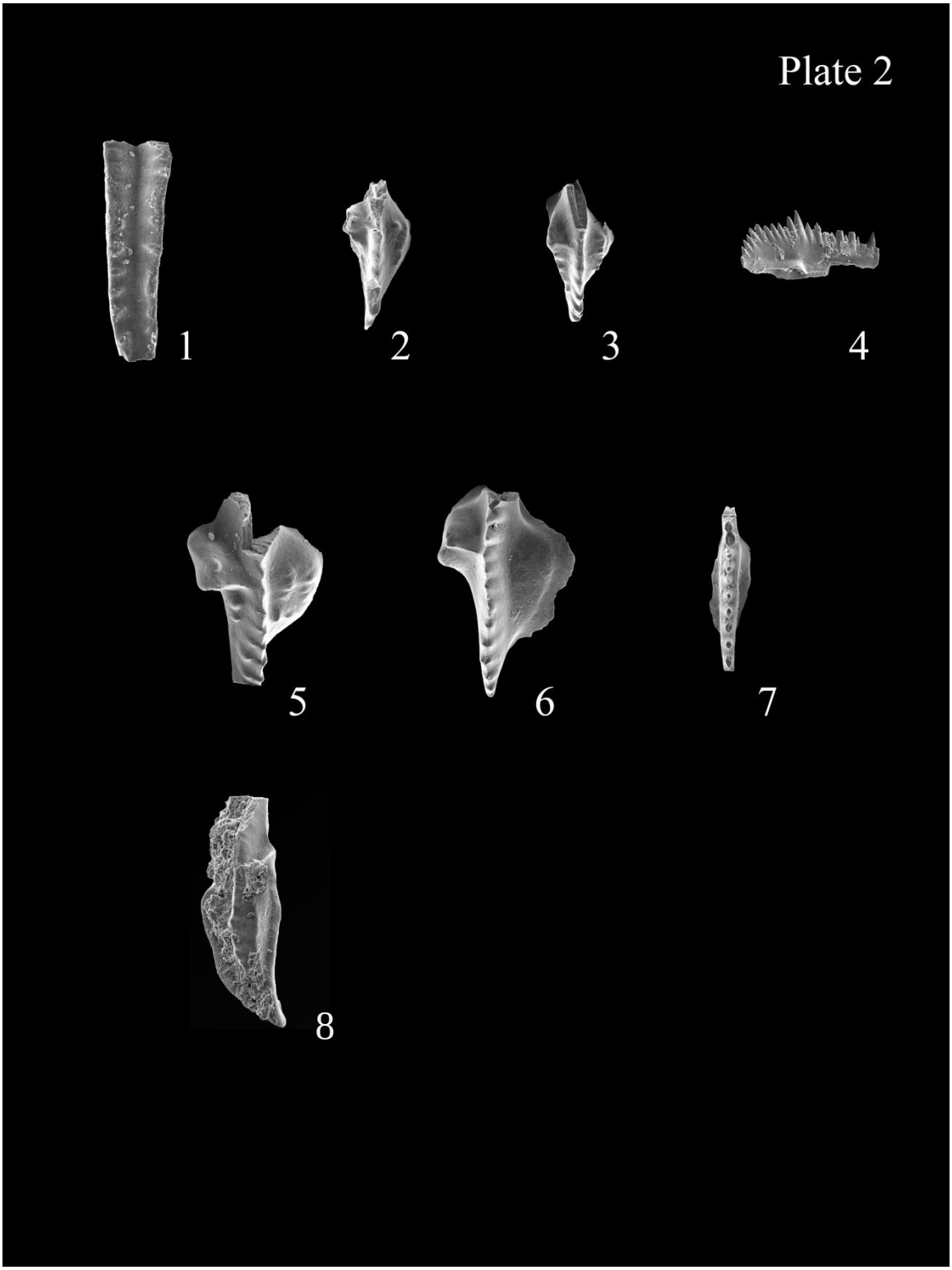
Plate 2
1
2
3
4
5
6
7
8

VITA

John Edward Hunt

Candidate for the Degree of

Master of Science

Thesis: CONODONT BIOSTRATIGRAPHY IN MIDDLE OSAGEAN TO UPPER CHESTERIAN STRATA, NORTH-CENTRAL OKLAHOMA, U.S.A.

Major Field: Geology

Biographical:

Education:

Completed the requirements for the Master of Science in geology at Oklahoma State University, Stillwater, Oklahoma in December, 2017.

Completed the requirements for the Bachelor of Science in geology at Brigham Young University, Provo, Utah in 2015.

Experience:

October 2017 to Present: Geologist I, Chesapeake Energy

May 2017 to Aug. 2017: Geology Intern, Chesapeake Energy

Jun. 2014 to Oct. 2015: Field Mapping Geologist, Brigham Young University

Sep. 2013 to Dec. 2014: Research Assistant, Brigham Young University

Professional Memberships:

Geological Society of America

American Association of Petroleum Geologists